Operational monitoring of snow cover using digital imagery

Cemal Melih Tanış

School of Electrical Engineering

Thesis submitted for examination for the degree of Master of Science in Technology.

Espoo 31.12.2019

Supervisor

Prof. Miina Rautiainen

Advisor

Dr. Ali Nadir Arslan

Aalto University
School of Electrical
Engineering

Aalto University
School of Electrical
Engineering

Aalto University, P.O. BOX 11000, 00076 AALTO
www.aalto.fi
Abstract of the master's thesis

Author Cemal Melih Tanış

Title Operational monitoring of snow cover using digital imagery

Degree programme Electronics and Nanotechnology

Major Space Science and Technology **Code of major** ELEC3039

Supervisor Prof. Miina Rautiainen

Advisor Dr. Ali Nadir Arslan

Date 31.12.2019 **Number of pages** 70+22 **Language** English

Abstract

Fractional snow cover (FSC) and snow depth (SD) are two important parameters used to calculate snow water equivalent and surface albedo, which are important physical quantities for applications in climatology, hydrology and meteorology. FSC is traditionally monitored using satellite data, but it is challenging for optical sensors to retrieve signals from the ground when forest canopy is present. Similar challenge exists for retrieving microwave signals from terrain with high slope rates. In addition to retrieval challenges, validation of FSC products are done using proxy parameters since in-situ FSC observations are very limited. This is because there are no devices or systems usable for continuous measurement of FSC and manual observation takes a lot effort and depends on subjective judgement. SD is traditionally observed by manual readings of snow sticks. Manual observations requires effort and presence of manpower, especially in remote areas. Also, temporal resolution of such observations are generally one day. In the last decades, manual observations are replaced with automated observations by ultrasonic and optical sensors in some countries, but the manual observation is still the primary method in many countries.

Using webcam photography for environmental monitoring is an emerging method. During the latest years, numerous environmental camera networks are established in different parts of the globe. These networks offer high resolution digital imagery in high temporal resolution. More digital imagery is also available from cameras and camera networks established for other purposes, such as monitoring ski tracks, traffic, harbours, urban areas etc. It is previously studied that environmental parameters are observed from digital images using image processing methods. A novel system is previously introduced by Tanis et al. for automated monitoring of different parameters from multiple camera networks. This system allows acquisition of images from different sources by defining camera networks on a toolbox, so that it can process and visualise the images on a processing chain customised by input from the user via graphical user interface. The toolbox is called Finnish Meteorological Institute Image Processing Toolbox (FMIPROT). It can work also on cloud, to create automated and continuous processing of digital imagery.

In this thesis, FSC and SD are estimated for multiple locations in Finland by processing images from MONIMET camera network for 2018 - 2019 season. Images are classified as snow covered or snow free in pixel level using an adaptive thresholding algorithm which determines a threshold value for the digital numbers (DN) of pixels in blue channel using histograms of the images. FSC is estimated by

using snow presence in the pixels from the classification and spatial resolution of the pixels calculated from georectification of the images. Images are georectified using perspective projection. SD is estimated using an algorithm to find the intersection of snow surface and snow sticks by thresholding and segmentation. Estimations are assessed using observations from in-situ measurements and observations by visual inspection. FMIPROT processing system is deployed on cloud and the near real time (NRT) monitoring is set up for the same parameters in same locations. The processing is integrated into "FMIPROT & Camera Network Portal" website so that the visualised NRT results are available for public.

Keywords digital imagery, snow cover, snow depth, webcam, webcam network, environmental monitoring, image processing, operational monitoring, near real time monitoring, cloud processing, georectification, orthorectification, optical remote sensing, remote sensing

Acknowledgements

First and foremost I would like to express my sincere gratitude to my advisor Dr. Ali Nadir Arslan and my supervisor Prof. Miina Rautiainen for their great support, mentorship and influence in every step towards this study.

I also wish to thank my manager, Dr. Kari Luojus for his support during my research experience in Finnish Meteorological Institute, to my tutor, Prof. Jaan Praks for his support during my studies in Aalto University, to the researchers in EU Life+ MONIMET project team, technicians and engineers in Finnish Meteorological Institute, Natural Resources Institute of Finland, University of Helsinki and University of Eastern Finland, for sharing their time, knowledge and measurements whenever I requested.

Parts of the work in this study was funded by European Commission through EU Life+ MONIMET Project (LIFE12ENV/FI/000409) during 2013–2017.

Cemal Melih Tanis
Otaniemi, 31.12.2019

Contents

List of Figures

List of Tables

Abbreviations

2D	2 Dimensions
3D	3 Dimensions
AWOS	Automatic weather observation station
CNES	Centre National D'Etudes Spatiales (The National Centre for Space Studies)
CNIF	Camera network information file
CPU	Central processing unit
CSV	Comma separated value
DEM	Digital elevation model
DN	Digital Number
EUROPHEN	European Phenology Camera Network
FinLTSER	Finnish Long-Term Socio-Ecological Research network
FMI	Finnish Meteorological Institute
FMIPROT	Finnish Meteorological Institute Image Processing Toolbox
FSC	Fractional snow cover
FTP	File transfer protocol
GCP	Ground control point
GPS	Global positioning system
GUI	Graphical user interface
HDF	Hierarchical Data Format
HTTP	Hyper text transfer protocol
HTML	Hyper text markup language
ICOS	Integrated Carbon Observation System
ICP	International Cooperative Programme
JPEG	Joint Photographic Experts Group
LUKE	Luonnonvarakeskus (Natural Resources Institute Finland)
MONIMET	Climate Change Indicators and Vulnerability of Boreal Zone: Applying Innovative Observation and Modeling Techniques
N/A	Not applicable
NRT	Near real time
PC	Personal computer
RMSE	Root mean square error
ROI	Region of interest
PRACTISE	Photo Rectification and Classification Software
SC	Snow cover
SD	Snow depth
SMEAR	Station for Measuring Ecosystem-Atmosphere Relations
SYKE	Suomen Ympäristökeskus (Finnish Environment Institute)
TSV	Tab separated value
UAS	Unmanned aerial system
UHEL	University of Helsinki
VTK	Visualization Toolkit

1 Introduction

1.1 Camera technology

In general terms, a camera is a device that captures an image of a view. History of the camera starts with camera obscura (dark room) which is experimented before the tenth century. Also referred as pinhole image, camera obscura is the phenomenon of the light reflected from objects passing through a small hole and then projected as the image of the object onto a screen on the other side. With the development of lenses, that phenomenon is used in a dark room or a box with a lens as an aid to drawing and painting after 16th century, and only during 19th century the images are started to be captured onto light sensitive material. After the invention of electronic sensors, digital cameras are developed. The same phenomenon is still used in digital cameras, only that the light is projected onto a sensor which the light intensity on the different parts of the sensor is read electronically and stored digitally, as shown in Figure 1.

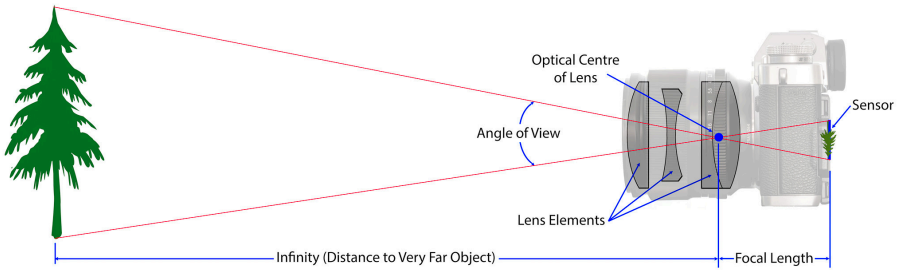

Figure 1: Formation of an image in a digital camera

The term camera is used for optical cameras, which stores detects and stores an image in the optical range of the electromagnetic spectrum. There are also cameras developed to capture images in other parts of the spectrum. Multispectral cameras capture images in multiple wavelengths, generally from 4 to 40 bands, starting from the optical range (0.6 μ m) to long wave infrared (14 μ m). Multispectral cameras are widely used in remote sensing for many decades, including sensing of snow cover, especially space-born [1, 2, 3]. Hyperspectral cameras captures in the similar spectral range in many more bands, for example 192 or 256, meaning more information about the scene is recorded, but in a lower resolution. Also, it is more costly and complicated to process hyperspectral data, as the number of bands are increasing. Hyperspectral cameras are also used in remote sensing, including snow cover[4, 5]. An optical camera can be considered as a multispectral camera with 3 bands, but there is a clear difference in the spectral response. Multispectral cameras are designed with narrow bandwidths but an optical camera has wider bandwidths in around red, green and blue colour light wavelengths, even overlapping with each other. Also, the sensitivity in infrared range is nonzero. Most cameras filter the light in the infrared range by a physical or programmable filter. This difference is illustrated in Figure 2 showing Sentinel 2 Multi Spectral Imager bands 1,2,3 and Stardot NetCam SC bands[6, 7].

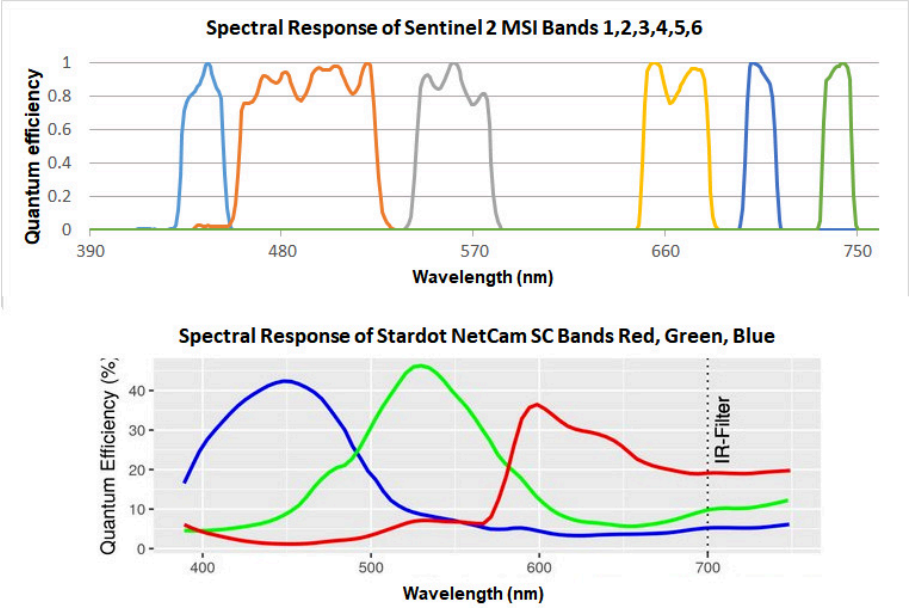

Figure 2: Spectral response of Multi Spectral Imager onbboard Sentinel 2 satellite (top): bands 1 (blue), 2 (orange), 3 (grey), 4 (yellow), 5 (blue), 6 (green) and Stardot NetCam SC camera (bottom): bands red (red), green (green) and blue (blue)[6, 7].

The image projected onto the camera sensor is read as light intensity for each pixel, which are the equally sized parts of the sensor. The intensity is read digitally, in 8 bits (digital number 0—255) for most cameras. The image is than stored in a file format with compression, because the raw image has a large data size. For example, Startdot NetCam SC has a sensor with 2592 pixels in width and 1944 pixels in height. Each pixel having 8 bits of data in three channels, then the raw image would be about 15 megabytes. Instead, the camera stores the images in Joint Photographic Experts Group (JPEG) format, which reduces the file size to 0.3—1.2 megabytes, depending on the image. JPEG is common in most non-professional cameras and in image software.

1.2 Webcam networks

Using webcam photography for environmental monitoring is an emerging method[8, 9, 10, 11, 12, 13, 14, 15]. During the latest years, numerous environmental camera networks are established in different parts of the globe. These networks offer high resolution digital imagery in high temporal resolution. Most of the image data is free, either directly available or with a registration policy. More digital imagery is also available from cameras and camera networks established for other purposes, such as monitoring ski tracks, traffic, harbours, urban areas etc[8, 16]. Most of the image data from such networks is available as live streams on web, but either they are not stored or stored in rolling archives where data is only available for a limited time. Depending on the application, the image data may also be stored for long term but it may be required to request the data from the owner. Even so, it is possible to

store images from live streams by simple cloud processing scripts. It is estimated that tens of thousand of outdoor webcams are available on web, offering free data in one way or another.

MONIMET Camera Network is a part of MONIMET project, established to monitor phenological activity of vegetation and snow cover in the boreal ecosystems in Finland[17, 18]. Multiple studies have done using the data during the project and after [9, 19, 20]. The network is consisting of 28 cameras producing 33 image time series in 14 sites[17]. The European Phenology Camera Network (EUROPhen) is one of the camera networks established in Europe which collects together digital cameras observing 50 flux sites across Europe[10, 21]. The network is open for more sites and cameras for those who want to contribute. It also offers guidance to set up phenology cameras for new contributors. Image data from the network is used in studies to monitor plant development in different ecosystem and land use types. PhenoCam network is a US based phenological camera network which also has cameras outside US in the collection[11, 22]. The network includes over 600 cameras in over 500 sites. Image data is free and available via PhenoCam web page with a registration. The website also offers already processed ROI time series of colour indices. The data is used in multiple studies for monitoring vegetation phenology[11, 23]. In Asia, another camera network for phenological monitoring, Phenological Eyes Network (PEN) is located[24, 25, 26]. The network has cameras in 37 sites, which are in different countries but mostly in Japan. Numerous studies are conducted using image data from PEN [13, 27, 28]. Australian Phenocam Network has cameras providing images from volunteering research sites in Australia[29, 30, 31]. 10 sites from the Terrestial Ecosystem Research Network (TERN) SuperSite Network is providing images for the camera network. Those sites are Long Term Ecological Research (LTER) sites which are providing different means of observations and measurements for ecological studies. The image data is free of charge under an open license. There are also cameras installed and used by the institutions which are not officialy declared as camera networks exists. For example, University of Eastern Finland has two cameras in Maaninka, observing a mineral agricultural field[32]. In Figure 3, locations of the cameras in three environmental camera networks and cameras of University of Eastern Finland are shown.

Potential applications of digital imagery from outdoor webcams are studied by Jacobs et al.[16] The study showed that the outdoor webcams provide images that have different types of land cover, ecosystem, urban areas, infrastructure, terrain types. Thousands of cameras, mostly located in US, Europe and parts of Asia can potentially provide observation of environmental parameters in large scale. Such parameters include snow cover, weather, cloud cover, vegetation and even wind speed. Also, since there is no installation and maintenance cost for using data from the cameras, they offer a lower cost alternative data source. Using the available cameras images would only cost as much as the processing system and the software. In Figure 4, locations of over 16000 webcams providing live images in 2003, at the time of the study [16] is shown.

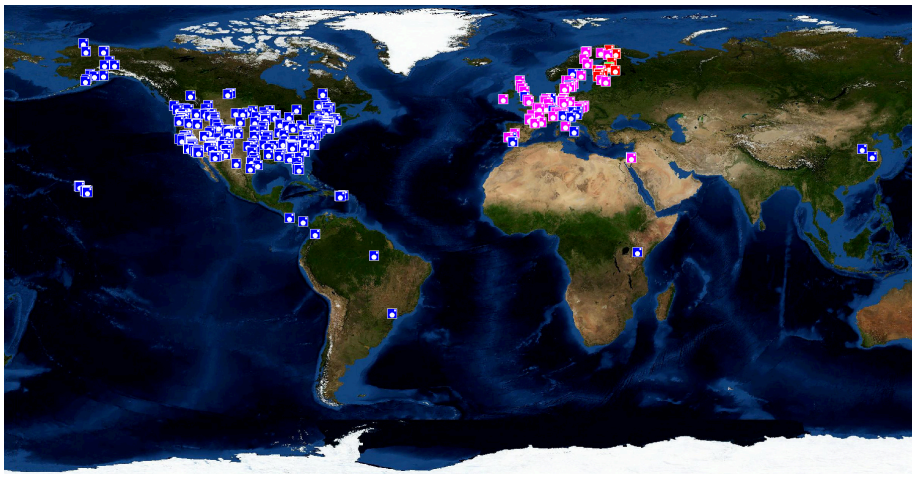

Figure 3: Map of the cameras of University of Eastern Finland (green) and in MONIMET Camera Network (red), The PhenoCam Network (blue) and European Phenology Camera Network (purple) (Background: NASA Blue Marble provided by DLR).

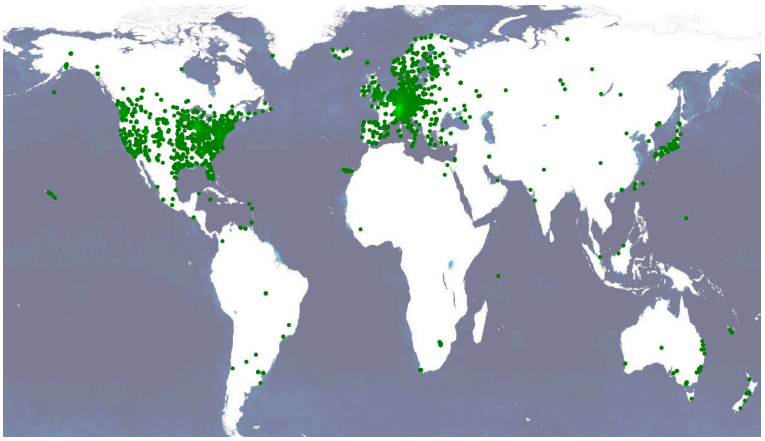

Figure 4: Locations of over 16000 webcams providing live images in 2003, at the time of the study [16].

1.3 Processing of webcam imagery

Vast amount of software packages are available for processing digital images. Using the open source community, researchers have developed numerous software packages and tools aimed for processing the images for environmental monitoring[33, 34, 35, 36]. For studies researchers have also developed their own programs[15, 37]. Different environmental parameters are extracted from images using the software, e.g. vegetation indices, sea ice extent, snow cover, snow depth. Some of the packages and tools are designed and disseminated so that other researchers can use them with their own image datasets.

Phenopix R package is one of the software packages that is developed for extracting vegetation phenology indices from image time series[33]. The package can compute

and report the ROI averaged indices and pixel values. The package provides a GUI for defining ROIs. Data fitering methods and post processing methods are also integrated into the package, which includes curve fitting, phenophase extraction and uncertainty analysis. Visualization options are also offered by the package. The software is developed in R programming language. PhenoCam GUI is a MATLAB based program which offers a GUI to define ROI and select data filtering and processing options to extract colour chromatic indices[36]. Another tool, PRACTICE, is developed to classify snow presence, which includes georectification of the images to estimate fractional snow cover[34]. The tool also has an optimization ruotine to estimate georectification parameters starting from the initial input, according to the ground control points (GCP). The python package, python-vegindex provides command line scripts for extracting vegetation indices from PhenoCam imagery[35]. The software is used in PhenoCam project to deliver standard data products which are visualised on the project web page.

Existing software packages and tools provide great features for processing time series of digital imagery. On the other hand, most software can handle image datasets which are already acquired by the user, or which have certain metadata format, or aimed for extracting only certain types of information. Some of them can be used to create near real time products but only for a specific application. Images from existing cameras and camera networks are distributed from different sources by different protocols. They have different filename formats and directory structures. To exploit the potential of existing and future camera networks to monitor environment in an operational manner with robust applications, it is crucial to develop user friendly toolboxes, establish platforms and create systems, for not only processing image datasets but also the acquisition of images from different camera networks using different protocols, processing images with a user friendly toolbox and creating operational services[8]. FMIPROT is a system and a toolbox to be used as a basis for this purpose. New features are implemented to the toolbox and processing algorithms are modified and improved in this thesis. FMIPROT acquires images from multiple camera networks, processes them and visualise the results. It can be deployed and run on the cloud using the files which it creates to store analysis configuration in, to create and maintain operational monitoring services. New processing algorithms can be added to the toolbox using the plugin system or by modifying the source code. Details of the toolbox is described in this study.

1.4 Snow cover

Snow cover has local, regional and global effects on atmospheric cycle, which are important for the Earth's climate system[38]. The surface energy balance strong depend on it because of the high albedo and low thermal conductivity of snow. It also effects the temperature, freezing and thawing of the soil and permafrost stability. Snow cover is also important in hydrology because it stores water, which is a high importance natural resource[38]. During the winter it affects the streamflow. When it melts, the rivers and reservoirs are fed by the water. Thus, it is important to monitor the snow cover. Two important parameters for snow cover monitoring are snow depth

(SD) and fractional snow cover (FSC). SD is used for the calculation of the snow water equivalent (SWE) variable, which indicated the water stored in snow. SWE can be defined as the vertical depth of the water if the snow is melted completely[38]. The unit of SWE is either millimetres or kilograms per square meters. It is calculated by the product of the snow depth and the density of the snow[39]. Since the density can change with the depth, the vertically integrated density of the snow is used. FSC also provides valuable information about the melting process and the energy balance[40]. The parameter is used in hydrology and climate models[40, 41].

There are different methods for the measurement of snow depth[38]. Manual, in-situ measurements of snow depth are commonly done either by snow sticks in a fixed location permanently or by graduated rods or rules for non-fixed measurements. The snow depth values are measured by an observer from the sticks, rods or rulers. This method is reliable, but it requires manpower[42]. Automatic measurements are done by instruments using ultrasonic or optical technology[38]. Those devices measure the distance from the sensor to the snow surface. The snow depth is calculated by subtracting the distance from the snow free ground distance to the sensor from the measured distance. Snow depth is also estimated by remote sensing methods. Microwave brightness temperature measurement from space-born passive radiometers are used in estimating SD but those sensors have coarse resolution readings and the accuracy of the methods depends on assumptions about the snowpack properties[43, 44, 45, 46, 47]. In latest years, estimation of snow depth using optical sensors on unmanned aerial systems (UAS)[48, 49] and webcams [42, 50, 51] is studied.

Snow presence on the ground is commonly observed qualitatively, for example stating if the snow exists, doesn't exists or exists on more or less than 50% of the surface[38, 52]. But the snow presence on the ground is not reported in-situ on a fractional level of percentages continuously. Finnish Environment Institute (SYKE) has about 150 snow courses that was being visited monthly and the FSC was reported by human observers[52] but they are not operational any more. Also, there is no automatic devices to report FSC. Instead, FSC is estimated for many decades using space-born instruments, including multispectral imagers and passive microwave radiometers[52, 53, 54]. Satellite derived products offer long time series of data, but they suffer from multiple challenges. Optical sensors cannot retrieve signals from the ground of dense forests, the illumination and frequency of sky-free cases in high latitudes in winter is low[52]. For microwave signals, complex terrain causes high uncertainty and the resolution of such sensors are quite low[54]. During the last decade, FSC is also estimated using optical sensors on UAS [55] and fixed cameras in various studies[9, 34, 37, 50].

1.5 Research objectives

In this study, near real time monitoring of two important parameters of snow cover, fractional snow cover and snow depth, by processing digital imagery from an environmental camera network, using specific algorithms are assessed. The study is contacted in Finland for multiple locations, using webcam images from MONIMET

camera network, taken in 2018 - 2019 season. Following research questions are discussed:

- How successful are the applied algorithms for producing snow cover information in Finland?
- Can webcams be used as a reliable data source for snow cover monitoring?
- Can the applied methods be used for operational, near real time monitoring of snow cover?
- Can the operational services be created using affordable cloud computing services?

2 Data

2.1 Webcam imagery

MONIMET Camera network image data is used for the study. 8 cameras from following sites, from south to north, are used: Tvärminne, Tammela, Hyytiälä, Värriö, Sodankylä Forest, Sodankylä Peatland, Lompolojankka and Kaamanen. The sites are chosen primarily according to the usability of the image field of views for snow monitoring, and the spatial coverage of Finland. All sites belong to the subarctic climate zone (Dfc) according to Köppen's climate classification[17]. Locations of the sites are seen in Figure 5 and Table 1.

Temporal coverage of the images is different for almost every camera used. Images taken between the dates 01.08.2018 to 30.06.2019 and times of day between 11:15 and 13:45, which corresponds to 5 to 6 images per day, are used for the study. For the operational monitoring, near real time images, taken in last one week are used. Temporal properties of the cameras are seen in Table 1.

Table 1: Cameras used in the study with their locations, temporal properties and parameters estimated from

Site / Camera	**Location**	**Studied temporal range**	**Image times of day**	**Number of images**	**Parameters estimated**
Tvärminne Landscape	59.844555°N, 23.249109°E	N/A	N/A	N/A	N/A
Tammela Ground	60.645983°N, 23.806501°E	01.08.2018 30.06.2019	11:15 13:45	969	FSC, SD
Hyytiälä Ground	61.847400°N, 24.295289°E	01.08.2018 30.06.2019	11:15 13:45	1625	FSC, SD
Värriö Ground	67.754920°N, 29.60989°E	01.08.2018 30.06.2019	11:15 13:45	1647	FSC
Sodankylä Forest Ground	67.361800°N, 26.638167°E	01.08.2018 30.06.2019	11:15 13:45	1655	FSC, SD
Sodankylä Peatland Ground	67.368517°N, 26.654483°E	01.08.2018 30.06.2019	11:15 13:45	1661	FSC, SD
Lompolo-jankka Ground	67.997393°N, 24.209355°E	01.08.2018 30.06.2019	11:15 13:45	1582	FSC
Kaamanen Ground	69.140583°N, 27.269817°E	01.08.2018 30.06.2019	11:15 13:45	1570	FSC

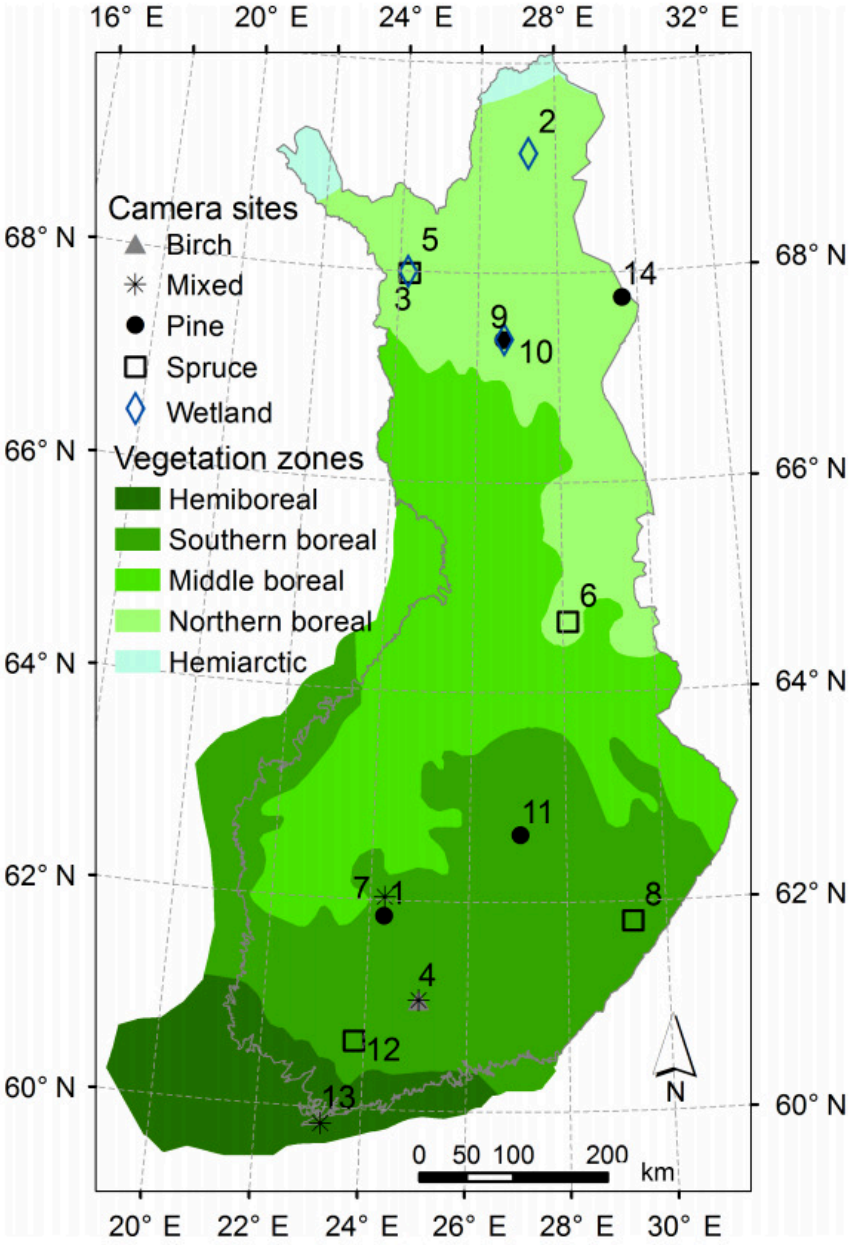

Figure 5: Map of the sites in MONIMET Camera Network, their dominant ecosystem and vegetation zones [17]. The cameras which are used in the study, from south to north, are: (13) Tvärminne, (12) Tammela, (1) Hyytiälä, (14) Värriö, (9) Sodankylä Forest, (10) Sodankylä Peatland, (5) Lompolojankka, (2) Kaamanen.

Tvärminne

Tvärminne site is located at the Tvärminne Zoological Station, which is a part of the Finnish Long-Term Socio Ecological Research network (FinLTSER)[17, 56]. The site has only one camera which has a view over the landscape towards north-west from the main building's roof. The landscape is more complex compared to the

other camera views in the study. It is at the shoreline of the archipelago, where forests, bedrocks, water surface, buildings and small flat areas at different elevation levels are visible. The camera model is Stardot NetCam SC and the image resolution is 5 megapixels. Temporal resolution of the images is 30 minutes. The camera is connected to the internet via cable network and uploads the images using FTP.

The view is not suitable to monitor snow cover using the methods in the study, but the complex terrain is the most suitable one for testing and visualizing the georectification process. In the study, visual examples are presented using the view of this camera.

Tammela

Tammela site is a part of ICP Forests level II sites[17]. Vegetation zone is southern boreal, and the dominant vegetation species is spruce (*Picae abies*). 3 cameras are installed in the site by LUKE but the camera with the crown view failed in May 2014. Multiple snow sticks are available in the ground camera view. The ground camera is used to study FSC and SD. The camera model is Stardot NetCam SC and the image resolution is 5 megapixels. Temporal resolution of the images is 30 minutes. Cameras are connected to the internet via cellular modem and uploads the images using FTP. FMI has a weather station in the site, named "Somero Salkoa."

Hyytiälä

Hyytiälä site is situated at the UHEL's Hyytiälä Forestry Field Station, which is a SMEAR II research site [17, 57, 58]. Vegetation zone is hemiboreal and the dominant vegetation species is Scots pine (*Pinus sylvestris*). Forest ground is dominated by dwarf shrubs and feather mosses. 2 cameras are installed in the site by UHEL. Multiple snow sticks are available in the ground camera view. The ground camera is used to study FSC and SD. The camera model is Stardot NetCam SC and the image resolution is 5 megapixels. Temporal resolution of the images is 30 minutes. Cameras are connected to the internet and uploads the images using FTP. FMI has a weather station near the site, named "Hyytiälä Juupajoki."

Värriö

Värriö site, which is a SMEAR I research station [17, 58, 59], is situated in Salla, eastern Lapland. Vegetation zone is northern boreal, and the dominant vegetation species is Scots pine (*Pinus sylvestris*). Forest ground has a variety of mosses, lichens and dwarf shrubs. 3 cameras are installed in the site by UHEL. The ground camera is used to study FSC and SD. The camera model is Stardot NetCam SC and the image resolution is 5 megapixels. Temporal resolution of the images is 30 minutes. Cameras are connected to the internet and uploads the images using FTP.

Sodankylä Forest

Sodankylä Forest site, which is a Class 1 site within the ICOS flux network, is situated in Arctic Research Center of FMI, in Sodankylä[17, 60]. Vegetation zone is northern boreal, and the dominant vegetation species is Scots pine (*Pinus sylvestris*). Forest ground has mosses, lichens and ericaceous shrubs. 3 cameras are installed in the site by FMI. Multiple snow sticks are available in the ground camera view. The ground camera is used to study FSC and SD. The camera model is Stardot NetCam SC and the image resolution is 5 megapixels. Temporal resolution of the images is 30 minutes. Cameras are connected to the internet via the cable network and uploads the images using FTP. FMI has a weather station in the site, named "Sodankylä Tähtelä."

Sodankylä Peatland

Sodankylä Peatland site is situated in an open fen, close to Arctic Research Center of FMI, in Sodankylä[17]. Vegetation zone is northern boreal, and it is dominated by large, treeless flarks with abundant sedge vegetation. 1 camera is installed in the site by FMI. Multiple snow sticks are available in the camera view. The camera is used to study FSC and SD. The camera model is Stardot NetCam SC and the image resolution is 5 megapixels. Temporal resolution of the images is 30 minutes. Cameras are connected to the internet via the cable network and uploads the images using FTP. FMI Arctic Space Centre has a weather station near the site, named "SUO0003 Station."

Lompolojankka

Lompolojankka site is an open mesotrohic sedge fen, which the camera field of view is mostly the drier part, dominated by dense stands of *Betula nana*[17, 60, 61, 62]. The site is part of ICOS network, where air and soil meteorology parameters are continuously measured. The site has one camera, which is used to study FSC. The camera model is Stardot NetCam SC and the image resolution is 5 megapixels. Temporal resolution of the images is 30 minutes.

Kaamanen

Kaamanen site is an open mesotrophic fen situated in Inari[17]. Vegetation zone is northern boreal, and the site has a surface pattern consisting of wet flarks and drier strings. 1 camera is installed in the site by FMI. The camera is used to study FSC. The camera model is Stardot NetCam SC and the image resolution is 5 megapixels. Temporal resolution of the images is 30 minutes. Cameras are connected to the internet and uploads the images using FTP.

2.2 Weather station data

In-situ snow depth observations are used for the validation of the snow depth estimation. The data is provided by FMI and it is under open data policy. The

observations are done by automatic weather stations. Provided format for the data is the common comma separated value. Unfortunately, not all the stations are in the exact same field as the corresponding camera. Three of the cameras used for SD estimation has a field of view over the forest ground, whereas the terrain where the station is more open. For the validation, this situation is considered as it is expected that the snow depth on the forest ground would be less than the snow depth in the relatively open fields. In Table 2, coordinates of the cameras and weather stations used for the SD estimation and the distance between them are reported. In Figure 6, the locations for Hyytiälä and Sodankylä Forest sites are shown on Google Earth imagery.

Table 2: Camera locations used in snow depth estimation and corresponding weather station locations used for validation.

Site name	**Camera location**	**Weather station location**	**Distance**
Tammela	60.645983°N, 23.806501°E	60.64668°N, 23.80559°E	94 m
Hyytiälä	61.847400°N, 24.295289°E	61.84591°N, 24.28696°E	470 m
Sodankylä Forest	67.361800°N, 26.638167°E	67.36663°N, 26.62901°E	665 m
Sodankylä Peatland	67.368517°N, 26.654483°E	67.36707°N, 26.65117°E	222 m

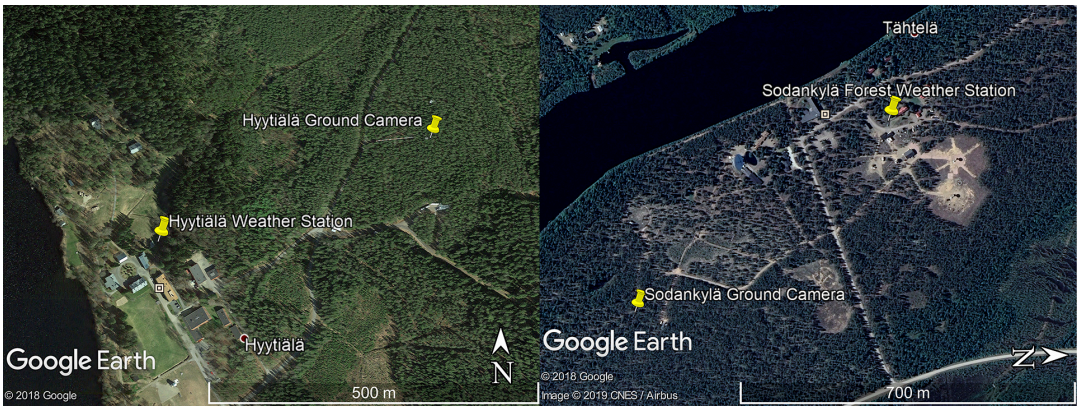

Figure 6: Locations of the cameras and weather stations on Google Earth imagery for Sodankylä Forest and Hyytiälä sites

2.3 Elevation data

Digital elevation model (DEM) data is used for georectification of the webcam imagery. The data is provided by National Land Survey of Finland. The data is open and free. The data is downloaded from the NLS pages on Kapsi Internet-käyttäjä [63] [64].

2 m resolution DEM is derived from laser scanning data. The grid size is 2m to 2m and the point density is at least 0.5 points/m^2. The data is in gridded text format. This data is not available for whole of Finland and it is used for all the sites with FSC study, except Kaamanen and Lompolojankka. 10 m resolution DEM is available for whole of Finland and the accuracy of the data 1.4 m. The data is in XYZ text format. This data is used for the Kaamanen and Lompolojankka site, since 2 m resolution data is not available. [63]

Visible comparison of two DEM datasets can be seen in Figure 7. The datasets are visualised using VTK, rendered from Tvärminne camera perspective.

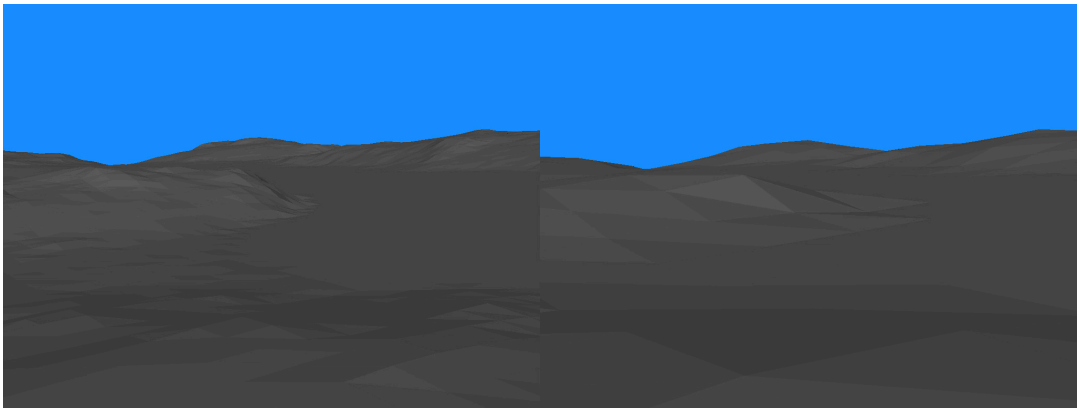

Figure 7: 2m (left) and 10m (right) resolution DEM rendered from Tvärminne Camera perspective

2.4 Auxiliary data

Satellite data from Google Earth is also used for the estimation and validation of camera orientation parameters. In the data, landmarks and their coordinates are used. Data source is reported by Google Earth for the following sites:

- Tvärminne: Landsat/Copernicus, Maxar Technologies, 2019.
- Sodankylä Peatland: CNES/Airbus, 2019.
- Lompolojankka: Maxar Technologies, 2019.
- Kaamanen: CNES/Airbus, 2019, Maxar Technologies, 2019.

3 Methods

3.1 Image processing system

FMIPROT is a toolbox for processing images from multiple camera networks, for vegetation phenology and snow cover monitoring. The toolbox itself is a processing system which includes acquisition and processing of the images and visualization of the results. The development of the toolbox has started with the project MONIMET, to process images from MONIMET camera network, and later it evolved into a system which supports acquisition from other camera networks.

The software is open source and it can be run on PCs and servers, which allows the user to create automated processing chains for operational monitoring. Multiple algorithms are implemented for processing images, but it also supports implementing more algorithms by user, either by modifying the code or by the integrated plugin system. The toolbox can be used with minimal computer skills as all features are available to use on a GUI, on Windows and multiple distributions of Linux. Latest version of the toolbox has the following features:

- Image acquisition from multiple camera networks
- Storing scenario options as files
- Generating HTML reports for scenario options and analyses results
- Multiple scenarios
- Multiple analyses in each scenario
- Mask/ROI creation by selection with GUI
- Filtering images and pixels according to different means of thresholds
- Downloading and handling images
- Quantitative image archive check
- Expandable algorithms by the plugin system
- Customizable plotting/mapping of results
- Windows and Linux support
- Configuring settings and running analysis from command line interface
- 3D Georectification preview tool to estimate and validate camera parameters

Following processing algorithms are available in the toolbox:

- Colour Fraction Extraction: Calculates fraction indices of the colours (also known as colour chromatic coordinates) using average values of DNs inside the ROI and also provides statistics of the DNs.

- Vegetation Indices: Calculates different vegetation indices using average values of DNs inside the ROI. The indices include green fraction index, red fraction index, green-red vegetation index and green excess index.
- Custom Colour Index: Calculates a custom colour index which its mathematical formula is entered by the user. The formula can include basic operations: sums, differences, multiplication and division. Parentheses are also used to indicate operation priority. Colour values are the average values of red, green and blue channels in ROIs.
- Snow cover fraction: Calculates FSC in the ROI, using the algorithm which is described in this thesis. It also provides the fraction of coverage without using the georectification.
- Snow depth: Calculates SD using a pole-like object in the image, which is selected as the ROI, using the algorithm described in this thesis.
- Time lapse animation: Creates a time-lapse animation by using the webcam images from a camera.
- Radial lens distortion correction: Corrects distorted camera images which has barrel type lens distortion using the algorithm described in this thesis and produces undistorted images.

All the features of the program are accessible by the GUI. It allows the user to manage the defined camera networks, change program settings, set up and save analysis options, download images, generate reports, start the processing chain, plot results, follow the log, manage plugins and use the georectification preview tool. The usage of the GUI is explained in the user manual in detail and tutorials are also available in the web page [32].

The software is coded in Python language. It runs in a loop initiated by a *Tkinter.Tk class instance*, just after the definitions of resources (e.g. storage directories, program configuration settings) and algorithm functions. Every call after that is done inside that loop. The loop waits for an input from the GUI to make that calls. The calls include updating the GUI, creating setups, saving setups, loading setups, changing configurations, running the processing chain, plotting results etc. After the calls are done and processes are completed, the loop turns back to the start to wait for input from the GUI, until the program is terminated. A simplified version of that workflow is illustrated in Figure 8. The program also can be run in "no-gui" mode, which the GUI library is not loaded, and the program directly goes into processing chain and exists when the chain is completed. This mode is intended for running scheduled analysis, for operational monitoring.

The processing chain is run according to the program settings and analysis options. Program settings include the choices like the directories for the images and results to be stored into, whether if the images should be downloaded from the repositories or not, using proxy for the connections, camera network parameters etc., which are the general options for using the program. On the other hand, analysis options are unique

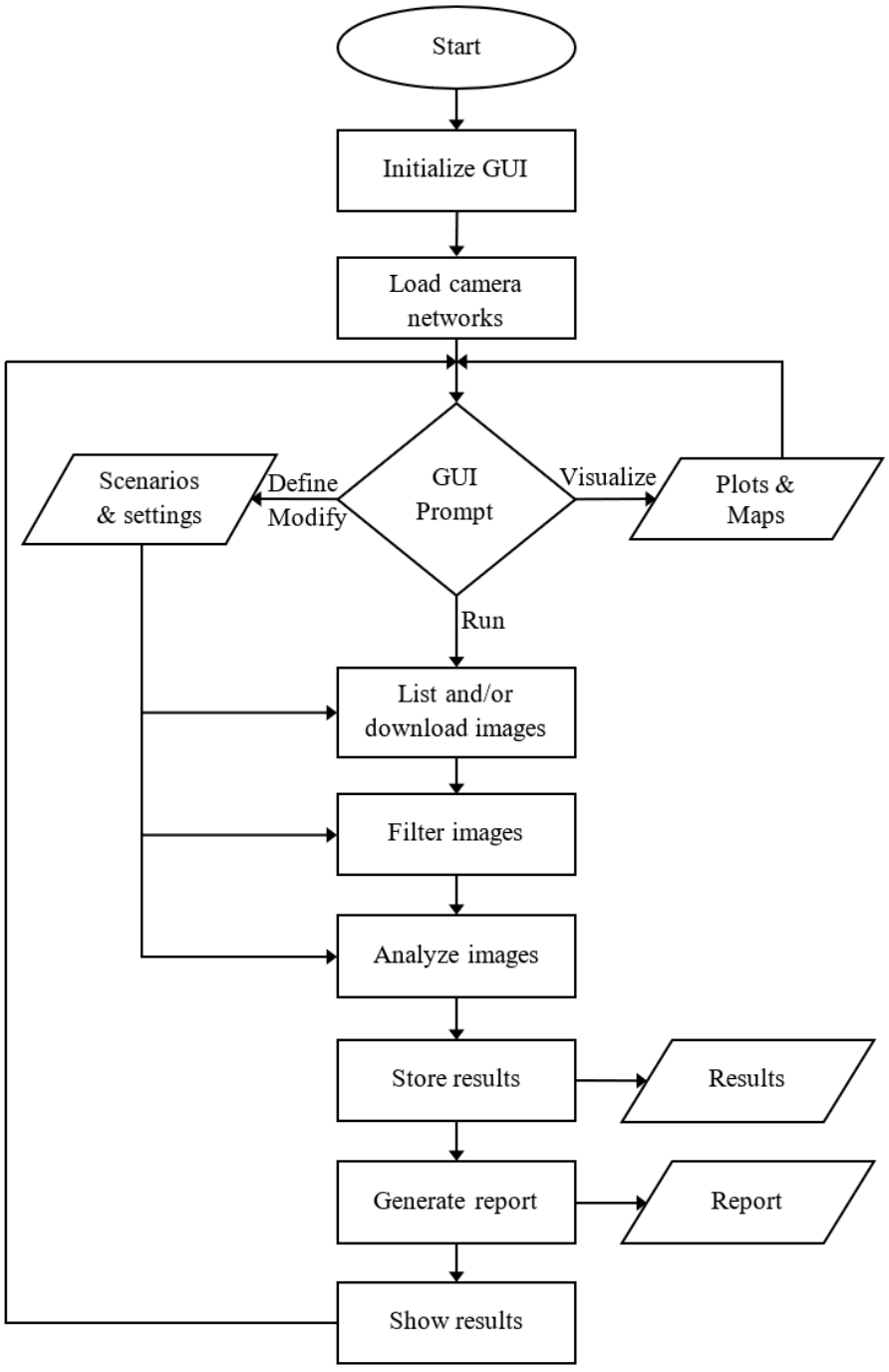

Figure 8: Simplified workflow of the program

for every study or operational monitoring. The concept of "setup/scenario/analysis" is designed to define and store those options for analyses to be done using images from multiple cameras and camera networks, in a systematic way. In this concept, a setup is the collective of all parameters which are kept in the memory of the program at once. A setup includes multiple scenarios, which a single camera and certain

parameters to refine which images to be used from that camera are chosen for each of them. A scenario includes multiple analyses to be done using the images obtained according to the scenario parameters. A setup can be saved in a file and then can be loaded back to the program to work with the same options. The structure is illustrated in Figure 9. The concept allows the user to create scheduled processing chains for operational monitoring. A setup can be created using GUI in a PC and then it can be scheduled to be called with the program in the cloud. When the program is directed to store the results in the same directory with each call using the exact same setup file, it checks the results that are produced before and runs the processing chain only for the images that are not processed yet. After the processing, it merges the results with the results for the older ones. This way, analyses of time series of images for long time intervals (e.g. one year) can be updated in much shorter time periods (e.g. hourly).

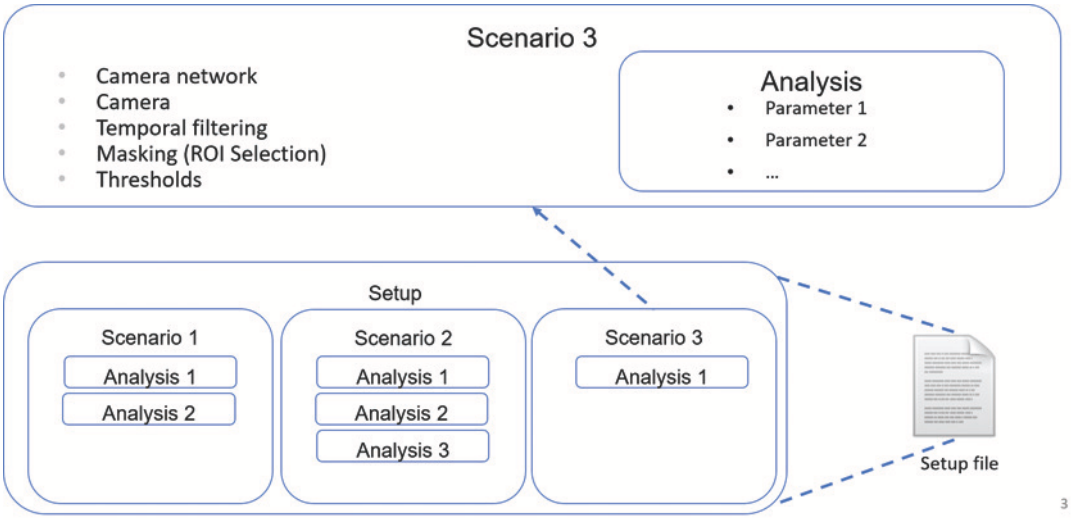

Figure 9: Setup/scenario/analysis concept structure

The output of the analyses is stored using simple and common file formats. For each run, the program saves a copy of the setup file and a report file in the results directory. Using the setup file, all the parameters in the setup can be viewed in GUI. The report file is in HTML and JS format. It is made of tables which the contents of the setup are reported and the time series results are visualised in plots and animations in videos. For each analysis that results in time series data, the program creates two text-based data files; in *tab separated values* (TSV) format and *comma separated values* (CSV) format. TSV files are visualised in GUI and CSV files are visualised in the HTML report. For each analysis that results in multi-dimensional arrays of data (e.g. images, maps) a *hierarchical data format* (HDF) file is created. For each analysis that results in a video animation, a video file is created. For each data file, a metadata file is created which includes information about the data file, such as the names of the parameters, camera name, analysis name, scenario name, dataset names etc. For each text-based data file and video animation, HTML files only showing the visualisation of the results are also created so that those can be

used without the extra information for the presentation of the results.

3.2 Camera Networks

The concept of camera networks used in the study is the collective of different camera groups, which consists of one of more cameras that belongs to an institution, collective, person, company, project or a similar entity. The cameras do not have be connected to each other physically or virtually, by any technology or device. Very existence of the cameras is the camera network, if they produce time series images. Even in the case that produced images are copied into a disk or computer, the camera can be used in this concept.

Generally, existing camera networks, especially environmental ones, have multiple cameras connected to a central infrastructure over the internet, where data is stored and maintained by the responsible entity. For example, MONIMET cameras are connected to internet by cable or cellular modems and they use FTP to upload images directly to FMI servers, or to other partners' servers, to be relayed to FMI servers. The data is disseminated through authenticated FTP connection and thorough the repositories in Zenodo website, by HTTP. The infrastructure and the protocols to store, maintain and disseminate the data may differ in different camera networks. Supporting different variations of the camera networks is achieved by using "camera network information file" (CNIF), a configuration file which keep the parameters of a camera network. The file includes the information needed to acquire the images, such as communication protocol, host address, filename format etc. for each camera in the network. The file is created and modified automatically by using FMIPROT GUI. Doing that, a camera network is defined in the toolbox. The format of the file is described in FMIPROT user manual, so that it can be created and modified programmatically, when needed. An entity can create and update such a file for users to easily use their camera data with FMIPROT. For example, MONIMET CNIF is hosted in FMIPROT website along with a short tutorial on how to use it. Using the CNIFs, FMIPROT can be used to multiple camera networks at once. Multiple camera networks with different configurations connected to FMIPROT is illustrated in Figure 10.

3.3 Cloud processing

Operational monitoring system is set up using cloud processing. FMIPROT is installed on a dedicated server provided by FMI. In the server, Debian operation system is installed along with the libraries required by FMIPROT. The scenarios used in the study are saved as separate setups so that when there is a problem in the processing chain, others are not affected, and it is also easier and safer to fix the problems.

The FMIPROT setups for the operational monitoring are prepared in a PC and uploaded to the server. Instead of the historical data, "latest one month" of images are selected in the setups for the operational monitoring. For the time of the day of the images, a larger window is selected, from 09:15 to 14:45. In addition, brightness

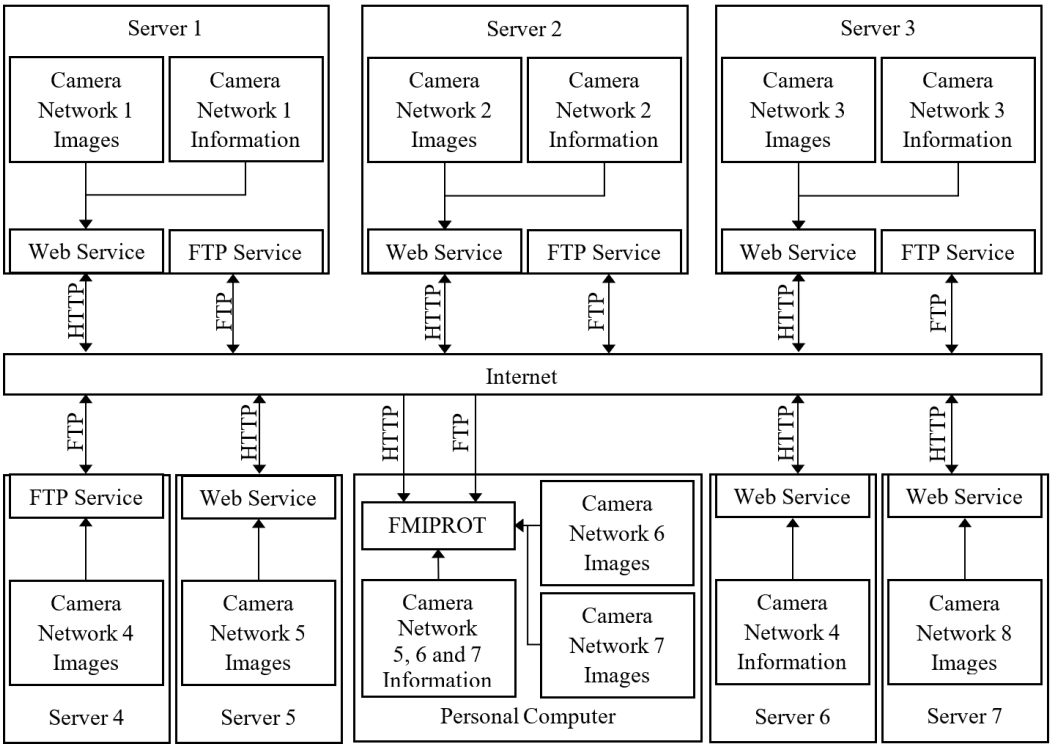

Figure 10: Multiple camera networks with different configurations connected to FMIPROT[8]

threshold is set up to 0.1 to filter out dark images taken in the winter mornings and evenings. Also, timelapse animation creation is added as an extra analysis for each scenario, so that the images can be seen as an animation alongside the results. All the setup parameters for the operational monitoring in given in the setup reports in Annex D.

For a more organized system, an additional script is written to call FMIPROT to run the setups from the job scheduler. This script also checks if the setups are already running because depending on the number of images and algorithm, previous runs may not have been finished when attempting another run. Scheduler is set to run the scripts every half an hour to check new images and analyse them. The script takes the directory which the setups are stored in, the directory which the results will be stored in, and the version of FMIPROT client or code that will be called. The version option is created so that different versions of the code or client can be used with different setups in the server. This provides the flexibility and safety when deploying and running multiple setups, as an update in the code or client may lead to a crash in the existing processing chains. That way, measures can be taken before changing the code and/or the processing chains, without breaking them. Optionally, a single setup in the directory can also be chosen to be run as an argument in the script. The script follows the procedure to call FMIPROT:

1. Activate the virtual environment and/or define any other environment variables

required by the operation system and/or libraries

2. List the setup files in the setup directory provided
3. Check if the setup directory exists, if not, exit the script
4. Check if file indicating the setups are already running exists, if it does, exit the script
5. Create an empty file with the setup directory name to indicate the setups in the folder are running
6. Check if a name is provided to run a single setup
7. List the setup files according to the previous step
8. Call the code for each setup file
9. Remove the empty file which is indicating the setups are running

The server is also set up to reach the results from the web. Result directories are set up in the processing chain so that the results are saved in a directory where can be reached from the web page domain, which is the website of FMIPROT: http://fmiprot.fmi.fi. In the website, a page is created for the operational monitoring to reach the results.

3.4 Snow cover detection algorithm

Snow cover detection in pixel level for estimating FSC is done by using an adaptive thresholding algorithm[37]. It is based on the statistical distribution of the reflectance of the surface, as the snow-covered area should have high reflectance compared to the snow-free area, but the reflectance difference in digital values (DN) changes with the total irradiance. The algorithm defines a threshold value for the DN of the pixels, according to the histogram of the DN. The first local minimum in the histogram which is higher than 127 is chosen as the threshold. This situation ideally occurs in the partial snow coverage case. If no local minimum is found, which is probably the no-snow or full-snow case, DN 127 is selected as the threshold. Then, the pixels with higher DN than the threshold are determined as snow covered and vice versa. The algorithm is applied on the values in the blue channel of the images. The histograms are extracted only within the ROI, not the whole image, and smoothed by averaging the 5 nearest points for each data point.

In the application of the algorithm, few modifications are done. Because of the fixed white balance and auto exposure settings of the cameras, distribution of the DN changes also according to the lightning conditions. In the original algorithm DN 127 is used as a starting point for the decision of the threshold because it is assumed that the snow covered pixels have a DN higher than 127 in blue channel[37], which is the middle point of the histogram. But it is seen in the images that the maximum value of DN in blue channel not only changes with the snow cover, but also with

the lightning, causing a shift in the extent of the histogram, thus the middle point. Especially for low or no snow cover cases, the maximum value of DN in the blue channel is much lower than the red and green channels. If the middle point is selected as 127 or the half of the maximum DN in the blue channel in those cases, then the classification would be incorrect. As the solution, the extent of the histograms are decided using all three channels, which is to be between 0 and the maximum value of the DN in all three channels. Then, the middle point is calculated as the middle of that extent. The remaining part of the decision of the threshold is still done with only the blue channel histogram. Also, pixels with DN 255 in any channels are filtered out using FMIPROT. One reason for that is a saturated pixel can be assumed have incorrect value and the other reason is that such a case may lead to the decision of the histogram extent incorrectly.

In Figure 11, one example for no snow, full snow and part snow is shown cases are shown with the original images and ROIs, blue channel histograms of the ROIs, calculated thresholds, and classified snow masks. The masked pixels inside the ROI in image (d) are the burned pixels, which have DN 255 in any of the channels.

3.5 Georectification of webcam imagery

The snow cover detection algorithm determines only if a pixel is snow covered or not but calculating FSC also requires the georectification of the images, since the ground resolution of the pixels in an image with oblique view is different for each pixel. Georectification of the image registers each pixel on the image to a point in the real world. Using that information, relative resolution of each pixel is found by calculating how much of the area in the real world corresponds to the same pixel in the image. After calculating the resolution of each pixel in the ROI, FSC can be calculated by using that "weight mask." The weight mask is calculated only once for an analysis, as it will be same for all the other images from the same camera with same ROI. In Figure 12, main steps for the calculation of fractional snow cover with snow cover detection and georectification is illustrated with an example image.

Perspective projection

The georectification of the camera images are done by an operation called perspective projection [65]. This operation is applied to the DEM data points after transforming the coordinates to the camera space. Then, perspective projection maps points in a 3D camera space to a 2D image plane. First, real world coordinates of the DEM data points are shifted to so that the camera is at the origin using Equation 1,

$$\begin{pmatrix} P_{tx} \\ P_{ty} \\ P_{tz} \\ 1 \end{pmatrix} = \begin{pmatrix} 1 & 0 & 0 & -C_x \\ 0 & 1 & 0 & -C_y \\ 0 & 0 & 1 & -C_z \\ 0 & 0 & 0 & 1 \end{pmatrix} \begin{pmatrix} P_{wx} \\ P_{wy} \\ P_{wz} \\ 1 \end{pmatrix} \tag{1}$$

where P_{ti} are the transformed coordinates, P_{wi} are the original coordinates in the real-world space, and C_i are the coordinates of the camera. Then, the viewing

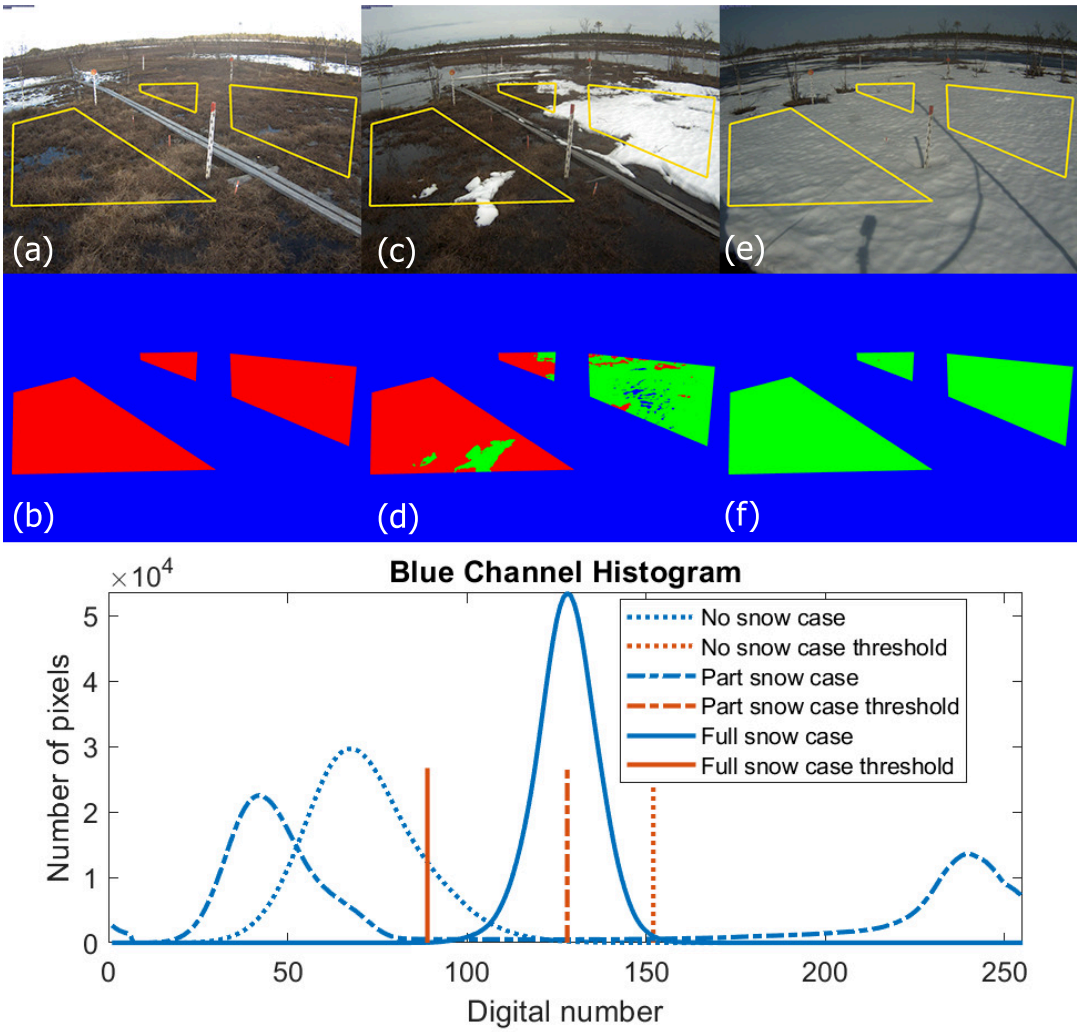

Figure 11: Snow cover detection examples for three cases from Sodankylä Peatland camera: (a) No snow case image and ROI, (b) No snow case snow mask, (c) Part snow case image and ROI, (d) Part snow case snow mask, (e) Full snow case image and ROI, (f) Full snow case snow mask, (g) Blue channel histograms and thresholds for those three cases. Colours for snow masks: Green - Snow covered pixels, Red - Snow free pixels, Blue - Masked pixels

transformation is applied using Equation 2,

$$\begin{pmatrix} P_{cx} \\ P_{cy} \\ P_{cz} \\ \omega \end{pmatrix} = \begin{pmatrix} U_x & U_y & U_z & 0 \\ V_x & V_y & V_z & 0 \\ N_x & N_y & N_z & 0 \\ 0 & 0 & 1/f & 1 \end{pmatrix} \begin{pmatrix} P_{tx} \\ P_{ty} \\ P_{tz} \\ 1 \end{pmatrix} \tag{2}$$

where P_{ci} are the coordinates in the camera space, P_{ti} are the coordinates from the previous operation, f is the focal length, w is a scaling factor of the projection, N is the direction of the camera unit vector, V is the unit vector showing which way is up (view up), and U is the unit vector orthogonal to both N and V. The vectors

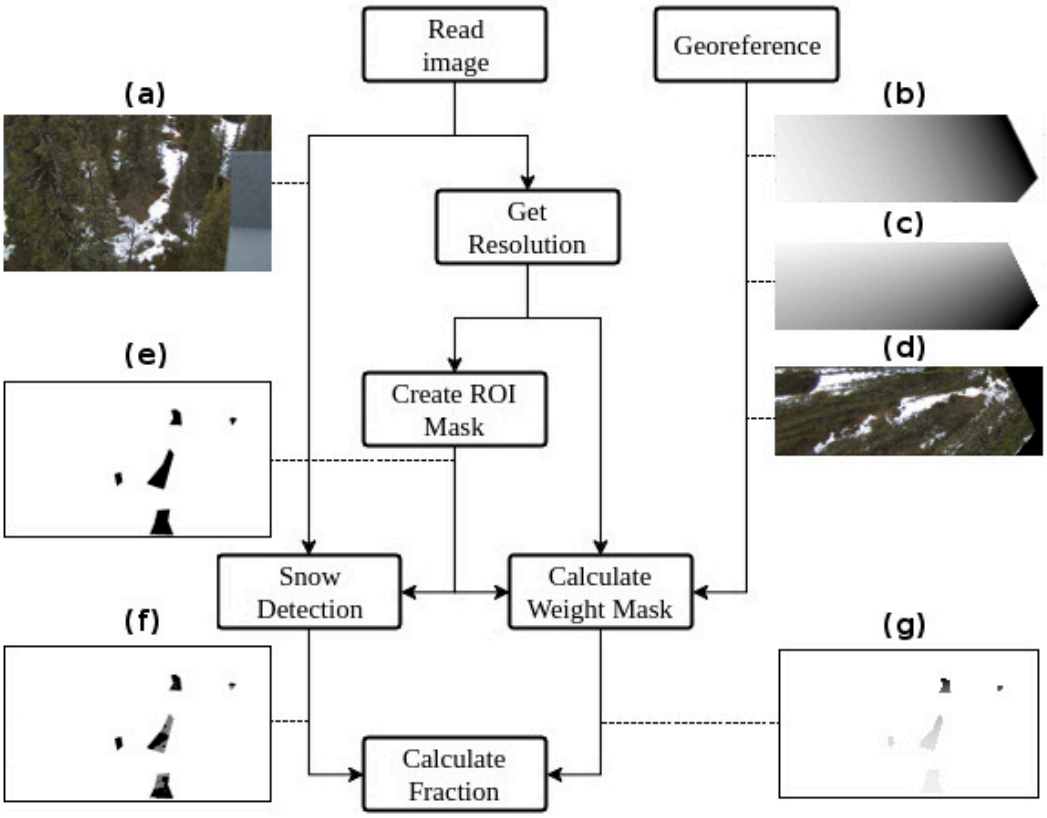

Figure 12: Main steps of FSC estimation[9]: (a) Webcam image; (b) Image pixel coordinates in y axis in the spatial grid; (c) Image pixel coordinates in x axis in the spatial grid; (d) Webcam image projected onto the spatial grid; (e) ROI mask; (f) Snow—no-snow in the ROI; and (g) Weightmask in the ROI.

N, V and U are calculated from the orientation parameters of the camera. Those parameters are the target direction (yaw, heading), the vertical direction (pitch) and the horizontal direction (roll) angles. The target direction is the geographical view direction of the camera, which is parallel to the ground. The angle is defined so that north is zero degrees and the it increases toward east, south, west and then back to north. Vertical direction is the angle between the camera direction vector and the plane parallel to the ground. The horizontal direction is the angle between the plane parallel to the ground and the vector orthogonal both to the camera direction vector and the plane parallel to the ground. Those angles are illustrated in Figure 13. Orientation parameters of the cameras used in the study are given in Table 3.

The vectors N, V and U are calculated using Equations 3,4,5 and 6,

$$N = \begin{pmatrix} \sin(y)\cos(p) \\ \cos(y)\cos(p) \\ -\sin(p) \end{pmatrix} \tag{3}$$

$$U_o = \begin{cases} N \times \frac{N_{xv}}{|N_{xy}|} & \text{if } N_z > 0 \\ \frac{N_{xy}}{|N_{xy}|} \times N & \text{if } N_z < 0 \end{cases} \tag{4}$$

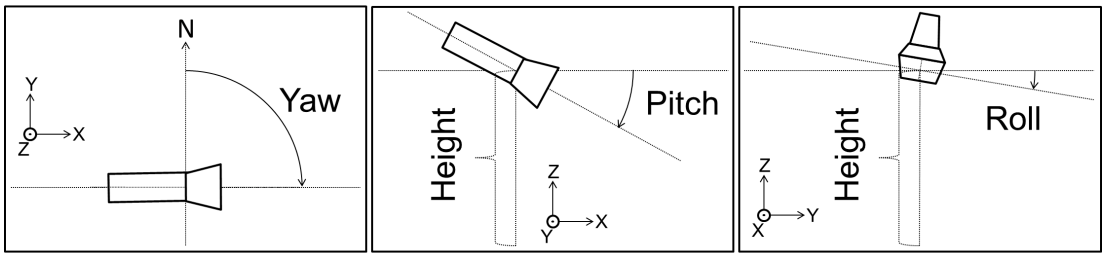

Figure 13: Camera orientation parameters: The target direction (yaw, heading), the vertical direction (pitch) and the horizontal direction (roll) angles

Table 3: Camera georectification parameters

Site / Camera	**Height**	**Yaw**	**Pitch**	**Roll**	**Focal length**	**Scale factor**
Tvärminne Landscape	16.10 m	306.0°	6.7°	-3.0°	4 mm	0.90
Tammela Ground	4.00 m	90.0°	23.3°	-1.0°	4 mm	0.77
Hyytiälä Ground	4.30 m	111.0°	42.0°	0.0°	4 mm	0.82
Värriö Ground	3.50 m	320.0°	30.0°	0.0°	4 mm	1.00
Sodankylä Forest Ground	2.46 m	96.0°	35.3°	0.0°	4 mm	0.74
Sodankylä Peatland Ground	2.08 m	23.4°	18.0°	-2.0°	4 mm	0.69
Lompolojankka Ground	2.50 m	341.0°	17.0°	3.0°	4 mm	0.7
Kaamanen Ground	2.60 m	55.5°	12.0°	-1.0°	4 mm	1.24

$$U = \frac{U_o + \begin{pmatrix} 0 \\ 0 \\ -tan(r) \end{pmatrix}}{\left| U_o + \begin{pmatrix} 0 \\ 0 \\ -tan(r) \end{pmatrix} \right|} \tag{5}$$

$$V = U \times N \tag{6}$$

where y is the yaw, p is the pitch and r is the roll angles. After the transformation, perspective projection is applied using Equations 7 and 8,

$$P_{px} = \frac{2fP_{cx}}{wP_{cz}} \tag{7}$$

$$P_{py} = \frac{2fP_{cy}}{wP_{cz}} \tag{8}$$

where P_{pi} is the coordinate in image plane and P_{ci} are the coordinates in the camera space.

The operation is applied to all points in the DEM data. As a result, a mapping of the real world coordinates to image plane coordinates is obtained.

Viewshed

The georectification algorithm calculates the corresponding pixel location for every point on the DEM. The image plane is two dimensional, but the actual perspective has a third dimension, which is the depth. The camera does not capture the depth as the third dimension, but the points that are visible in an image are the ones that has are the closest to the camera in the third dimension. From the position of the camera, the points that are behind a closer point on the surface of the DEM are not visible on the image, as there are not photons reaching to the camera from those points. The distribution of the visibility around a viewpoint is called viewshed [66]. Viewshed of the camera should be calculated for all the points on DEM so that the invisible points can be excluded from the georectification process.

Viewsheds for the cameras are calculated with an algorithm using reference planes[66]. The algorithm was developed as a solution to the computer time consumption of the many algorithms that are using sight lines, which is why it is preferred for the toolbox and the study. The algorithm defines reference planes that passes through the viewpoint and adjacent points. The base idea is that if a point further away in the direction of those adjacent points is visible, than it should be above this reference plane. For each point in the DEM, the visibility of the point is decided according to that idea and the reference plane defined for each point. The viewshed for Tvärminne Landscape Camera is shown in Figure 14 as an example. In the Figure, elevation raster, coloured from blue to yellow, is overlaid on Google Earth imagery and invisible locations according to the calculated viewshed are masked as red. The camera location is shown with a yellow pin icon. The camera is 16.10 m above the ground. Maximum and minimum elevation in the raster are 0 m (blue) and 18.60 m (yellow).

Simulation of camera model with VTK

Instead of calculating each matrix in the georectification algorithm using the mathematical relations, The Visualization Toolkit (VTK) libraries are used. VTK is an open source library for computer graphics, which is mostly used with scientific data [67]. One of the basic features of VTK is rendering 3D data to be drawn onto computer screen, viewed from a perspective, which can be used as the simulation of a camera capturing images over a terrain. In this simulation, the perspective projection is done by using the properties of the "camera" class in VTK. When a camera class in VTK is initiated with the camera specific and camera orientation parameters, it provides all the transformation matrices for the camera. The camera class also

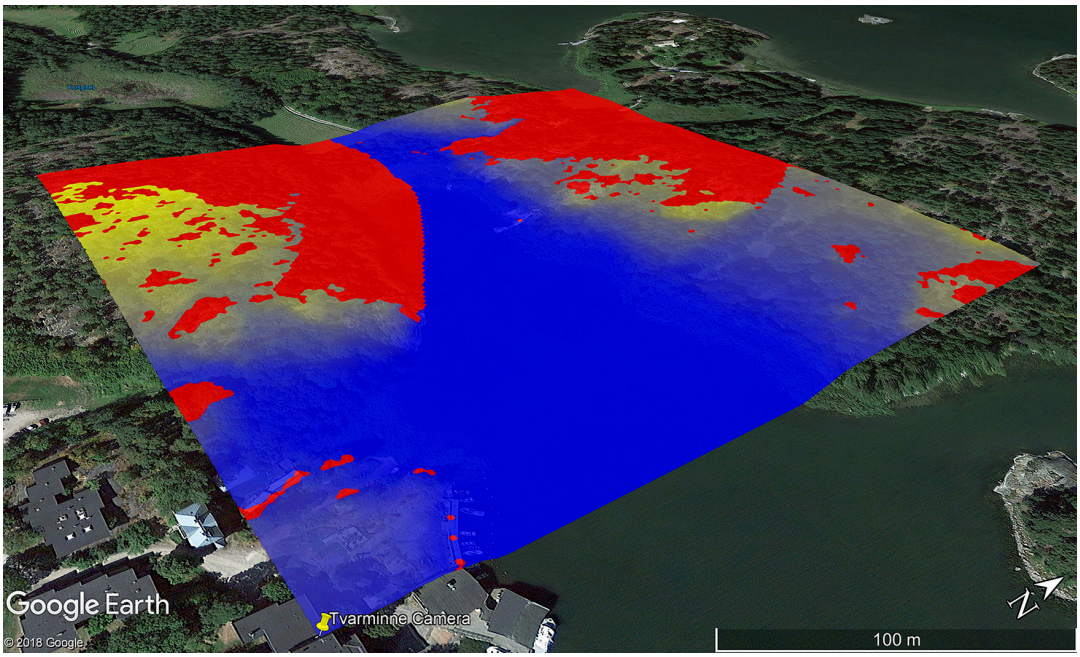

Figure 14: Elevation and the viewshed around Tvärminne Landscape Camera overlaid on Google Earth imagery. (Blue to yellow: elevation where visible, red: not visible)

provides a composite matrix which can be used to convert world coordinates to image pixel coordinates directly. This matrix is called "Composite projection transform matrix" in the library and using the composite matrix, pixel coordinates for each point in the DEM is directly calculated by Equation 9,

$$\begin{pmatrix} P_{px} \\ P_{py} \\ P_{pz} \\ 1 \end{pmatrix} = M \times \begin{pmatrix} P_{wx} \\ P_{wy} \\ P_{wz} \\ 1 \end{pmatrix} \tag{9}$$

where P_{wi} are the real-world coordinates, P_{pi} are the image coordinates and M is the transformation matrix.

Georectification preview tool

Measurement of the camera orientation is required for the georectification, but it may not always be available. The camera may be in a remote location where travelling to may not always possible. The camera may be destroyed, moved or removed after obtaining images, without the measurements. Even when there is a measurement, it is subject to error. Also, zoom of a camera is not measurable and not always reported by the camera software. For the georectification process, the parameters of the camera should be as correct as possible. For that matter, a tool is designed and integrated into the toolbox to estimate, fix and validate the camera specific and camera orientation parameters. Georectification preview tool is designed using VTK libraries. For such a simulation using the library, three elements are required: The

data, the camera and the interactor.

The data to be rendered is generated from the DEM. Original DEM data is point data, which is the elevation value for each location in the area. VTK supports point data but rendering points in space does not result in visible surfaces. First, a surface-like object should be created using DEM data. After the DEM data is interpolated into desired resolution, VTK Polydata model is used to create a mesh of the terrain surface. The mesh is "knitted" by creating triangles with the DEM data points, including X and Y components, so that it is placed into the data space with the real coordinates. The mesh of the terrain surrounding the field of view of Tvärminne landscape camera is shown in Figure 15 as an example.

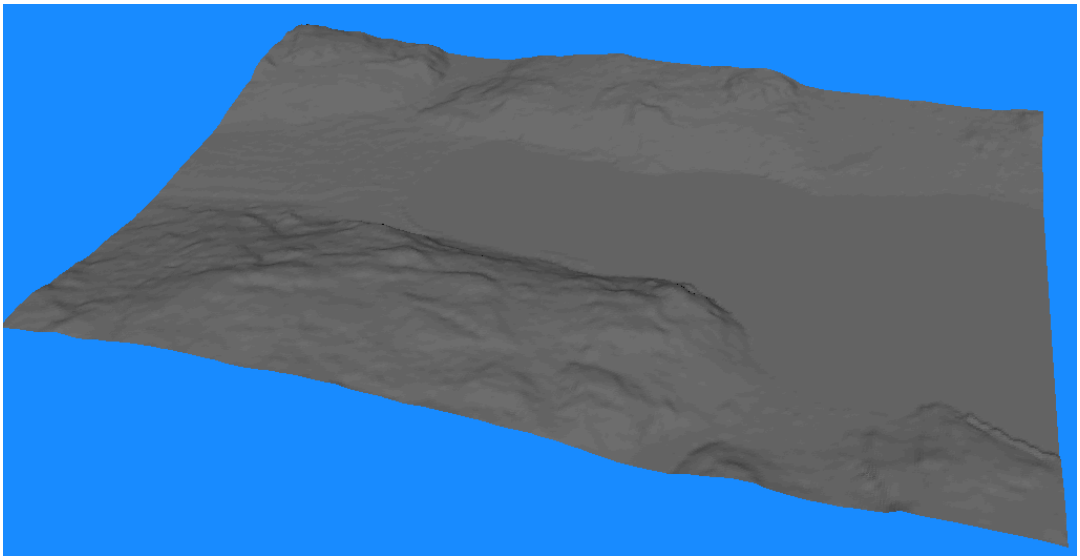

Figure 15: The mesh of the terrain surrounding the field of view of Tvärminne landscape camera

The camera class in VTK has many properties, but 5 of them are necessary to correctly place the camera in the data space:

1. Position
2. Focal point
3. View up vector
4. Roll (horizontal direction)
5. Zoom (scale factor)

Position, roll and zoom properties can directly be set, but the focal point position and the view up vector should be calculated from the orientation and camera specific parameters, as described in the previous section. When those properties are set, the renderer draws the terrain from the camera view position and direction. The

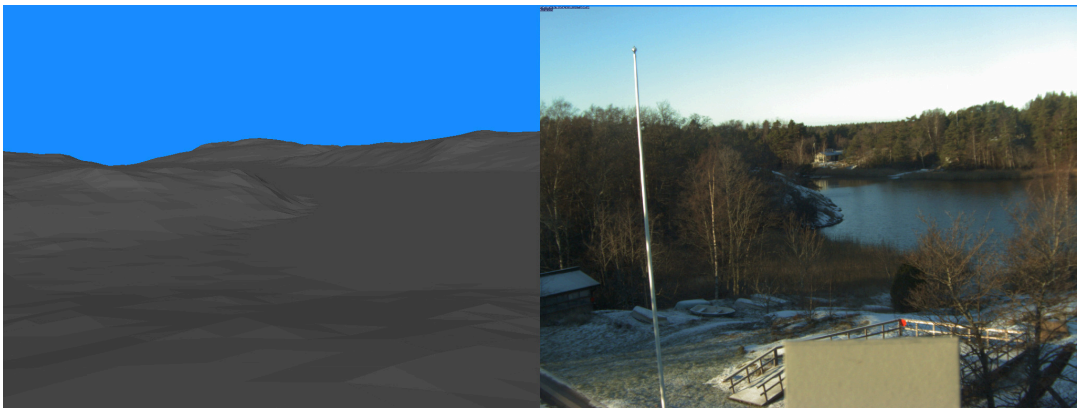

Figure 16: The terrain surrounding the field of view of Tvärminne landscape camera seen from the camera position and view direction (left) and an example camera image from the same camera (right)

same data in Figure 15 is seen with the camera parameters of Tvärminne landscape camera and an example camera image from the same camera is seen in Figure 16.

The interactor class allows the user to interact with the renderer, such as triggering an event when the user clicks on the renderer without, move the pointer over, press a button etc. The purpose of the tool is to see the change in the view when camera parameters are changed and get information about points on the surface, such as the real word coordinates, image pixel coordinates, distance to camera etc. so that use some control points to find the correct camera parameters. For that, the interactor class is coded so that when the mouse pointer is over a point on the surface, report some information about the point. A transparent copy of the preview image is also added to the renderer so that the points on the surface can be inspected according to the landmarks and the image can be compared visually. In Figure 17, the preview can be seen for the same camera and camera view in Figure 16, with the information about the point at the right corner of the terrace in the view.

The interactor also creates a dialog when a point on the window is clicked. In this dialog, camera parameters can be changed. When the changes are applied, the renderer changes the view of the camera accordingly in the renderer window. In the new view, the perspective and the control points are checked again to see the improvement in the error. If there are enough landmarks on the view, one can even find the camera parameters by using the tool and the control points which can be extracted from a satellite image. Google Earth is used to extract such control points for some cameras in the study: Lompolojankka and Kaamanen.

Lens distortion correction

It is visible from the images that the images from some of the cameras has systematic distortions in the image. Easier to notice over the horizon line, the points in the images are shifted in a radial direction, towards the centre of the image. This type of distortion is called barrel distortion, which is commonly seen in wide angle lenses

Figure 17: The preview can be seen for the same camera and camera view in Figure 16, with the information about the point at the right corner of the terrace in the view.

[68]. The distortion is modelled by Equation 10:

$$r_u = r_d \left(1 + k r_d^2\right) \tag{10}$$

where r_u is the distance from the pixel to the centre of the distortion in the undistorted image, r_d is the same distance in the distorted image, and k is the lens specific coefficient [69]. The distances are calculated by Equation 11,

$$r_i = \sqrt{(x_i - x_0)^2 + (y_i - y_0)^2} \tag{11}$$

where x_i and y_i are the normalised coordinates of the pixels and x_0 and y_0 are the normalised coordinates of the centre of the distortion and r_i is the distance of the pixel to the centre of the distortion [69]. Equation 10 indicates that a part of the normalised coordinates of the undistorted image will be bigger than 1.0, which means some of the points will not be mapped into the corrected image. The size of the lost area is dependent on the coefficient k, specific to the lens. That situation can be seen in the example in Figure 18. Lens correction coefficients for the cameras are found empirically, and given in Table 4.

Radial lens correction algorithm is integrated into the functions of the georectification algorithm, which is integrated into the functions of the fractional snow

Figure 18: Radial lens correction: Image from Sodankylä Peatland camera, taken on 02.08.2018 (left) and the undistorted image produced with the algorithm applied with $k = 0.13$ (right).

Table 4: Lens specific correction coefficients for the cameras used in the study

Site / Camera	**Lens correction coefficient**
Tvärminne Landscape	0.025
Tammela Ground	0.000
Hyytiälä Ground	0.025
Värriö Ground	0.080
Sodankylä Forest Ground	0.080
Sodankylä Peatland Ground	0.130
Lompolojankka Ground	0.050
Kaamanen Ground	0.100

cover algorithm. Georectification algorithm produces mapping for the camera images without the distortion. For snow cover detection, the distorted images are used so that there is no data loss in the input data. Distortion correction is applied to the snow – no-snow classified image, which is used with the weight mask produced by the georectification algorithm, using the coordinates with the distortion correction, so that all input and output data is consistent.

ROI Selection

One of the properties of the perspective projection is that the distance between two points in the image plane decreases with the depth in the 3D space for two points. Due to this effect, two parallel lines in space intersect at a single point in the image plane. From the spatial resolution of a pixel point of view, it means that some pixels in an image may have relatively very low spatial resolution and sometimes theoretically infinite, depending on the terrain and the viewing direction. Moreover, the algorithm used for the georectification only processes a certain subset of the

DEM data, as it is practically impossible to process all the data in the theoretical field of view, depending on the camera. In that case, if a point in the real world corresponds to a pixel in the image plane, but it is out of bounds for the processed part of DEM data, then the calculation for that pixel is incorrect. In Figure 19, the spatial resolution for the pixels for the images from Tvärminne Landscape Camera is presented. It is seen that this effect is visible especially where the parallel lines that have smaller angle with the optical axis. Furthest points of the water surface on the middle of the image (marked with green rectangle in the figure) corresponds to an area of about 30 times of the area corresponds to the pixels on the hill just next to them (marked with yellow rectangle). This ratio for some pixels on the hills at the behind (marked with magenta rectangles) goes more than 100. This effect is not only a problem in complex terrain, but also for flat terrain, especially if the vertical angle of the camera (pitch) is very low.

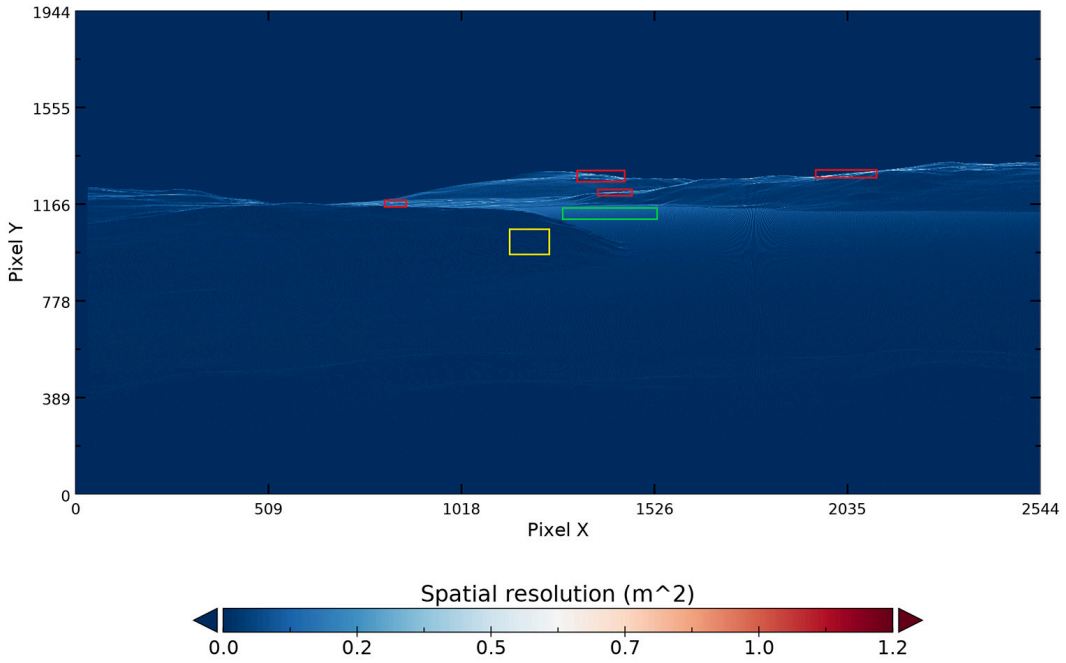

Figure 19: Spatial resolution of the pixels for Tvärminne camera images

In FSC estimation algorithm, the resulting weight mask is multiplied with the snow – no-snow image to calculate the fraction. In such an operation, if the weight mask has values which are significantly different from each other, the effect of the pixels with the smaller values will become ineffective, which means the snow coverage information from those pixels are not actually used in the algorithm. Because of that, for the estimation of FSC, the weight masks should be checked beforehand to select the ROI correctly. In the toolbox, that can be done by running a georectification analysis with the same georectification parameters used in the FSC algorithm. This selection will also greatly reduce the required computing time, as the required spatial extent for the process can be chosen much smaller. ROIs selected for all the analyses are seen in the setup reports in Annex C.

3.6 Snow depth estimation algorithm

The algorithm is using image segmentation to detect where snow surface intersects a pole-like object, for example, a snow stick. The algorithm is introduced with a preliminary feasibility study using images of a camera in Sodankylä SPICE observation site[70]. It is later studied using camera images from MONIMET Sodankylä Peatland site, Gressoney la Trinitè Dejola and Careser dam[42].

The intersection to be detected can only be detected if the object is dark coloured, or it has markers that are dark coloured. For this algorithm, correct selection of ROI is crucial. The ROI should be drawn on a snow free preview image so that the bottom of the pole-like object can be selected. The ROI can be wider than the object, but top and the bottom should be as precise as possible. Because the height of object is provided by the user, it is not a must to draw ROI until the top of the object. Any point which the height is known on the object can be used as the top of the ROI. For example, only the 100 cm part of a 120 cm snow stick can be selected, if it is indicated that the object is 100 cm. That type of selection comes in handy especially when the view of the object is obscured, for example by a branch that is bent by the weight of the snow on it.

The following steps are applied in the algorithm. In Figure 20, the steps are shown on an example. One of steps, "shape filtering" in the original algorithm is excluded here because it leads to incorrect segmentation for some of the cameras due to the difference in the marker sizes in pixels.

1. Cropping the image: The image is cropped to the bounding box of the ROI, because all the segmentation should be done inside the ROI.

2. Gaussian filter, if selected as a parameter: The noise in the images prevent the segmentation of the markers do be done correctly. Applying gaussian filter on the image smoothens the edges of markers. Number of neighbour pixels for the filter is given by the user.

3. Thresholding: The image is classified as binary according to the threshold value given by the user. This is done so that pixels on the markers have one value and pixels on the snow and/or light parts of the pole-like object have the other value.

4. Segmentation: Regions of the same values (contours) are detected by segmentation. These shapes are the markers.

5. Marker height detection: Heights of the markers are obtained by reading the bounding box coordinates of the markers. In the code, the height is the difference between the marker and the top of the pole-like object, because the pixel indices are increasing from the top of the image to the bottom in the library.

6. Depth calculation: Using the object height in centimetres provided by the user, the height of the lowest marker in pixels (a in Figure 20), and the height

of object in pixels (b in Figure 20) are used to calculate the height of the interception in centimetres, meaning the snow depth, as in Equation 12.

$$\text{Snow depth} = \text{Object height} \times \left(1 - \frac{a}{b}\right) \tag{12}$$

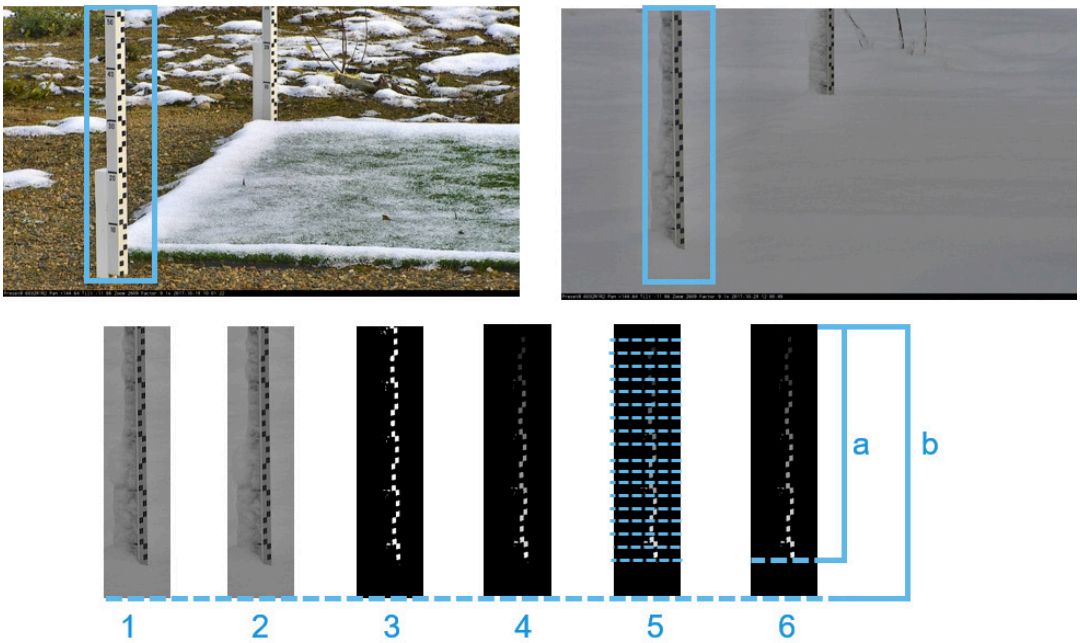

Figure 20: Snow depth algorithm illustrated. Top left: ROI selection in snow free image; top right: ROI preview in snow covered image; bottom: algorithm steps numbered as the description; a: the height of the lowest marker in pixels; b: the height of object in pixels.

3.7 Validation and error estimation

Validation of the estimated parameters are done by direct comparison of the estimated values to the reference values and then calculating statistical metrics. Root mean square error (RMSE) is used for the error quantification in the comparisons. $RMSE$ is calculated by the Equation 13,

$$RMSE = \sqrt{\frac{1}{N}\sum (v_{estimated} - v_{reference})^2} \tag{13}$$

where N is the number of comparisons, $v_{estimated}$ is the value of the estimated parameter and $v_{reference}$ is the value of the reference observation.

Datasets are generated for the direct comparison of FSC by visually inspecting the images and subjectively estimating the snow cover fraction in the ROI. For a human observer, it is challenging to make a precise decision for such an observation, the FSC values are recorded as values with 10% intervals (0, 10%, 20%, ... 90%,

100%). This method relies on subjective observations, but it is shown in a previous study that the subjective error for such an observation is around 10% [9]. Using that datasets, RMSE is calculated for the value pairs, and linear regression lines on scatter plots are provided.

Comparison of FSC values are also done separately for the early seasons and the melting seasons, as the lightning conditions and the distribution of the snow on the ground is different not only for the ecosystem type, but also for the seasons. The seasons are defined according to the reference data created by visual inspection. The early season starts one day before the first snow cover on the ground and ends one day after the last partly snow cover case before winter. The melting season starts one day before the first partly snow cover case after winter and ends one day after the last partly snow cover case before summer. According to those conditions, first and lasts days for the seasons for each site are given in Table 5.

Table 5: Early season and melting season dates

Site	**Early season**	**Melting season**
Tammela	26.10.2018 - 09.01.2019	14.02.2019 - 17.04.2019
Hyytiälä	25.10.2018 - 02.01.2019	24.02.2019 - 26.04.2019
Värriö	27.09.2018 - 04.12.2018	25.04.2019 - 21.05.2019
Sodankylä Forest	04.10.2018 - 09.12.2018	28.04.2019 - 12.05.2019
Sodankylä Peatland	04.10.2018 - 10.12.2018	26.04.2019 - 09.05.2019
Lompolojankka	04.10.2018 - 06.12.2018	19.04.2019 - 21.05.2019
Kaamanen	05.10.2018 - 11.12.2018	12.04.2019 - 09.05.2019

Reference data for SD is obtained from automatic weather stations, which uses well established measurement devices. The SD data is also quality controlled by the providing institution. On the other hand, SD is not always homogenous in the field. What should or can be observed from a snow stick is sometimes different from the measurement on the points where the measurement device is targeted. Also, for three of the cameras, the measurement providing station is at a distance from the camera field of view, which has a different terrain. That is why, smaller datasets are generated for the comparison by reading the snow sticks visible in the camera field of views. Using that smaller datasets, RMSE is calculated for the value pairs, and linear regression lines on scatter plots are provided.

For the accuracy assessment of the georectification, relatively lower resolution of orthoimages from each camera are overlaid on Google Earth imagery. For the GCPs with coordinate information, GCPs locations are marked on Google Earth imagery and on orthoimages. Error between corresponding GCP markers are measured using the measurement tool in Google Earth. For the GCPs with distance information, such as distance from the camera or distances between GCPs, the GCPs are marked on orthoimages and the distances are measured using the measurement tool in Google Earth. For the sites without any in-situ measured GCPs, Google Earth imagery and the common sense in the shapes and sizes of the objects in the orthoimages are used.

4 Results and Discussion

4.1 Georectification

Georectification of the camera field of views are fairly consistent with the GCPs and Google Earth imagery. The error in the positions of the GCPs are mostly around 2 m, which is lower than the accuracy of the GPS devices that is used to measure the locations of the cameras and GCPs. Thus, it can be said the a georectified image is not highly accurate in the pixel level, but it is sufficiently accurate for FSC analyses as only the weighting mask create from the rectification is used. As the error in the locations are lower than the accuracy of the GPS devices, RMSE for the georectification is not calculated.

In Tammela site, the GCPs are measured by the distance to the camera and each other. In Figure 21, the measurements of GCPs are shown on the right and the GCPs marked in Google Earth imagery with an orthorectifed image overlaid is shown on the left. In Table 6, in-situ measurements and Google Earth measurements are listed. It is seen from the table that the maximum error is about 49 cm, which is under the DEM resolution and similar to the error in the study [34].

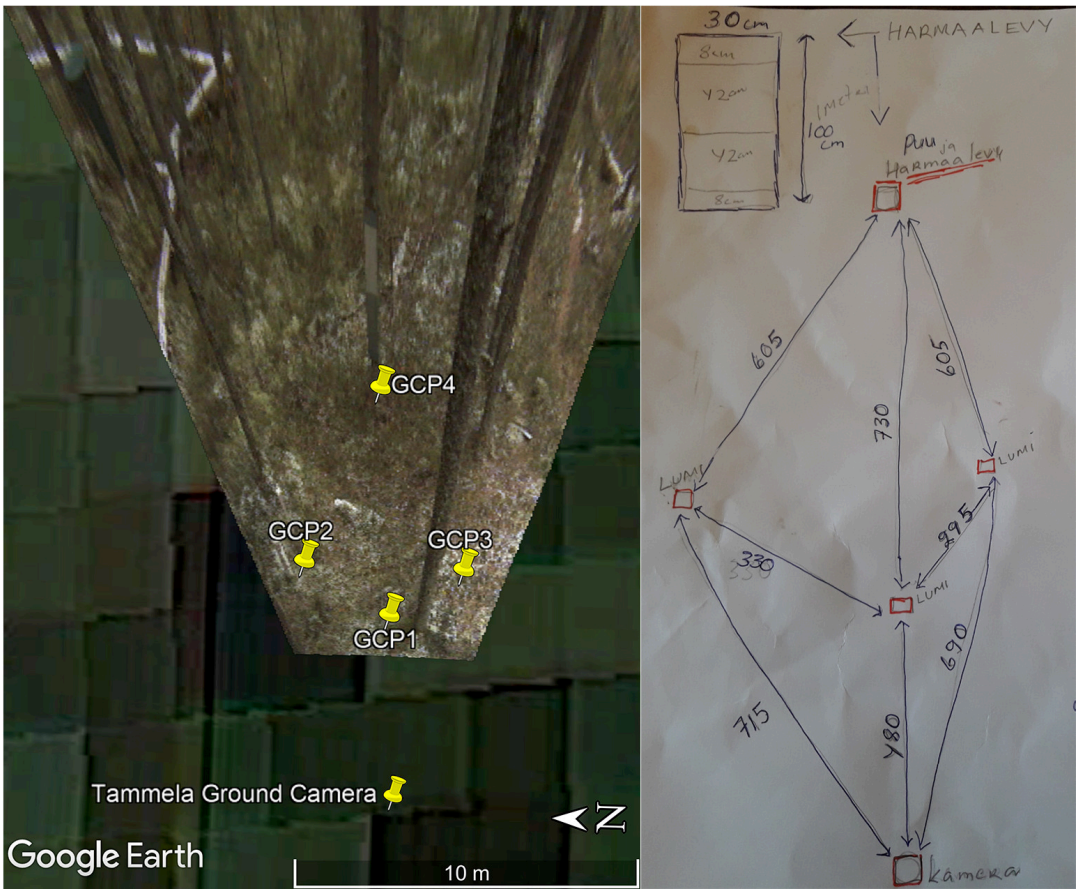

Figure 21: GCPs of Tammela site marked on the orthoimage overlaid on Google Earth imagery (left) and in-situ distance measurements (right)

Table 6: Distances between GCPs in Tammela

Line	In-situ Distance	Calculated Distance
Camera—GCP1	4.80 m	5.15 m
Camera—GCP2	7.15 m	7.24 m
Camera—GCP3	6.90 m	6.85 m
GCP1—GCP2	3.30 m	2.96 m
GCP1—GCP3	2.95 m	2.57 m
GCP1—GCP4	7.30 m	6.81 m
GCP2—GCP4	6.05 m	5.76 m
GCP3—GCP4	6.05 m	5.99 m
Camera—GCP2	7.15 m	7.24 m
Camera—GCP3	6.90 m	6.86 m

The assessment of the accuracy of the georectification is done similary for other cameras. The GCPs on the orthoimages are presented in Annex A. For Värriö and Kaamanen images there are no in-situ GCP measurements. For Kaamanen camera, the orientation parameters are decided according to the orthoimage most consistent with the Google Earth imagery, by visual inspection. For Värriö, the resolution is too high for such an optimisation. Instead, the parameters are decided so that the orthoimage shows a common sense in the distance between trees, shape of the walking board etc. The scale of the orthoimage may be incorrect, but the ratio of the spatial resolutions of the pixels would be sufficient for the FSC estimation, as the ROI is very close to the camera and the camera vertical angle (pitch) is quite low not to create much difference between the spatial resolutions of the pixels.

4.2 Fractional snow cover

Fractional snow cover estimations by image processing and visual observation from the camera images, scatter plots for all year, early season and melting season are seen in Figure 22,24, 26, 28, 30, 32 and 34 for each camera. Fractional snow cover estimations by image processing and visual observation from the camera images for early season and melting season are seen in Figure 23,25, 27, 29, 31, 33 and 35 for each camera. In general it is seen that the values from the image processing follows the trends in the values from the visual observations in early and melting seasons. Calculated RMSE values for the comparisons for all data, early seasons and melting seasons for each camera is given in Table 7. It is seen that the error is lower for forest cameras in early season and for peatland cameras in melting season, which are around 20% for all except Tammela camera. It is also seen that for Kaamanen camera both seasons have low RMSE and for Tammela camera both seasons have high RMSE. For overall data, RMSE is still under 33% for all cameras. For the interpretation of the results, the reference data subjectivity should also be considered. Especially in the early season of peatlands, the snow cover hard to estimate for an observer.

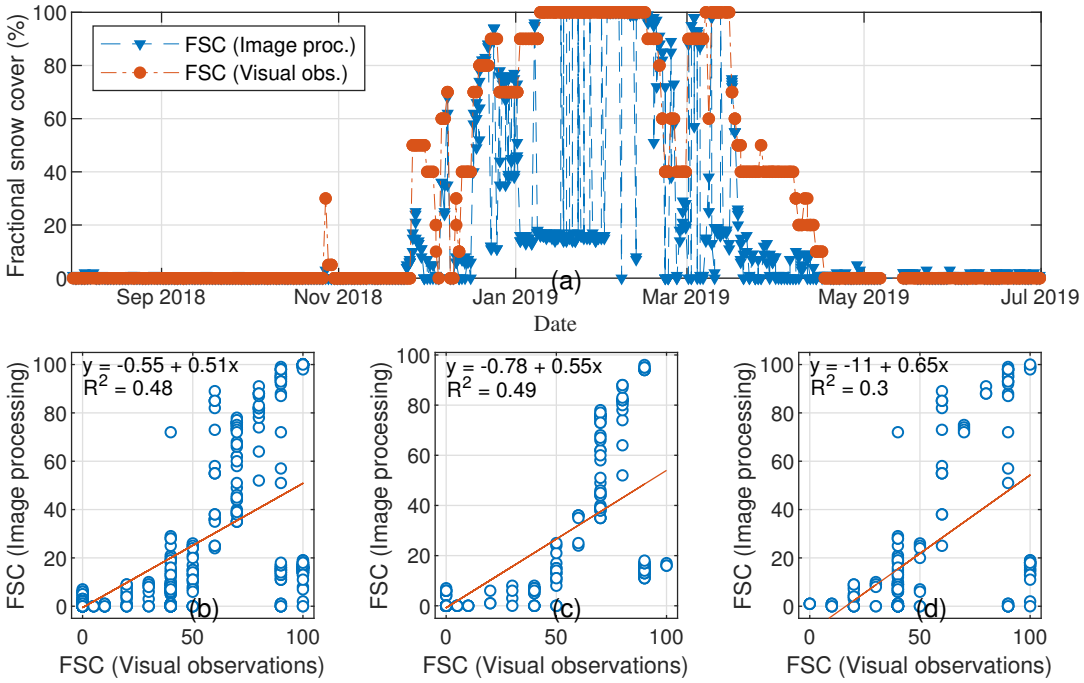

Figure 22: (a) Fractional snow cover estimations by image processing and visual observation from Tammela Spruce Ground camera images, scatter plots for (b) all year, (c) early season and (d) melting season.

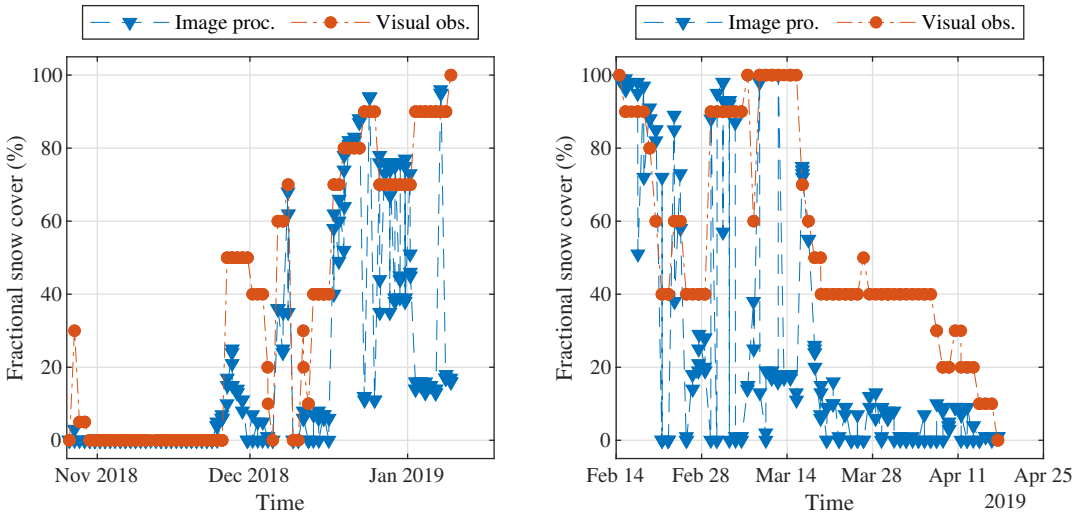

Figure 23: Fractional snow cover estimations by image processing and visual observation from Tammela Spruce Ground camera images for early season (left) and melting season (right).

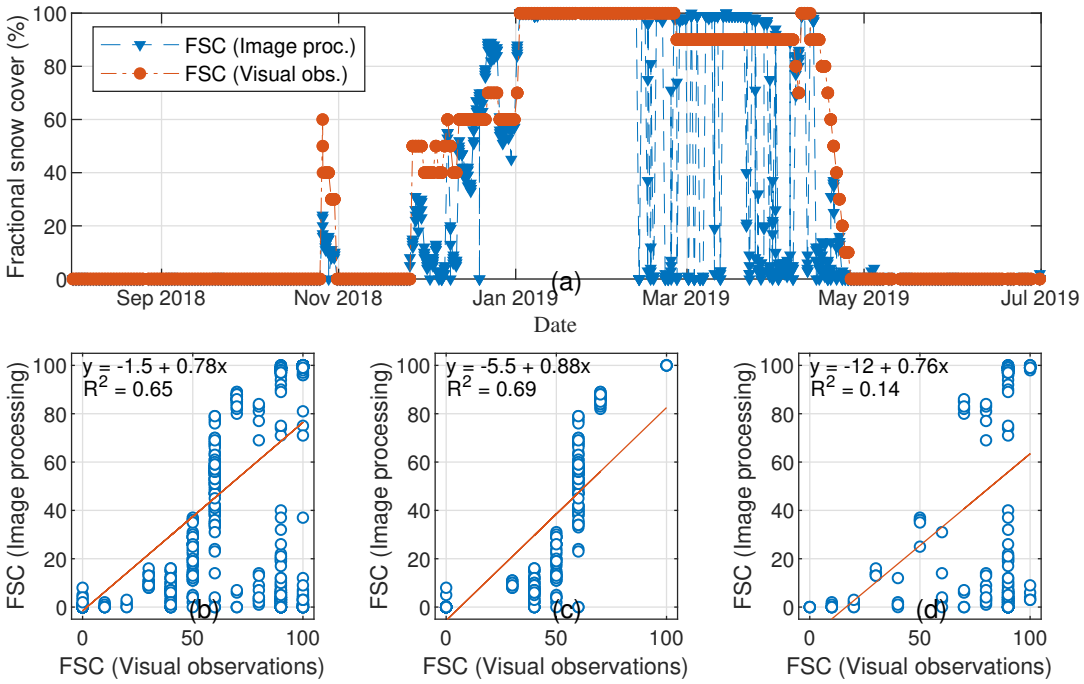

Figure 24: (a) Fractional snow cover estimations by image processing and visual observation from Hyytiälä Pine Ground camera images, scatter plots for (b) all year, (c) early season and (d) melting season.

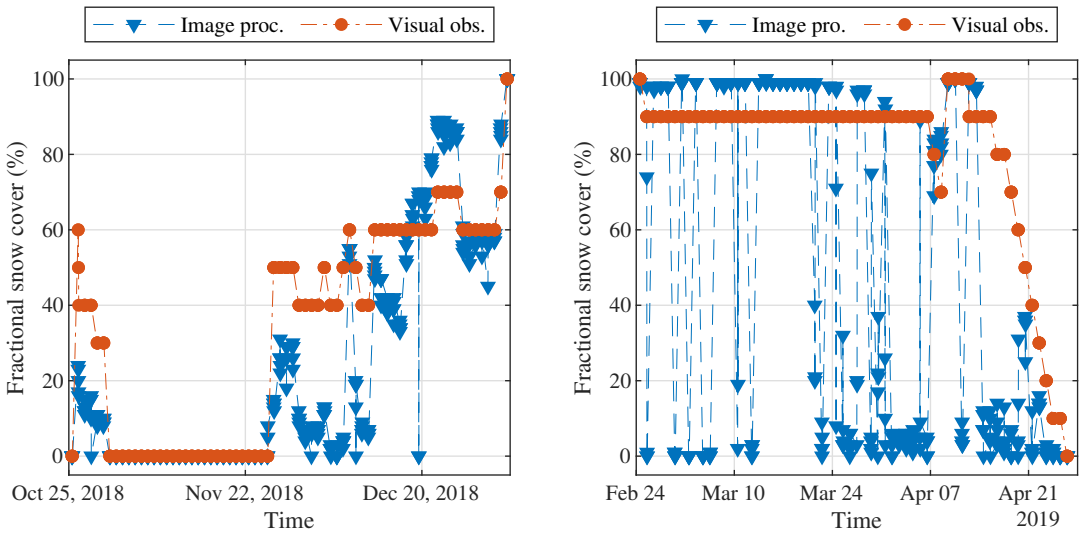

Figure 25: Fractional snow cover estimations by image processing and visual observation from Hyytiälä Pine Ground camera images for early season (left) and melting season (right).

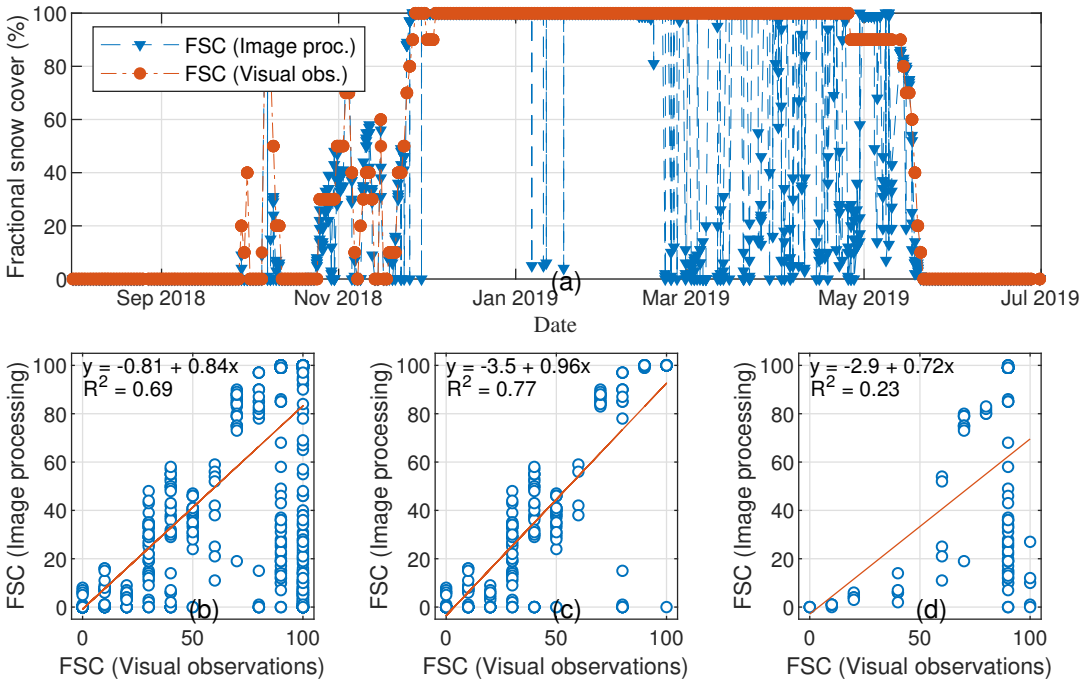

Figure 26: (a) Fractional snow cover estimations by image processing and visual observation from Värriö Pine Ground camera images, scatter plots for (b) all year, (c) early season and (d) melting season.

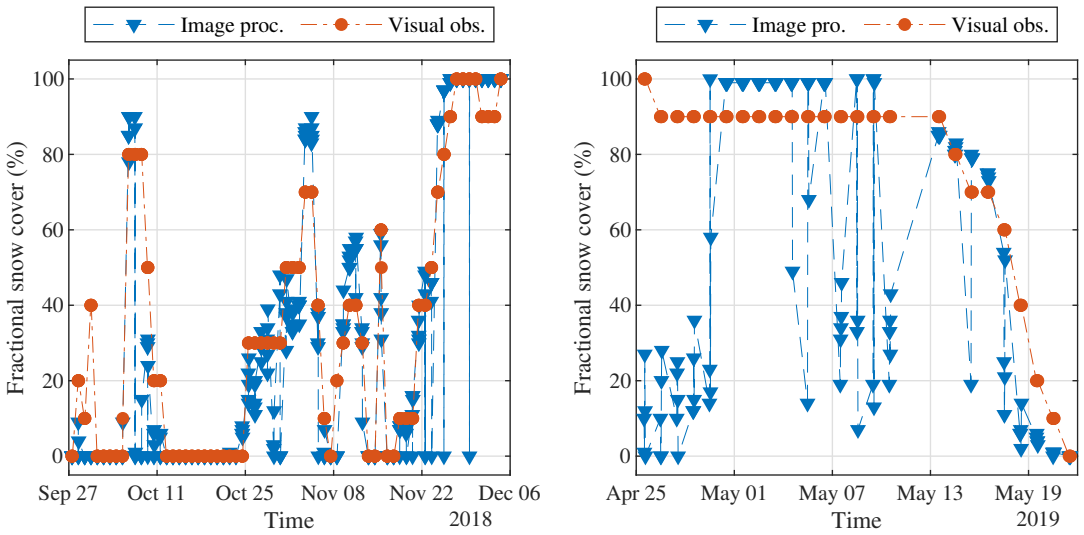

Figure 27: Fractional snow cover estimations by image processing and visual observation from Värriö Pine Ground camera images for early season (left) and melting season (right).

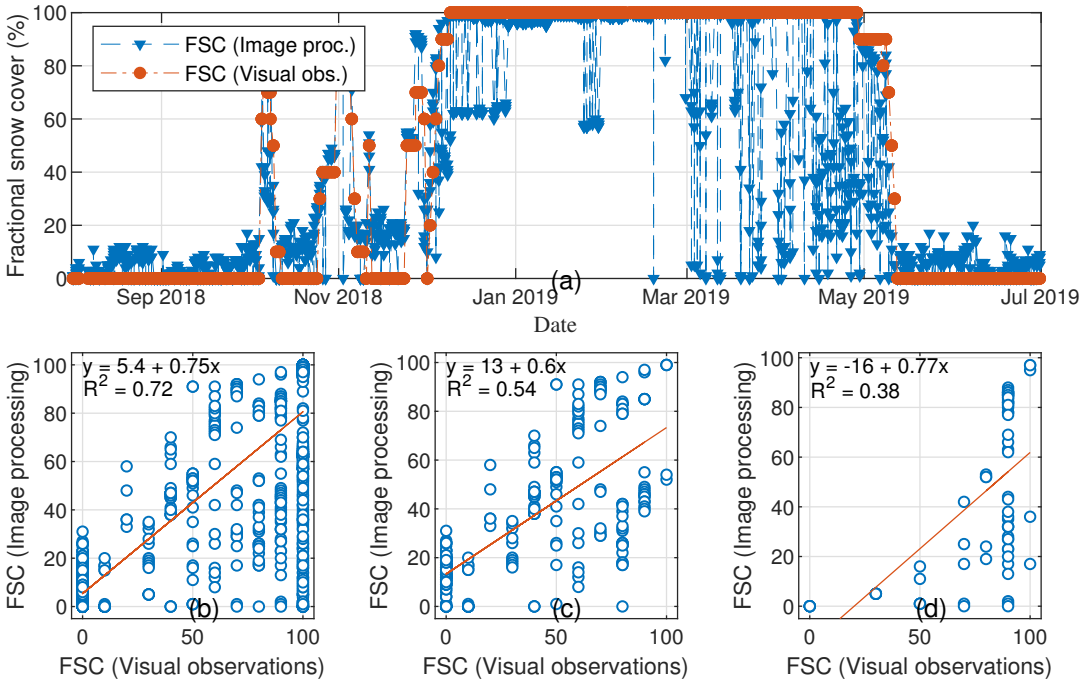

Figure 28: (a) Fractional snow cover estimations by image processing and visual observation from Sodankylä Pine Ground camera images, scatter plots for (b) all year, (c) early season and (d) melting season.

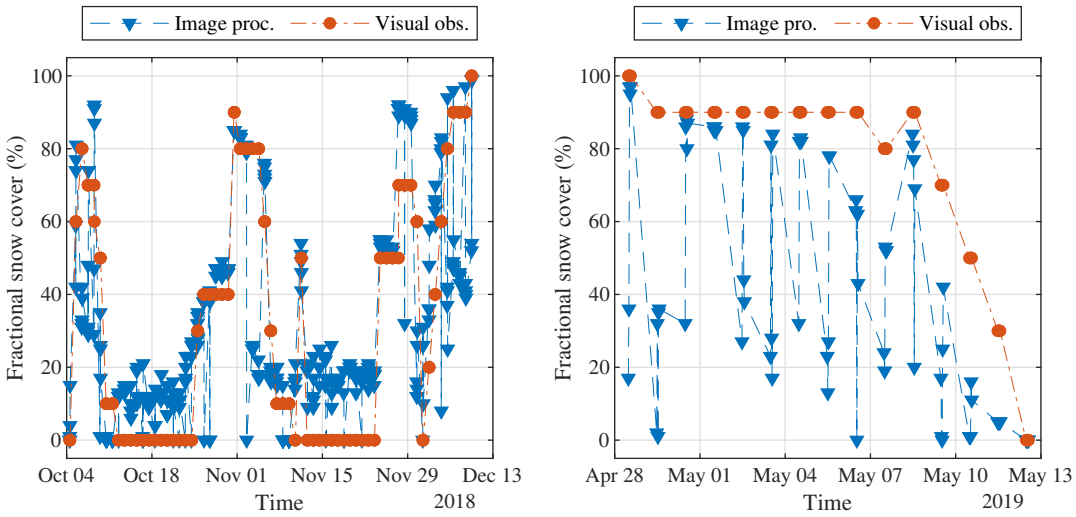

Figure 29: Fractional snow cover estimations by image processing and visual observation from Sodankylä Pine Ground camera images for early season (left) and melting season (right).

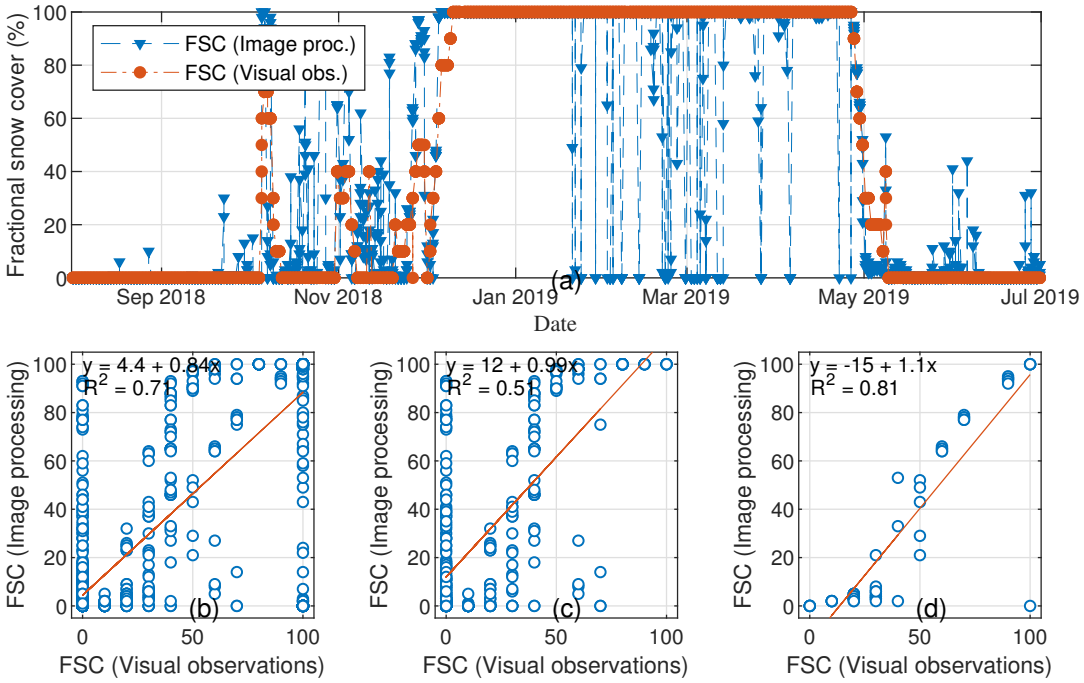

Figure 30: (a) Fractional snow cover estimations by image processing and visual observation from Sodankylä Pine Peatland camera images, scatter plots for (b) all year, (c) early season and (d) melting season.

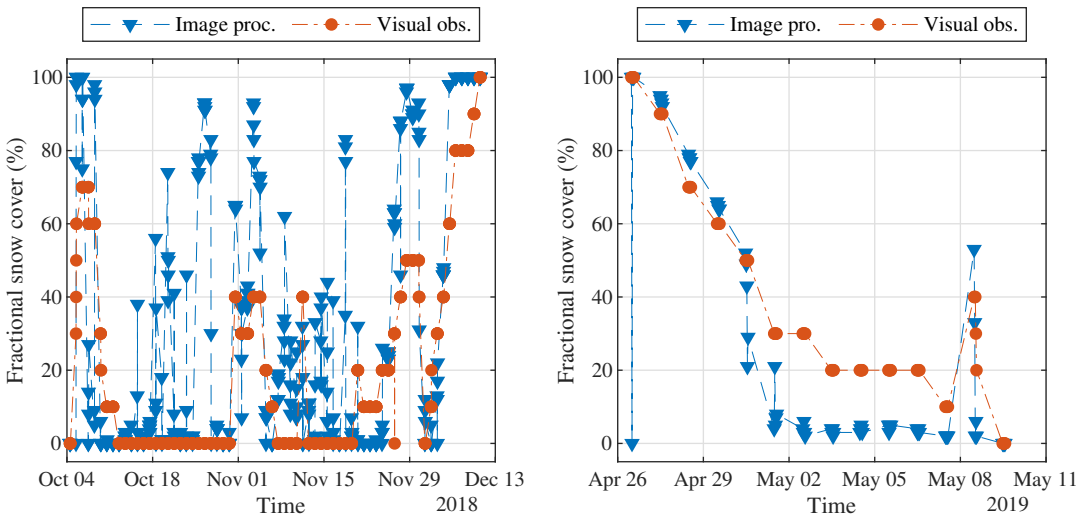

Figure 31: Fractional snow cover estimations by image processing and visual observation from Sodankylä Pine Peatland camera images for early season (left) and melting season (right).

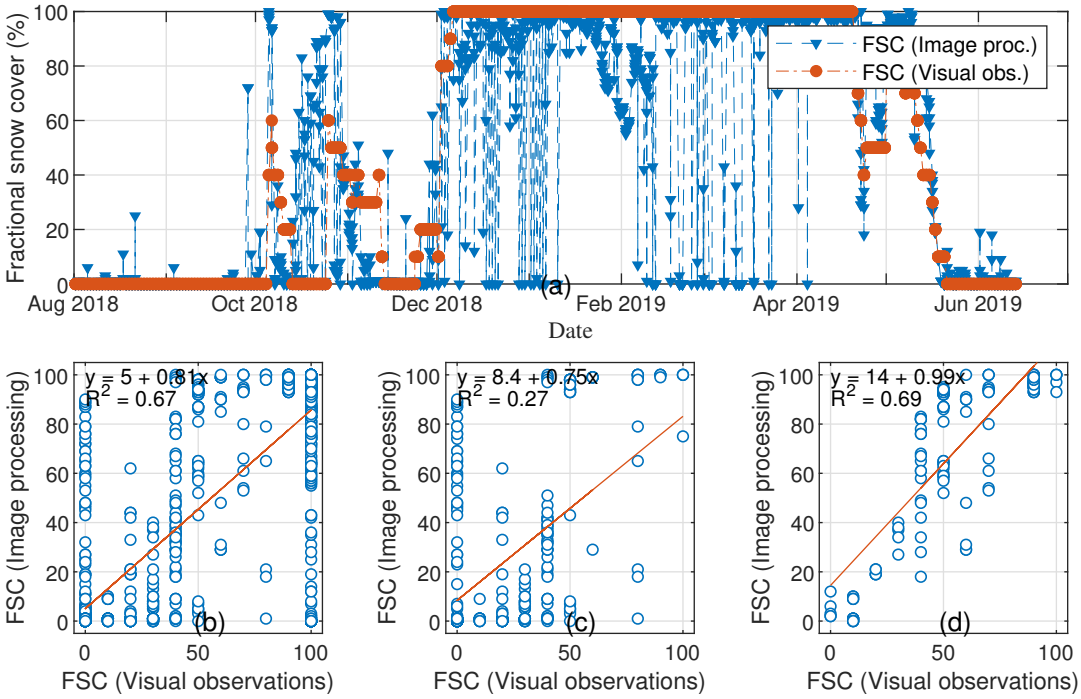

Figure 32: (a) Fractional snow cover estimations by image processing and visual observation from Lompolojankka Wetland Ground camera images, scatter plots for (b) all year, (c) early season and (d) melting season.

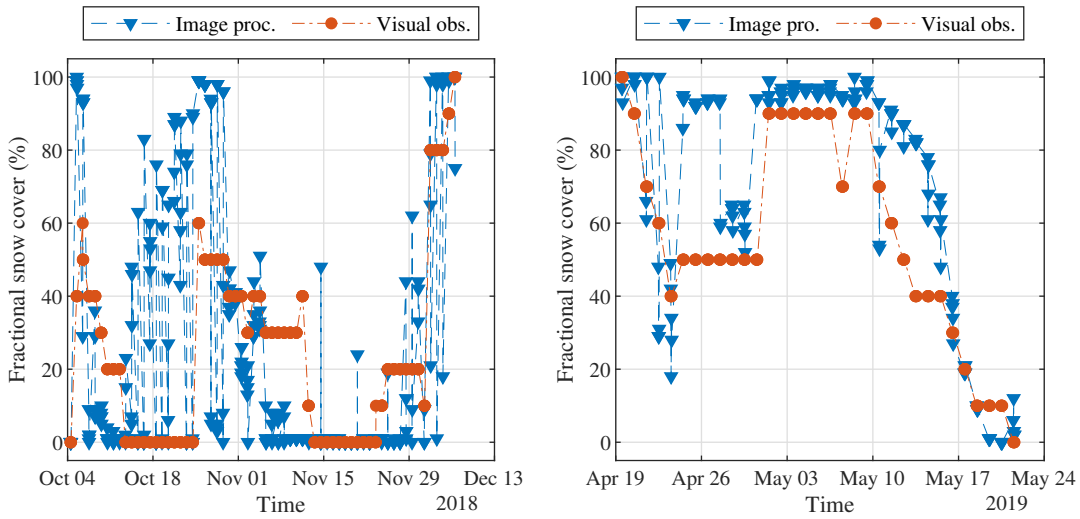

Figure 33: Fractional snow cover estimations by image processing and visual observation from Lompolojankka Wetland Ground camera images for early season (left) and melting season (right).

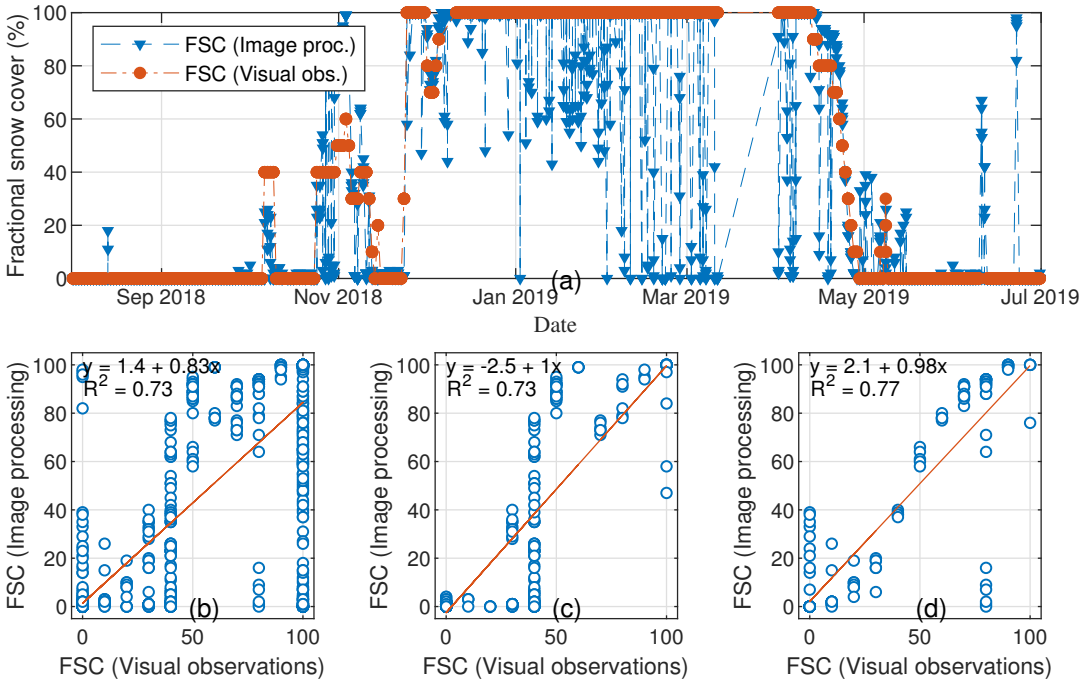

Figure 34: (a) Fractional snow cover estimations by image processing and visual observation from Kaamanen Wetland Ground camera images, scatter plots for (b) all year, (c) early season and (d) melting season.

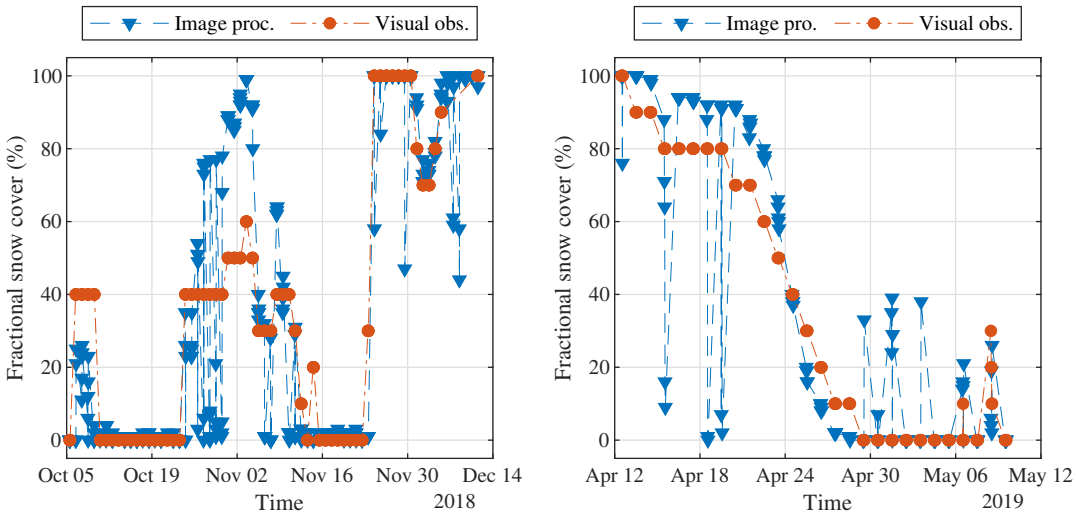

Figure 35: Fractional snow cover estimations by image processing and visual observation from Kaamanen Wetland Ground camera images for early season (left) and melting season (right).

Table 7: RMSE for FSC estimates.

Site	**Overall (%)**	**Early season(%)**	**Melting season(%)**
Tammela	32.44	31.46	42.82
Hyytiälä	28.41	19.44	53.63
Värriö	28.84	18.45	42.81
Sodankylä Forest	26.19	22.96	42.58
Sodankylä Peatland	26.44	29.16	19.25
Lompolojankka	27.98	31.33	23.07
Kaamanen	24.99	20.62	19.74

It is seen in the inspection of the images and the results that some of the high error sources identified in [9] are also valid for the analyses. The most common source of error is the phenomena of the shades cast over the surface due to the natural and artificial objects, including snow roughness, that blocks the sunlight in sunny days (Figure 36a,b). This phenomena is observer in all cameras, mostly from middle of February to the full melting of snow. This contribution to the error is very high for forest cameras, in melting season as there are many trees around the view and density of the trees creates shades and high contrast in the image. Another common source is the litter and lichen for forest cameras (Figure 36c,d), which are classified as no-snow instead of snow for the litter and vice versa for the lichen. Light coloured reflections from the water in peatlands is also observerd but it is not common (Figure 36e). Unlike the previous study[9], orientation and focus changes in the camera views are not observed in analyses. Accumulation of snow and frost on the camera housing occurs, but those images are not included in the comparison as reference data is not created for them.

There is another error source that is observed in the study for Sodankylä Peatland and Lompolojankka site. The colour of the vegetation in early season is close to brown-yellow, sometimes in a very light tone, especially when the illumination is higher (Figure 36f). This is also valid for Kaamanen site, but distribution of such vegetation is more even. For Sodankylä and Lompolojankka, only in a part of ground has the phenomenon, which effect the histogram and changes the threshold for the snow classification to be lower than the "bright vegetation" values. It is though that the high error for those two peatland cameras mostly caused by that phenomena. This error source is similar to the one in [34], which the limestone on the ground is classified as snow. A special case exists for Lompolojankka camera. In winter, under full snow cover, branches from the trees near camera are bent down due to the snow on them inside the ROI (Figure 36g), the high snow roughness is commonly observed (Figure 36h) and trails of snowmobiles are present (Figure 36h). Both phenomena explains many days of 80%—99% snow cover values in the middle of the winter.

The error sources listed above are shown in Figure 36.

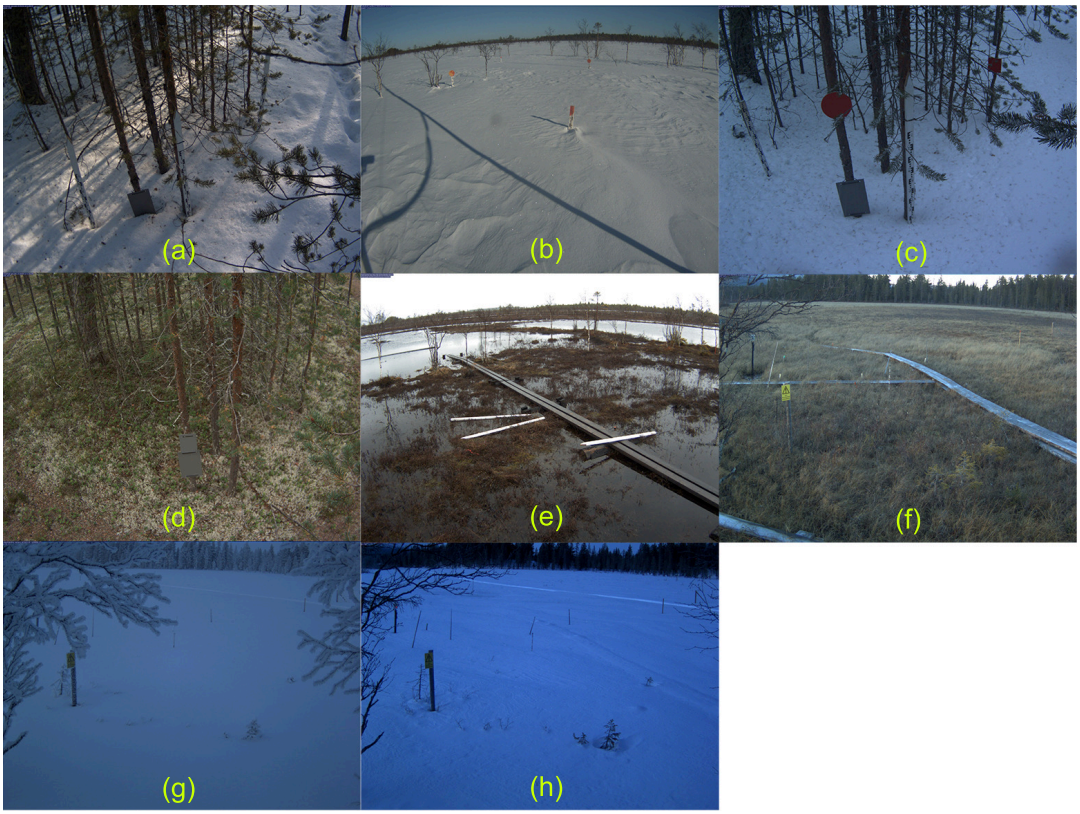

Figure 36: High error sources for FSC algorithm

4.3 Snow Depth

Snow depth estimations by image processing and by visual observations from the images from the cameras and in-situ measurements from automatic weather stations in the sites with the automatic weather station is located in a distance are given in Figure 37, 38 and 39. It is seen for those sites that the trends in the snow depth estimations are consistent with the trend in the automatic weather station measurements, but there is a nonlinear bias which the image processing is underestimating. As mentioned, this is expected due to the location difference with the camera and the AWOS. The difference in estimations and measurements for Hyytiälä and Sodankylä Forest sites are similar to each other, as in the case for the difference between the locations, both in distance and in the difference of terrain, which is seen in Figure 6 and in Table 2. The difference in estimations and measurements for Tammela site is rather different than other two sites. The difference is quite low in the early season and much higher in the melting season. The distance between the camera and the AWOS for the site is quite low, and it is known that the AWOS is still inside the forested area. It can be said that the accumulation is snow is similar, as the terrain and vegetation is similar, but there may be another factor that increases melting speed.

For Sodankylä Peatland site, it is seen in Figure 40 that the estimation from the image processing are very consistent with the measurements from the AWOS. It is seen that the algorithm correctly estimates the snow depth, although there are still many days after mid-February that the estimations are totally incorrect, very similar to the case in FSC. It is also inspected and seen that the source of this error is due to the diffuse illumination by the shadows which are detected as markers in the ROI. The RMSE for the comparison is calculated as 13.21 cm, altough is seen from the time plots that the error for the images without the shadow problem is much lower. The illumination problem is also seen in the images from other cameras. For Tammela and Hyytiälä, the effect in error is low because the snow depth is quite low but for Sodankylä it is quite high.

Comparison with visual observations of the snow depth from the snow sticks for the three sites confirms that the expected difference with the AWOS measurements. The values from the visual observations are much closer to the estimations from the image processing and the calculated RMSE values are similar to the the value for Sodankylä Peatland site. The RMSE values are calculated for the comparisons with the visual observations for the three cameras as 10.57 cm for Tammela, 9.89 cm for Hyytiälä and 10.57 cm for Sodankylä Forest sites. In Figure 41, scatter plots for the comparisons and the linear regression lines are presented. In Table 8, RMSE values are presented for all sites. The error is higher than the error calculated in study [71], which has a correction algorithm applied on the core algorithm and quite lower than than the study [50].

Apart from the illumination, it is inspected that there are two more sources for high errors: Number of pixels along the snow stick and litters on the ground. The snow stick in Tammela camera view is the furthest away from the camera so the number of pixels along the snow stick is minimum. Because of that, the segmentation is harder to achieve. For Tammela and Hyytiälä camera, size of litter on the ground

in pixels is comparable to the size of the snow stick markers in pixels and they fall inside the ROI drawn around the snow stick. Because of that they are detected as markers visible under the snow depth.

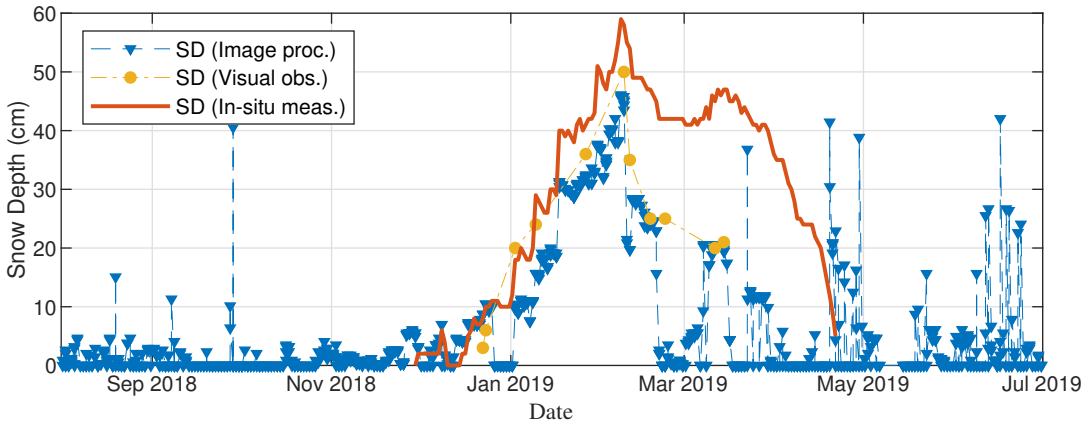

Figure 37: Snow depth estimations by image processing and by visual observations from Tammela Spruce Ground camera images and snow depth measurements from the nearby automatic weather station.

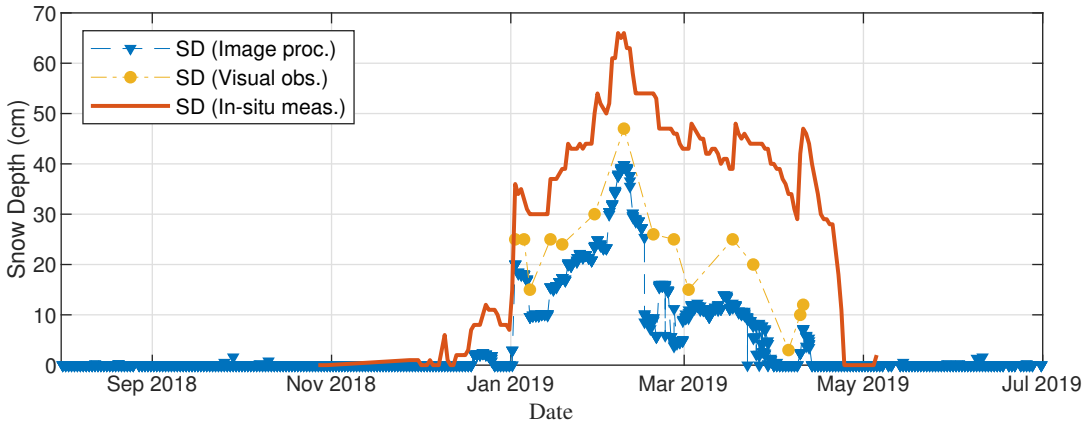

Figure 38: Snow depth estimations by image processing and by visual observations from Hyytiälä Pine Ground camera images and snow depth measurements from the nearby automatic weather station.

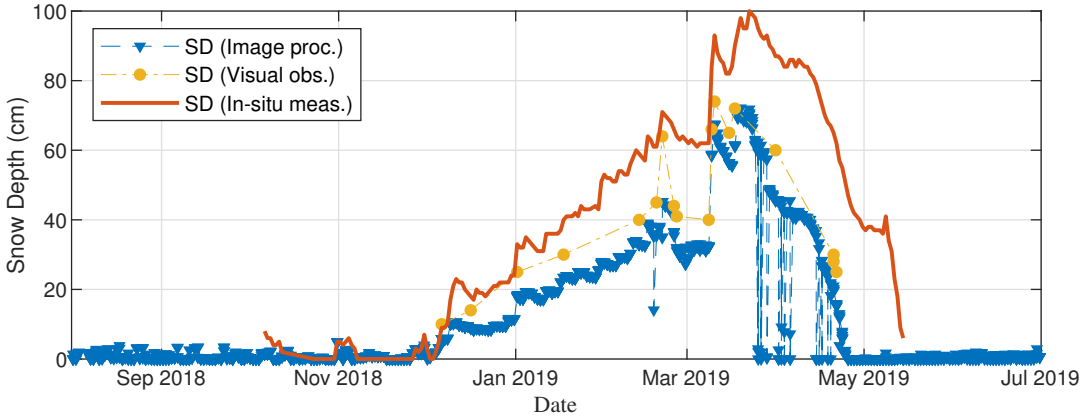

Figure 39: Snow depth estimations by image processing and by visual observations from Sodankylä Pine Ground camera images and snow depth measurements from the nearby automatic weather station.

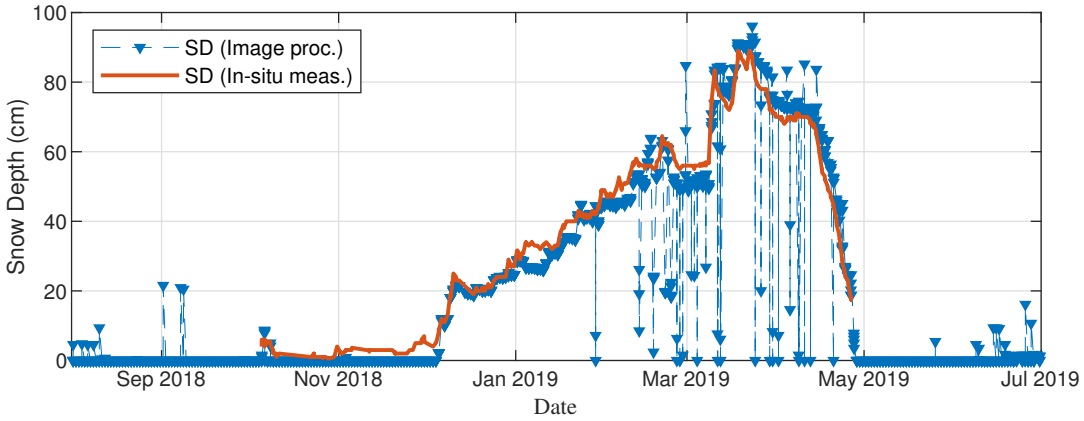

Figure 40: Snow depth estimations from Sodankylä Pine Peatland camera images and snow depth measurements from the nearby automatic weather station

Table 8: RMSE for SD estimates.

Site	**Overall (cm)**
Tammela	10.57
Hyytiala	9.89
Sodankyla Forest	10.57
Sodankyla Peatland	13.21

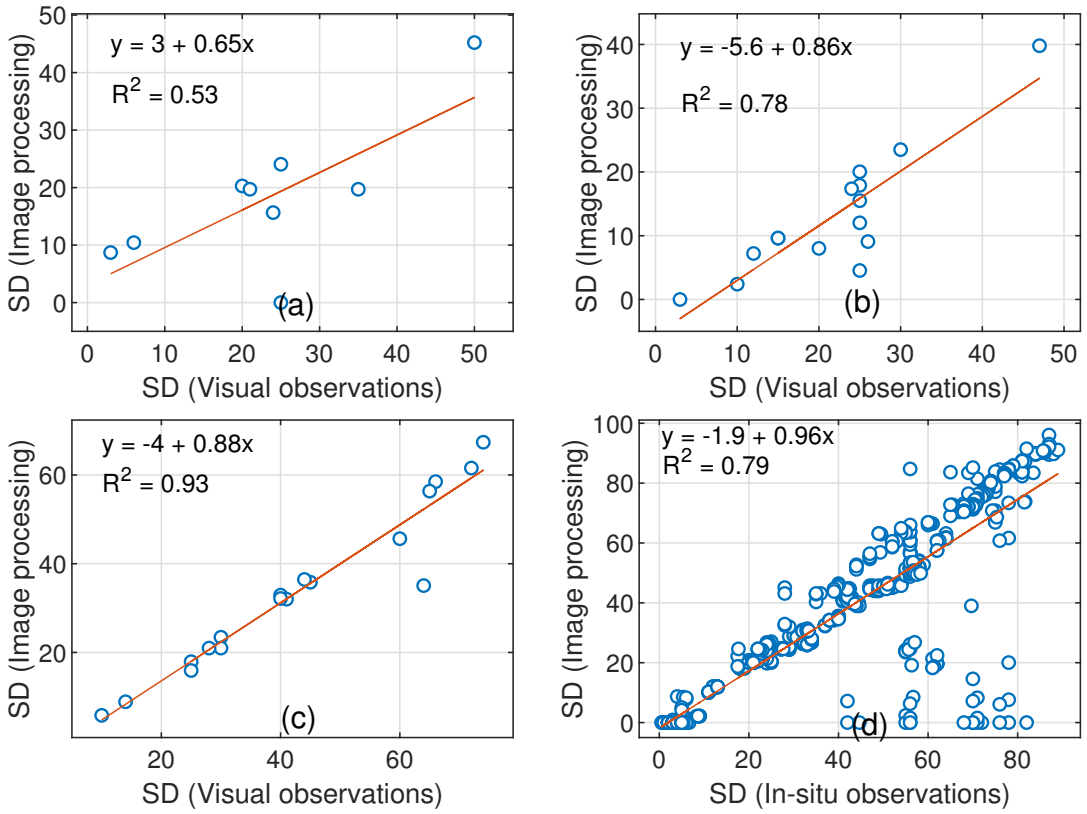

Figure 41: Scatter plots and regression lines for snow depth estimates a) Tammela Spruce Ground Camera b) Hyytiälä Pine Ground camera c) Sodankylä Pine Ground camera d) Sodankylä Peatland Camera

4.4 Cloud processing

On the FMI server, snow cover monitoring analyses are running alongside with other processes. The near real time results are accessible in FMIPROT & Camera Network Portal web page. Printouts of the results at the time of study are given in Annex B. Since the creation of animations take relatively longer time, the setups are run at 12:00 and 15:00 Finnish time, which results in a latency of 3 hours. The processing chain works well in the cloud but there has been blocks in the camera views, probably due to snow storms and fast melting and re-freezing of the snow on the camera housing, in Sodankylä Forest, Sodankylä Peatland, Lompolojankka and Kaamanen. The blockings have results in incorrect results in early November. This situation disturbs the NRT results, but on the other hand it is also a notification to clear the cameras from the snow.

For testing the system if it can be deployed and run in an affordable, cheap cloud computing infrastructure, a private server with the minimal configuration from is rented and the processing chains are copied into the server. It is seen that only 1 shared CPU, 2 GB of memory and 50 GB of disk space is sufficient to run the same system, not only for snow cover but also the website, updates of the camera network (such as fetching latest images) and vegetation monitoring results which is also running in the FMI server. In Figure 42, daily CPU usage of the private server is seen. The longer peaks corresponds to the snow cover monitoring runs.

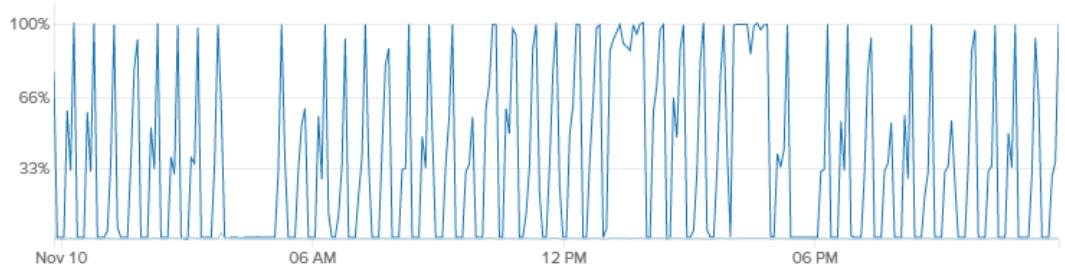

Figure 42: Daily CPU usage in the private server

It is identified that the run times of the processes can be about 30% shorter with a further improvement in FMIPROT toolbox. The current code runs the calculation for filtering out dark images for all the images in latest month for each run, which is unnecessary. Instead, the data filtering should be run only for the images that are not processed in the previous run. This improvement is listed for the next improvement of the toolbox. After this improvement, it can be said that the snow cover monitoring setups can be run more frequently on the same system.

5 Conclusions

Snow depth estimation with the applied method using webcam imagery showed promising results. The method can be used in available webcam images which has a snow stick or other appropriate pole-like object, both for creating continuous, near real time datasets in locations where snow depth data is not available and decrease the required manpower and cost in locations where snow depth data with manual measurements is present. The method cannot estimate snow depth under 2 cm, due to the distance of the sticks, the size of the markers and vegetation or uneven soil level that blocks the view in the lower part the snow stick. Thus, it can be said that the with properly manufactured and installed sticks, optimised for this method can report the low snow depth and snow on-off information. Furthermore, data filtering methods can be applied to the estimated time series data for improving the performance.

Fractional snow cover estimation with the applied method using webcam imagery showed promising results under specific conditions, for example in early season for forest sites and melting season for peatland sites. Unlike the study in [9], raw results are presented and assessed in this study, rather than daily averaged values because the processing system used and developed further for creating near real time monitoring does not have features for post processing of the results yet. On the other hand, one can add such methods to the system. Most problematic issue is found as the illumination dependence. The method works well in uniform illumination, which mostly occurs in the cloudy days. On sunny or partly sunny days, the method mostly does not work, but the difference of those values with the ground truth is so high that data filtering methods can be applied or developed to filter out such results. Also, the case occurs mostly in late winter where snow cover is still 100% so in applications such as extracting phenophases it would not be a problem. For using the data as a complementary source for satellite derived products, such as filling the gap for cloudy days, only the cases of uniform illumination would be used.

It is shown that FMIPROT can be used to create near real time processing systems in a robust way for snow cover monitoring. The system can be deployed in the cloud with basic cloud processing knowledge. Monitoring setups can be prepared in a personal computer instance. The georectification tool also offers optimization for the camera orientation parameters. The toolbox is also cost-effective, even though it is not optimised for performance yet. The example cloud processing system shows that when the camera images are present in online repositories, FMIPROT can be deployed and run on a 10$/month cloud system alongside a website that shows the results to create an operational monitoring system with about 10 cameras. This operational monitoring system would be sufficient to obtain estimates of snow depth and fractional snow cover in regional scale with a latency of less than an hour. This monitoring system can be extended to country scale by increasing the cloud computing capacity. The processing system provides HTML reports so the results and data can be hosted even without a dedicated web page. In the reports, direct links to the raw data is available so that the data can be used by anyone. The toolbox should be used via command line interface in the cloud to create operational

monitoring services. Usage of the toolbox via command line interface is described in the user manual. As a future work, web page and processing chain script templates can be created to create such services in a more robust way.

The toolbox is open source and it also has simple plugin system, so that different algorithms can also be implemented or the current algorithms can be modified. In latest years, machine learning algorithms are studied to extract information for environmental monitoring[15, 50, 72]. Machine learning algorithms can also be implemented to the toolbox, either directly or with slight modifications in the base code, depending on the application. Together with conventional algorithms and machine learning algorithms, the system hold a great potential for obtaining information in an automated, near real time approach, to be used environmental and other applications, including hydrology, agriculture, wildlife, vegetation, coastal monitoring, meteorology, logistics etc.

References

[1] S. Metsämäki, J. Pulliainen, M. Salminen, K. Luojus, A. Wiesmann, R. Solberg, K. Böttcher, M. Hiltunen, and E. Ripper, "Introduction to globsnow snow extent products with considerations for accuracy assessment," *Remote Sensing of Environment*, vol. 156, pp. 96–108, 2015.

[2] F. Paul, S. Winsvold, A. Kääb, T. Nagler, and G. Schwaizer, "Glacier remote sensing using sentinel-2. part ii: Mapping glacier extents and surface facies, and comparison to landsat 8," *Remote Sensing*, vol. 8, no. 7, p. 575, 2016.

[3] R. Solberg, B. Wangensteen, J. Amlien, H. Koren, S. Metsämäki, T. Nagler, K. Luojus, and J. Pulliainen, "A new global snow extent product," in *Proceedings of ESA Living Planet Symposium, ESA Special Publication SP-686, Bergen, Norway, 26 June–02 July*, Citeseer, 2010.

[4] X. Zhang, C. Liao, J. Li, and Q. Sun, "Fractional vegetation cover estimation in arid and semi-arid environments using hj-1 satellite hyperspectral data," *International Journal of Applied Earth Observation and Geoinformation*, vol. 21, pp. 506–512, 2013.

[5] A. W. Nolin and J. Dozier, "A hyperspectral method for remotely sensing the grain size of snow," *Remote sensing of Environment*, vol. 74, no. 2, pp. 207–216, 2000.

[6] J. Staab, "Applying Computer Vision for Monitoring Visitor Numbers," Master's thesis, Julius Maximilian University of Würzburg, Hahnbergweg 24, 69118 Heidelberg, 2017.

[7] ESA, "Sentinel-2 Spectral Response Functions (S2-SRF)," tech. rep., European Space Agency, 12 2019.

[8] C. M. Tanis, M. Peltoniemi, M. Linkosalmi, M. Aurela, K. Böttcher, T. Manninen, and A. N. Arslan, "A system for acquisition, processing and visualization of image time series from multiple camera networks," *Data*, vol. 3, no. 3, 2018.

[9] A. N. Arslan, C. M. Tanis, S. Metsämäki, M. Aurela, K. Böttcher, M. Linkosalmi, and M. Peltoniemi, "Automated webcam monitoring of fractional snow cover in northern boreal conditions," *Geosciences*, vol. 7, no. 3, 2017.

[10] L. Wingate, J. Ogée, E. Cremonese, G. Filippa, T. Mizunuma, M. Migliavacca, C. Moisy, M. Wilkinson, C. Moreaux, G. Wohlfahrt, *et al.*, "Interpreting canopy development and physiology using the europhen camera network at flux sites," *Biogeosciences Discussions*, 2015.

[11] A. D. Richardson, K. Hufkens, T. Milliman, D. M. Aubrecht, M. Chen, J. M. Gray, M. R. Johnston, T. F. Keenan, S. T. Klosterman, M. Kosmala, *et al.*, "Tracking vegetation phenology across diverse north american biomes using phenocam imagery," *Scientific data*, vol. 5, p. 180028, 2018.

[12] K. Hufkens, G. Filippa, E. Cremonese, M. Migliavacca, P. D'Odorico, M. Peichl, B. Gielen, L. Hörtnagl, K. Soudani, D. Papale, *et al.*, "Assimilating phenology datasets automatically across icos ecosystem stations," *International agrophysics*, vol. 32, no. 4, pp. 677–687, 2018.

[13] S. Tsuchida, K. Nishida, K. Iwao, W. Kawato, H. Oguma, and A. Iwasaki, "Phenological eyes network for validation of remote sensing data," *Journal of the Remote Sensing Society of Japan*, vol. 25, no. 3, pp. 282–288, 2005.

[14] R. Holman, J. Stanley, and T. Ozkan-Haller, "Applying video sensor networks to nearshore environment monitoring," *IEEE Pervasive Computing*, vol. 2, no. 4, pp. 14–21, 2003.

[15] M. Xiao, M. Rothermel, M. Tom, S. Galliani, E. Baltsavias, and K. Schindler, "Lake ice monitoring with webcams.," *ISPRS Annals of Photogrammetry, Remote Sensing & Spatial Information Sciences*, vol. 4, no. 2, 2018.

[16] N. Jacobs, W. Burgin, N. Fridrich, A. Abrams, K. Miskell, B. H. Braswell, A. D. Richardson, and R. Pless, "The global network of outdoor webcams: properties and applications," in *Proceedings of the 17th ACM SIGSPATIAL International Conference on Advances in Geographic Information Systems*, pp. 111–120, ACM, 2009.

[17] M. Peltoniemi, M. Aurela, K. Böttcher, P. Kolari, J. Loehr, J. Karhu, M. Linkosalmi, C. M. Tanis, J.-P. Tuovinen, and A. N. Arslan, "Webcam network and image database for studies of phenological changes of vegetation and snow cover in finland, image time series from 2014 to 2016," *Earth System Science Data*, vol. 10, no. 1, pp. 173–184, 2018.

[18] "MONIMET." http://monimet.fmi.fi. Accessed: 2019-08-30.

[19] M. Linkosalmi, M. Aurela, J.-P. Tuovinen, M. Peltoniemi, C. M. Tanis, A. N. Arslan, P. Kolari, K. Böttcher, T. Aalto, J. Rainne, J. Hatakka, and T. Laurila, "Digital photography for assessing the link between vegetation phenology and co_2 exchange in two contrasting northern ecosystems," *Geoscientific Instrumentation, Methods and Data Systems*, vol. 5, no. 2, pp. 417–426, 2016.

[20] M. Peltoniemi, M. Aurela, K. Böttcher, P. Kolari, J. Loehr, T. Hokkanen, J. Karhu, M. Linkosalmi, C. M. Tanis, S. Metsämäki, *et al.*, "Networked web-cameras monitor congruent seasonal development of birches with phenological field observations," *Agricultural and forest meteorology*, vol. 249, pp. 335–347, 2018.

[21] "EuroPhen." http://europhen.org/. Accessed: 2019-08-30.

[22] "PhenoCam An Ecosystem Phenology Camera Network." https://phenocam.sr.unh.edu/. Accessed: 2019-08-30.

[23] G. Filippa, E. Cremonese, M. Migliavacca, M. Galvagno, O. Sonnentag, E. Humphreys, K. Hufkens, Y. Ryu, J. Verfaillie, U. M. di Cella, *et al.*, "Ndvi derived from near-infrared-enabled digital cameras: Applicability across different plant functional types," *Agricultural and Forest Meteorology*, vol. 249, pp. 275–285, 2018.

[24] "Phenological Eyes Network (PEN)." http://www.pheno-eye.org. Accessed: 2019-08-30.

[25] S. Nagai, T. Akitsu, T. M. Saitoh, R. C. Busey, K. Fukuzawa, Y. Honda, T. Ichie, R. Ide, H. Ikawa, A. Iwasaki, *et al.*, "8 million phenological and sky images from 29 ecosystems from the arctic to the tropics: the phenological eyes network," *Ecological research*, vol. 33, no. 6, pp. 1091–1092, 2018.

[26] K. Nishida, "Phenological eyes network (pen)-a validation network for remote sensing of the terrestrial ecosystems," *AsiaFlux Newsl*, vol. 21, pp. 9–13, 2007.

[27] T. Mizunuma, T. Koyanagi, M. Mencuccini, K. N. Nasahara, L. Wingate, and J. Grace, "The comparison of several colour indices for the photographic recording of canopy phenology of fagus crenata blume in eastern japan," *Plant Ecology & Diversity*, vol. 4, no. 1, pp. 67–77, 2011.

[28] T. M. Saitoh, S. Nagai, N. Saigusa, H. Kobayashi, R. Suzuki, K. N. Nasahara, and H. Muraoka, "Assessing the use of camera-based indices for characterizing canopy phenology in relation to gross primary production in a deciduous broad-leaved and an evergreen coniferous forest in japan," *Ecological Informatics*, vol. 11, pp. 45–54, 2012.

[29] "Australian Phenocam Network." https://phenocam.org.au. Accessed: 2019-08-30.

[30] "TERN - Terrestrial Ecosystem Research Network." https://www.tern.org.au/. Accessed: 2019-08-30.

[31] T. B. Brown, K. R. Hultine, H. Steltzer, E. G. Denny, M. W. Denslow, J. Granados, S. Henderson, D. Moore, S. Nagai, M. SanClements, *et al.*, "Using phenocams to monitor our changing earth: toward a global phenocam network," *Frontiers in Ecology and the Environment*, vol. 14, no. 2, pp. 84–93, 2016.

[32] "FMIPROT & Camera Network Portal." http://fmiprot.fmi.fi. Accessed: 2019-08-30.

[33] G. Filippa, E. Cremonese, M. Migliavacca, M. Galvagno, M. Forkel, L. Wingate, E. Tomelleri, U. M. Di Cella, and A. D. Richardson, "Phenopix: Ar package for image-based vegetation phenology," *Agricultural and Forest Meteorology*, vol. 220, pp. 141–150, 2016.

[34] S. Härer, M. Bernhardt, J. Corripio, and K. Schulz, "Practise-photo rectification and classification software (v. 1.0).," *Geoscientific Model Development Discussions*, vol. 6, no. 1, 2013.

[35] "tmilliman/python-vegindex: Python package to generate vegetation index timeseries from PhenoCam images." https://github.com/tmilliman/python-vegindex. Accessed: 2019-08-30.

[36] "PhenoCam Software Tools." https://phenocam.sr.unh.edu/webcam/tools/. Accessed: 2019-08-30.

[37] R. Salvatori, P. Plini, M. Giusto, M. Valt, R. Salzano, M. Montagnoli, A. Cagnati, G. Crepaz, and D. Sigismondi, "Snow cover monitoring with images from digital camera systems," *European Journal of Remote Sensing*, vol. 43, 2011.

[38] A. Haberkorn, "European snow booklet – an inventory of snow measurements in europe," 2019.

[39] B. Goodison, H. Ferguson, and G. McKay, "Measurement and data analysis," *Handbook of snow*, pp. 191–274, 1981.

[40] V. V. Salomonson and I. Appel, "Estimating fractional snow cover from modis using the normalized difference snow index," *Remote sensing of environment*, vol. 89, no. 3, pp. 351–360, 2004.

[41] S. J. Metsämäki, S. T. Anttila, H. J. Markus, and J. M. Vepsäläinen, "A feasible method for fractional snow cover mapping in boreal zone based on a reflectance model," *Remote sensing of Environment*, vol. 95, no. 1, pp. 77–95, 2005.

[42] M. Bongio, A. N. Arslan, C. M. Tanis, and C. De Michele, "Snow depth estimation by time-lapse photography: Finnish and italian case studies," *The Cryosphere Discussions*, vol. 2019, pp. 1–35, 2019.

[43] J. Pulliainen and M. Hallikainen, "Retrieval of regional snow water equivalent from space-borne passive microwave observations," *Remote sensing of environment*, vol. 75, no. 1, pp. 76–85, 2001.

[44] L. Leppänen, A. Kontu, J. Vehviläinen, J. Lemmetyinen, and J. Pulliainen, "Comparison of traditional and optical grain-size field measurements with snowpack simulations in a taiga snowpack," *Journal of Glaciology*, vol. 61, no. 225, pp. 151–162, 2015.

[45] A. Kontu, J. Lemmetyinen, J. Vehviläinen, L. Leppänen, and J. Pulliainen, "Coupling snowpack-modeled grain size parameters with the hut snow emission model," *Remote sensing of environment*, vol. 194, pp. 33–47, 2017.

[46] J. L. Foster, C. Sun, J. P. Walker, R. Kelly, A. Chang, J. Dong, and H. Powell, "Quantifying the uncertainty in passive microwave snow water equivalent observations," *Remote Sensing of environment*, vol. 94, no. 2, pp. 187–203, 2005.

[47] X. Li, L. Zhang, L. Weihermüller, L. Jiang, and H. Vereecken, "Measurement and simulation of topographic effects on passive microwave remote sensing over mountain areas: A case study from the tibetan plateau," *IEEE Transactions on Geoscience and Remote Sensing*, vol. 52, no. 2, pp. 1489–1501, 2013.

[48] Y. Bühler, M. S. Adams, R. Bösch, and A. Stoffel, "Mapping snow depth in alpine terrain with unmanned aerial systems (uass): potential and limitations," *The Cryosphere*, vol. 10, no. 3, pp. 1075–1088, 2016.

[49] B. Vander Jagt, A. Lucieer, L. Wallace, D. Turner, and M. Durand, "Snow depth retrieval with uas using photogrammetric techniques," *Geosciences*, vol. 5, no. 3, pp. 264–285, 2015.

[50] K. S. J. Brown, *Snow Depth Measurement via Automated Image Recognition*. PhD thesis, Colorado State University. Libraries, 2019.

[51] A. R. Hedrick and H.-P. Marshall, "Automated snow depth measurements in avalanche terrain using time-lapse photography," in *2014 International Snow Science Workshop*, 2014.

[52] S. Metsämäki, O.-P. Mattila, J. Pulliainen, K. Niemi, K. Luojus, and K. Böttcher, "An optical reflectance model-based method for fractional snow cover mapping applicable to continental scale," *Remote Sensing of Environment*, vol. 123, pp. 508–521, 2012.

[53] K. Rittger, T. H. Painter, and J. Dozier, "Assessment of methods for mapping snow cover from modis," *Advances in Water Resources*, vol. 51, pp. 367–380, 2013.

[54] A. Frei, M. Tedesco, S. Lee, J. Foster, D. K. Hall, R. Kelly, and D. A. Robinson, "A review of global satellite-derived snow products," *Advances in Space Research*, vol. 50, no. 8, pp. 1007–1029, 2012.

[55] H. Liang, X. Huang, Y. Sun, Y. Wang, and T. Liang, "Fractional snow-cover mapping based on modis and uav data over the tibetan plateau," *Remote Sensing*, vol. 9, no. 12, p. 1332, 2017.

[56] "Finnish Environment Institute > Finnish Long-Term Socio-Ecological Research network FinLTSER." https://www.syke.fi/projects/lter. Accessed: 2019-08-30.

[57] P. Hari, E. Nikinmaa, T. Pohja, E. Siivola, J. Bäck, T. Vesala, and M. Kulmala, "Station for measuring ecosystem-atmosphere relations: Smear," in *Physical and physiological forest ecology*, pp. 471–487, Springer, 2013.

[58] "SMEAR." http://www.atm.helsinki.fi/SMEAR/. Accessed: 2019-08-30.

[59] P. Hari, M. Kulmala, T. Pohja, T. Lahti, E. Siivola, L. Palva, P. Aalto, K. Hämeri, T. Vesala, S. Luoma, *et al.*, "Air pollution in eastern lapland: challenge for an environmental measurement station.," *Silva Fennica*, vol. 28, 1994.

[60] "ICOS Carbon Portal." https://www.icos-cp.eu/. Accessed: 2019-08-30.

[61] M. Aurela, A. Lohila, J.-P. Tuovinen, J. Hatakka, T. Riutta, and T. Laurila, "Carbon dioxide exchange on a northern boreal fen," *Boreal Environment Research*, vol. 14, pp. 699–710, 2009.

[62] A. Lohila, M. Aurela, J. Hatakka, M. Pihlatie, K. Minkkinen, T. Penttilä, and T. Laurila, "Responses of n2o fluxes to temperature, water table and n deposition in a northern boreal fen," *European journal of soil science*, vol. 61, no. 5, pp. 651–661, 2010.

[63] "National Land Survey of Finland." https://www.maanmittauslaitos.fi/. Accessed: 2019-08-30.

[64] "Maanmittauslaitoksen avoimien kartta-aineistojen latauspalvelu." http://kartat.kapsi.fi/. Accessed: 2019-08-30.

[65] J. G. Corripio, "Snow surface albedo estimation using terrestrial photography," *International Journal of Remote Sensing*, vol. 25, no. 24, pp. 5705–5729, 2004.

[66] J. Wang, G. J. Robinson, and K. White, "Generating viewsheds without using sightlines," *Photogrammetric engineering and remote sensing*, vol. 66, no. 1, pp. 87–90, 2000.

[67] W. J. Schroeder, B. Lorensen, and K. Martin, *The visualization toolkit: an object-oriented approach to 3D graphics*. Kitware, 2004.

[68] P. Drap and J. Lefèvre, "An exact formula for calculating inverse radial lens distortions," *Sensors*, vol. 16, no. 6, p. 807, 2016.

[69] K. Gribbon, C. Johnston, and D. G. Bailey, "A real-time fpga implementation of a barrel distortion correction algorithm with bilinear interpolation," in *Image and Vision Computing New Zealand*, pp. 408–413, 2003.

[70] C. M. Tanis, A. N. Arslan, and T. Laine, "Poster: Snow depth estimation using digital imagery," in *Workshop: Towards a better harmonization of snow observations, modeling and data assimilation in Europe*, pp. 194–195, October 2017.

[71] M. Bongio, A. N. Arslan, C. M. Tanis, and C. De Michele, "Snow depth estimation by time-lapse photography: Finnish and italian case studies," *The Cryosphere Discussions*, vol. 2019, pp. 1–35, 2019.

[72] H. J. Munoz, *CSEWIS: Cloud and Snow Estimates from Webcam Image Streams*. PhD thesis, 2018.

A Annex: Orthoimages and GCPs

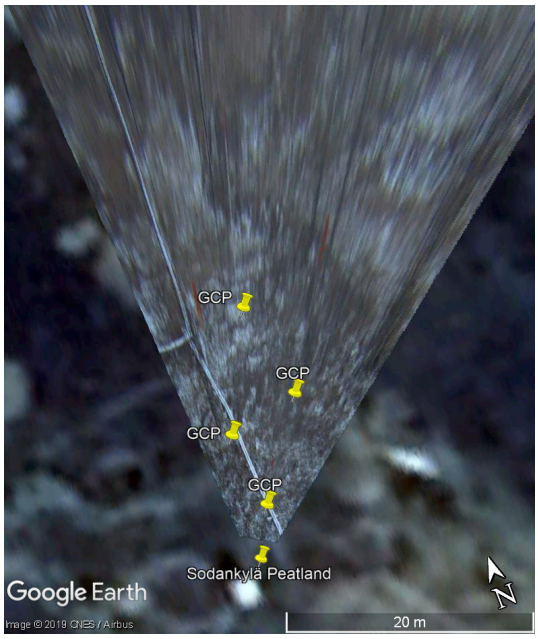

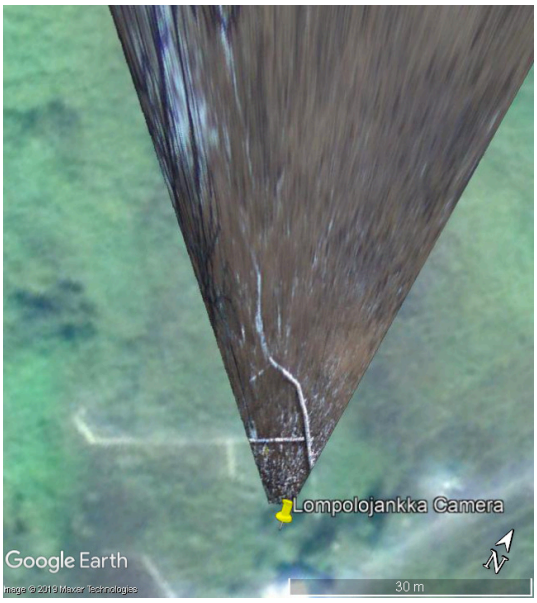

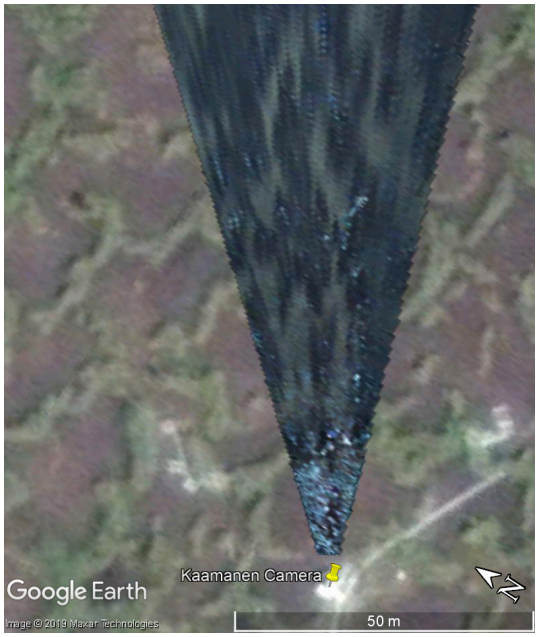

B Annex: NRT Monitoring on the web page

FMIPROT & Camera Network Portal

Fractional snow cover monitoring with MONIMET Camera Network

Results

7 setups are defined for operational monitoring. Click on the buttons to switch to the results of the setups.

1 2 3 4 5 6 7

sodankyla

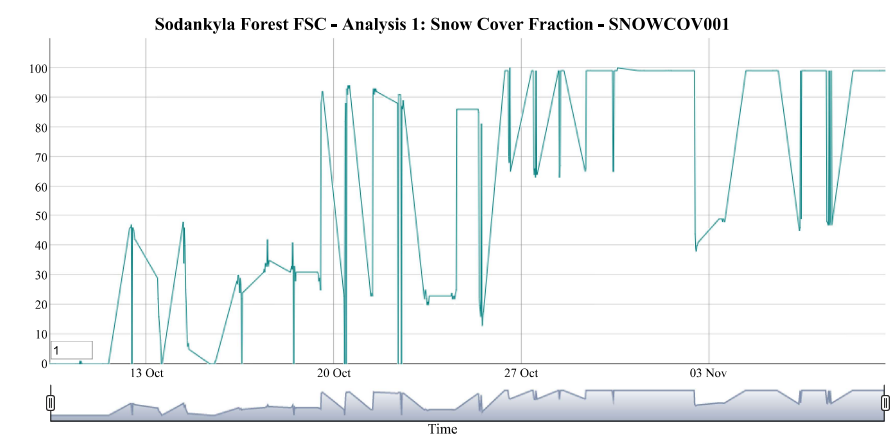

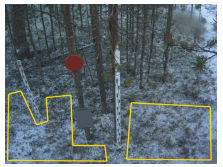

>Setup report page
>Download/Open data file
Plot:
Snow Cover Fraction
Reset plot | Toggle help

>Setup report page
>Download/Open data file

FMIPROT & Camera Network Portal

Snow depth monitoring with MONIMET Camera Network

Results

4 setups are defined for operational monitoring. Click on the buttons to switch to the results of the setups.

1 2 3 4

sodankyla

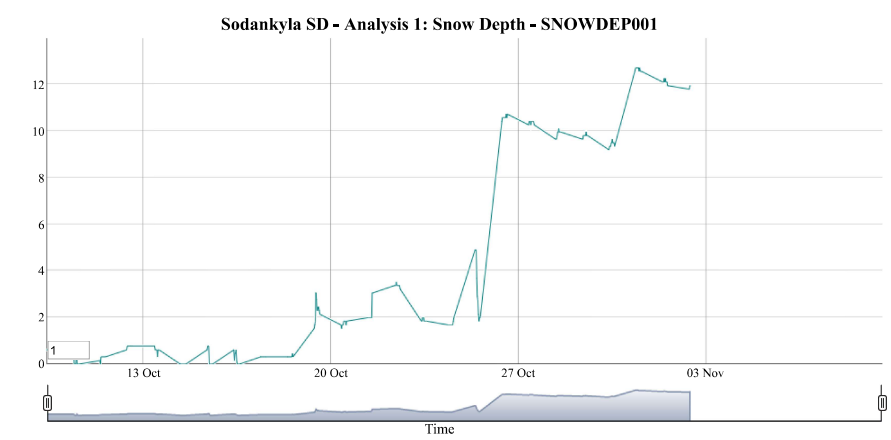

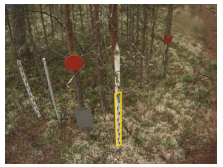

>Setup report page
>Download/Open data file
Plot:
Snow Depth
Reset plot | Toggle help

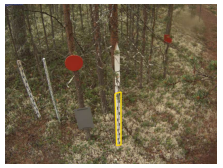

>Setup report page
>Download/Open data file

C Annex: Setup reports of historical analyses

FMIPROT Setup Report | FMIPROT Webpage

Go to: Tammela FSC | Hyytiala FSC | Varrio FSC | Sodankyla Forest FSC | Sodankyla Peatland FSC | Lompolojankka FSC | Kaamanen FSC | Tammela SD | Hyytiala SD | Sodankyla SD | Sodankyla Peatland SD

Tammela FSC

Camera Selection

Camera Network	Camera Name
MONIMET	Tammela Spruce Ground

Temporal Selection

Date and time intervals

	Start	End
Date	2018-08-01	2019-06-30
Time	11:15:00	13:45:00

Masking/ROIs

Run analyses also for each polygon (ROI) separately: False

0.9879,0.4424,0.8652,0.4384,0.8394,0.6929,0.7485,0.697,0.7333,0.901,0.5227,0.903,0.5121,0.9798

Polygon	Coordinates
1	0.1227,0.9475,0.0894,0.7818,0.247,0.5495,0.2394,0.4182,0.3636,0.3576,0.4924,0.398,0.6545,0.4081,0.6318,0.6768,0.4364,0.6707,0.45,(
2	0.9894,0.9798

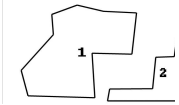

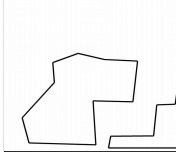

Thresholds

Type	Value	Minimum	Maximum
Image Threshold	Brightness	0.1	1.0
Image Threshold	Luminance	0.0	1.0
ROI Threshold	Red Fraction	0.0	1.0
ROI Threshold	Green Fraction	0.0	1.0
ROI Threshold	Blue Fraction	0.0	1.0
Pixel Threshold	Red Channel	0.0	254.0
Pixel Threshold	Green Channel	0.0	254.0
Pixel Threshold	Blue Channel	0.0	254.0

Analyses

Analysis No	Analysis Name	Analysis Parameters	
		Parameter	Value
1	Snow Cover Fraction - SNOWCOV001	Include Red Channel	Not Selected
		Include Green Channel	Not Selected
		Include Blue Channel	Selected
		Store mid-step and extra output data	Selected
		Use georectification	Selected
		Spatial extent	4;-4.6;13;3.6
		Spatial Extent Coordinate System	ETRS-TM35FIN(EPSG:3067) GEOID with Camera at (
		Spatial resolution	0.001
		DEM Dataset	NLS-DEM2
		Camera coordinates	60.64598306;23.80650111
		Camera coordinate system	WGS84(EPSG:4326)
		Camera Height	4
		Horizontal position	-1
		Target Direction	90
		Vertical position	23.3
		Focal length	4
		Scaling factor	0.77
		Interpolate DEM Data	Selected
		Flat terrain	Not Selected
		Radial Center	0.0;0.0
		Horizontal coefficient	0.0
		Vertical Coefficient	0.0

Hyytiala FSC

Camera Selection

Camera Network	Camera Name
MONIMET	Hyytiala Pine Ground

Temporal Selection

Date and time intervals

	Start	End
Date	2018-08-01	2019-06-30
Time	11:15:00	13:45:00

Masking/ROIs

Run analyses also for each polygon (ROI) separately: False

Polygon	Coordinates
1	0.1136,0.4525,0.1364,0.402,0.0909,0.2303,0.1682,0.196,0.2,0.2566,0.247,0.2606,0.2712,0.4768,0.3394,0.4646,0.2939,0.0828, 0.6606,0.0384,0.9333,0.3535,0.9121,0.4606,0.9818,0.5293,0.9591,0.8566,0.8894,0.9596,0.5258, 0.9859,0.503,0.2586,0.4636,0.2586,0.4606,0.5293,0.4652,0.5515,0.5136,0.5576,0.5258,0.9838,0.2455,0.9616

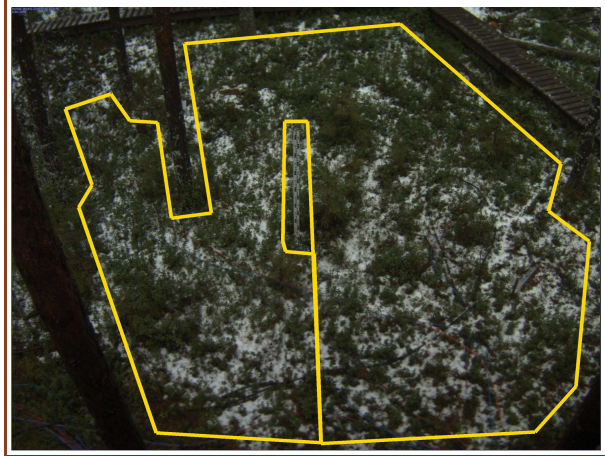

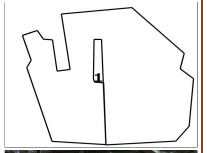

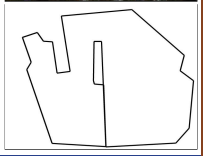

Thresholds

Type	Value	Minimum	Maximum
Image Threshold	Brightness	0.1	1.0
Image Threshold	Luminance	0.0	1.0

ROI Threshold	Red Fraction	0.0	1.0
ROI Threshold	Green Fraction	0.0	1.0
ROI Threshold	Blue Fraction	0.0	1.0
Pixel Threshold	Red Channel	0.0	254.0
Pixel Threshold	Green Channel	0.0	254.0
Pixel Threshold	Blue Channel	0.0	254.0

Analyses

Analysis No	Analysis Name	Parameter	Value
1	Snow Cover Fraction - SNOWCOV001	Include Red Channel	Not Selected
		Include Green Channel	Not Selected
		Include Blue Channel	Selected
		Store mid-step and extra output data	Selected
		Use georectification	Selected
		Spatial extent	1.7;-5;10;1
		Spatial Extent Coordinate System	ETRS-TM35FIN(EPSG:3067) GEOID with Camera at Origin
		Spatial resolution	0.00075
		DEM Dataset	NLS-DEM2
		Camera coordinates	61.84740;24.29529
		Camera coordinate system	WGS84(EPSG:4326)
		Camera Height	4.3
		Horizontal position	0.0
		Target Direction	111
		Vertical position	42
		Focal length	4
		Scaling factor	0.82
		Interpolate DEM Data	Selected
		Flat terrain	Not Selected
		Radial Center	0.0;0.0
		Horizontal coefficient	0.025
		Vertical Coefficient	0.025

Varrio FSC

Camera Selection

Camera Network	Camera Name
MONIMET	Varrio Pine Ground

Temporal Selection

Date and time intervals

	Start	End
Date	2018-08-01	2019-06-30
Time	11:15:00	13:45:00

Masking/ROIs

Run analyses also for each polygon (ROI) separately: False

Polygon	Coordinates
1	0.5727,0.3899,0.4409,0.5131,0.4136,0.6869,0.4091,0.9899,0.9742,0.9717,0.9909,0.4848,0.8955,0.4606,0.8636, 0.3818,0.8197,0.3838,0.8091,0.4768,0.75,0.5677,0.6439,0.602,0.6318,0.402,0.6212,0.3697,0.5697,0.3576

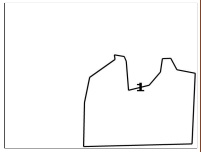

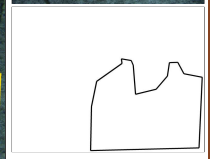

Thresholds

Type	Value	Minimum	Maximum
Image Threshold	Brightness	0.1	1.0
Image Threshold	Luminance	0.0	1.0
ROI Threshold	Red Fraction	0.0	1.0
ROI Threshold	Green Fraction	0.0	1.0
ROI Threshold	Blue Fraction	0.0	1.0
Pixel Threshold	Red Channel	0.0	254.0
Pixel Threshold	Green Channel	0.0	254.0
Pixel Threshold	Blue Channel	0.0	254.0

Analyses

Analysis No	Analysis Name	Parameter	Value
1	Snow Cover Fraction - SNOWCOV001	Include Red Channel	Not Selected
		Include Green Channel	Not Selected
		Include Blue Channel	Selected
		Store mid-step and extra output data	Selected
		Use georectification	Selected
		Spatial extent	-4.5;2.5;-0.5;8
		Spatial Extent Coordinate System	ETRS-TM35FIN(EPSG:3067) GEOID with Camera at Origin
		Spatial resolution	0.0006
		DEM Dataset	NLS-DEM2
		Camera coordinates	67.75492;29.60989
		Camera coordinate system	WGS84(EPSG:4326)
		Camera Height	3.5
		Horizontal position	0.0
		Target Direction	320
		Vertical position	30
		Focal length	4
		Scaling factor	1
		Interpolate DEM Data	Selected
		Flat terrain	Not Selected
		Radial Center	0.0;0.0
		Horizontal coefficient	0.08
		Vertical Coefficient	0.08

Sodankyla Forest FSC

Camera Selection

Camera Network	Camera Name
MONIMET	Sodankyla Pine Ground

Temporal Selection

Date and time intervals

	Start	End
Date	2018-08-01	2019-06-30
Time	11:15:00	13:45:00

Masking/ROIs

Run analyses also for each polygon (ROI) separately: False

Polygon	Coordinates
1	0.9725,0.9747,0.9688,0.6427,0.5956,0.6174,0.5739,0.9697
2	0.0123,0.9773,0.017,0.5631,0.0748,0.5442,0.1496,0.7551,0.2027,0.7311,0.1951, 0.5846,0.3106,0.5694,0.3191,0.8838,0.4706,0.8838,0.4801,0.9823

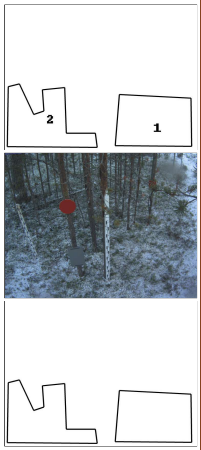

Thresholds

Type	Value	Minimum	Maximum
Image Threshold	Brightness	0.1	1.0
Image Threshold	Luminance	0.0	1.0
ROI Threshold	Red Fraction	0.0	1.0
ROI Threshold	Green Fraction	0.0	1.0
ROI Threshold	Blue Fraction	0.0	1.0
Pixel Threshold	Red Channel	0.0	254.0
Pixel Threshold	Green Channel	0.0	254.0
Pixel Threshold	Blue Channel	0.0	254.0

Analyses

Analysis No	Analysis Name	Analysis Parameters

Parameter	Value
Include Red Channel	Not Selected
Include Green Channel	Not Selected
Include Blue Channel	Selected
Store mid-step and extra output data	Selected
Use georectification	Selected
Spatial extent	1.3;-2.2;3.4;1.8
Spatial Extent Coordinate System	ETRS-TM35FIN(EPSG:3067) GEOID with Camera at Origin
Spatial resolution	0.0005
DEM Dataset	NLS-DEM2
Camera coordinates	67.3618;26.638167
Camera coordinate system	WGS84(EPSG:4326)
Camera Height	2.46
Horizontal position	0.0
Target Direction	96
Vertical position	35.3
Focal length	4
Scaling factor	0.74
Interpolate DEM Data	Selected
Flat terrain	Not Selected
Radial Center	0.0;0.0
Horizontal coefficient	0.08
Vertical Coefficient	0.08

Sodankyla Peatland FSC

Camera Selection

Camera Network	Camera Name
MONIMET	Sodankyla Pine Peatland

Temporal Selection

Date and time intervals

	Start	End
Date	2018-08-01	2019-06-30
Time	11:15:00	13:45:00

Masking/ROIs

Run analyses also for each polygon (ROI) separately: False

Polygon	Coordinates
1	0.9864,0.3455,0.6333,0.297,0.6379,0.4566,0.9652,0.6424
2	0.5379,0.4,0.3833,0.3212,0.3818,0.2949,0.5424,0.2909
3	0.0288,0.4424,0.1985,0.3838,0.5939,0.7293,0.0242,0.7475

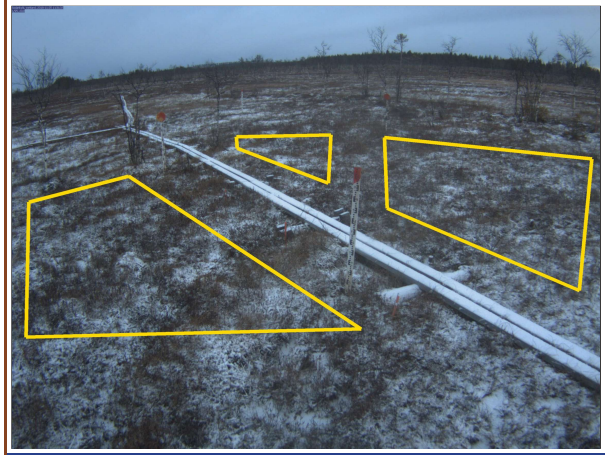

Thresholds

Type	Value	Minimum	Maximum
Image Threshold	Brightness	0.1	1.0
Image Threshold	Luminance	0.0	1.0
ROI Threshold	Red Fraction	0.0	1.0
ROI Threshold	Green Fraction	0.0	1.0
ROI Threshold	Blue Fraction	0.0	1.0

	Pixel Threshold	Red Channel	0.0	254.0
	Pixel Threshold	Green Channel	0.0	254.0
	Pixel Threshold	Blue Channel	0.0	254.0

Analyses

Analysis No	Analysis Name	Analysis Parameters	
		Parameter	Value
1	Snow Cover Fraction - SNOWCOV001	Include Red Channel	Not Selected
		Include Green Channel	Not Selected
		Include Blue Channel	Selected
		Store mid-step and extra output data	Selected
		Use georectification	Selected
		Spatial extent	-1.5;2;9.5;14
		Spatial Extent Coordinate System	ETRS-TM35FIN(EPSG:3067) GEOID with Camera at Origin
		Spatial resolution	0.0005
		DEM Dataset	NLS-DEM2
		Camera coordinates	67.368517;26.654483
		Camera coordinate system	WGS84(EPSG:4326)
		Camera Height	2.08
		Horizontal position	-2
		Target Direction	23.4
		Vertical position	18
		Focal length	4
		Scaling factor	0.69
		Interpolate DEM Data	Selected
		Flat terrain	Not Selected
		Radial Center	0.0;0.0
		Horizontal coefficient	0.13
		Vertical Coefficient	0.13

Lompolojankka FSC

Camera Selection

Camera Network	Camera Name
MONIMET	Lompolojankka Wetland Ground

Temporal Selection

Date and time intervals

	Start	End
Date	2018-08-01	2019-06-30
Time	11:15:00	13:45:00

Masking/ROIs

Run analyses also for each polygon (ROI) separately: False

Polygon	Coordinates
1	0.5833,0.4444,0.9727,0.7515,0.9742,0.9697,0.397,0.9818,0.3015,0.9051,0.0727,0.8323,0.0955,0.7232,0.2485,0.7172,0.2439,0.4384
2	0.9803,0.5838,0.6121,0.3273,0.6182,0.2525,0.8197,0.2545,0.8364,0.3131,0.8894,0.2949,0.9,0.2606,0.9848,0.2485
3	0.4485,0.3758,0.2652,0.3737,0.2591,0.2929,0.3152,0.2909,0.4182,0.3111
4	0.5576,0.297,0.5606,0.2404,0.3152,0.2162,0.203,0.2101,0.2106,0.2566,0.303,0.2545,0.3485,0.2505

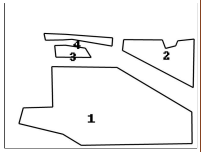

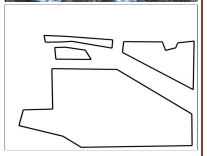

Thresholds

Type	Value	Minimum	Maximum
Image Threshold	Brightness	0.1	1.0
Image Threshold	Luminance	0.0	1.0
ROI Threshold	Red Fraction	0.0	1.0
ROI Threshold	Green Fraction	0.0	1.0
ROI Threshold	Blue Fraction	0.0	1.0
Pixel Threshold	Red Channel	0.0	254.0
Pixel Threshold	Green Channel	0.0	254.0
Pixel Threshold	Blue Channel	0.0	254.0

Analyses

Analysis No	Analysis Name	Analysis Parameters	
		Parameter	Value
1	Snow Cover Fraction - SNOWCOV001	Include Red Channel	Not Selected
		Include Green Channel	Not Selected
		Include Blue Channel	Selected
		Store mid-step and extra output data	Selected
		Use georectification	Selected
		Spatial extent	-23;2;0;31
		Spatial Extent Coordinate System	ETRS-TM35FIN(EPSG:3067) GEOID with Camera at Origin
		Spatial resolution	0.001
		DEM Dataset	NLS-DEM10
		Camera coordinates	67.997393;24.209355
		Camera coordinate system	WGS84(EPSG:4326)
		Camera Height	2.5
		Horizontal position	3
		Target Direction	341
		Vertical position	17
		Focal length	4
		Scaling factor	0.7
		Interpolate DEM Data	Selected
		Flat terrain	Not Selected
		Radial Center	0.0;0.0
		Horizontal coefficient	0.05
		Vertical Coefficient	0.05

Kaamanen FSC

Camera Selection

Camera Network	Camera Name
MONIMET	Kaamanen Wetland Ground

Temporal Selection

Date and time intervals

	Start	End
Date	2018-08-01	2019-06-30
Time	11:15:00	13:45:00

Masking/ROIs

Run analyses also for each polygon (ROI) separately: False

Polygon	Coordinates
1	0.9909,0.297,0.4121,0.3091,0.1197,0.3273,0.0076,0.3556,0.0061,0.9919,0.7667,0.9939,0.7712,0.899,0.8561,0.9091,0.85,0.5192,0.9879,0

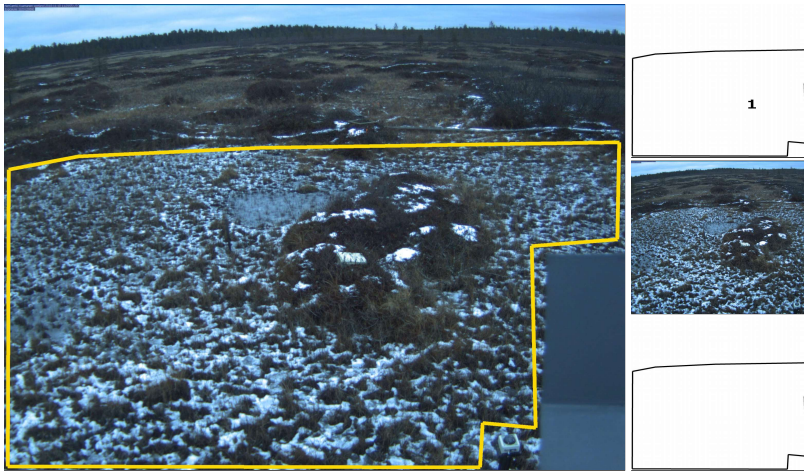

Thresholds

Type	Value	Minimum	Maximum
Image Threshold	Brightness	0.1	1.0
Image Threshold	Luminance	0.0	1.0
ROI Threshold	Red Fraction	0.0	1.0
ROI Threshold	Green Fraction	0.0	1.0
ROI Threshold	Blue Fraction	0.0	1.0
Pixel Threshold	Red Channel	0.0	254.0
Pixel Threshold	Green Channel	0.0	254.0
Pixel Threshold	Blue Channel	0.0	254.0

Analyses

Analysis No	Analysis Name	Analysis Parameters	
1	Snow Cover Fraction - SNOWCOV001	**Parameter**	**Value**
		Include Red Channel	Not Selected
		Include Green Channel	Not Selected
		Include Blue Channel	Selected
		Store mid-step and extra output data	Selected
		Use georectification	Selected
		Spatial extent	3.5;0;23;17
		Spatial Extent Coordinate System	ETRS-TM35FIN(EPSG:3067) GEOID with Camera at C
		Spatial resolution	0.001
		DEM Dataset	NLS-DEM10
		Camera coordinates	69.140583;27.269817
		Camera coordinate system	WGS84(EPSG:4326)
		Camera Height	2.6
		Horizontal position	-1
		Target Direction	55.5
		Vertical position	12
		Focal length	4
		Scaling factor	1.24
		Interpolate DEM Data	Selected
		Flat terrain	Not Selected
		Radial Center	0.0;0.0
		Horizontal coefficient	0.1
		Vertical Coefficient	0.1

Tammela SD

Camera Selection

Camera Network	Camera Name
MONIMET	Tammela Spruce Ground

Temporal Selection

Date and time intervals

	Start	End
Date	2018-08-01	2019-06-30
Time	11:15:00	13:45:00

Masking/ROIs

Run analyses also for each polygon (ROI) separately: False

0.5116,0.7051,0.4848,0.7063,0.4866,0.918

Polygon	Coordinates
1	0.4893,0.9168,0.5071,0.918

Thresholds

Type	Value	Minimum	Maximum
Image Threshold	Brightness	0.1	1.0
Image Threshold	Luminance	0.0	1.0
ROI Threshold	Red Fraction	0.0	1.0
ROI Threshold	Green Fraction	0.0	1.0
ROI Threshold	Blue Fraction	0.0	1.0
Pixel Threshold	Red Channel	0.0	255.0
Pixel Threshold	Green Channel	0.0	255.0
Pixel Threshold	Blue Channel	0.0	255.0

Analyses

Analysis No	Analysis Name	Analysis Parameters	
		Parameter	Value
1	Snow Depth - SNOWDEP001	Height of the object	120
		Threshold Value	65
		Gaussian filter sigma	1
		Bias	0

Hyytiala SD

Camera Selection

Camera Network	Camera Name
MONIMET	Hyytiala Pine Ground

Temporal Selection

Date and time intervals

	Start	End
Date	2018-08-01	2019-06-30
Time	11:15:00	13:45:00

Masking/ROIs

Run analyses also for each polygon (ROI) separately: False

Polygon	Coordinates
1	0.4749,0.5094,0.4937,0.5087,0.4953,0.2683,0.4697,0.2697,0.4734,0.508

Thresholds

Type	Value	Minimum	Maximum
Image Threshold	Brightness	0.1	1.0
Image Threshold	Luminance	0.0	1.0
ROI Threshold	Red Fraction	0.0	1.0
ROI Threshold	Green Fraction	0.0	1.0
ROI Threshold	Blue Fraction	0.0	1.0
Pixel Threshold	Red Channel	0.0	255.0
Pixel Threshold	Green Channel	0.0	255.0
Pixel Threshold	Blue Channel	0.0	255.0

Analyses

Analysis No	Analysis Name	Analysis Parameters	
		Parameter	Value
1	Snow Depth - SNOWDEP001	Height of the object	125
		Threshold Value	40
		Gaussian filter sigma	1
		Bias	0

Sodankyla Forest SD

Camera Selection

Camera Network	Camera Name
MONIMET	Sodankyla Pine Ground

Temporal Selection

Date and time intervals

	Start	End
Date	2018-08-01	2019-06-30
Time	11:15:00	13:45:00

Masking/ROIs

Run analyses also for each polygon (ROI) separately: False

Polygon	Coordinates
1	0.5473,0.8801,0.5265,0.8851,0.5189,0.5606,0.5473,0.5492

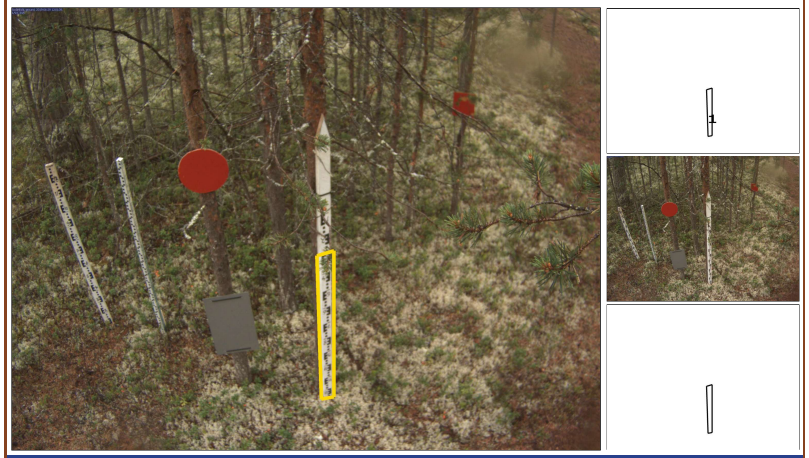

Thresholds

Type	Value	Minimum	Maximum
Image Threshold	Brightness	0.1	1.0
Image Threshold	Luminance	0.0	1.0
ROI Threshold	Red Fraction	0.0	1.0
ROI Threshold	Green Fraction	0.0	1.0
ROI Threshold	Blue Fraction	0.0	1.0
Pixel Threshold	Red Channel	0.0	255.0
Pixel Threshold	Green Channel	0.0	255.0
Pixel Threshold	Blue Channel	0.0	255.0

Analyses

Analysis No	Analysis Name	Analysis Parameters	
		Parameter	Value
1	Snow Depth - SNOWDEP001	Height of the object	100
		Threshold Value	80
		Gaussian filter sigma	1
		Bias	0

Sodankyla Peatland SD

Camera Selection

Camera Network	Camera Name
MONIMET	Sodankyla Pine Peatland

Temporal Selection

Date and time intervals

	Start	End
Date	2018-08-01	2019-06-30
Time	11:15:00	13:45:00

Masking/ROIs

Run analyses also for each polygon (ROI) separately: False

Polygon	Coordinates
1	0.5644,0.6477,0.5767,0.6503,0.5928,0.4141,0.5767,0.4154

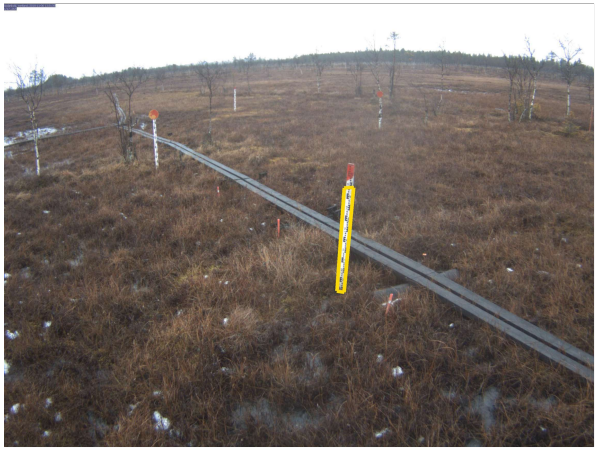

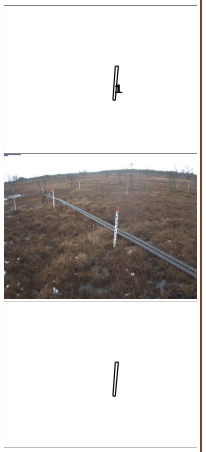

Thresholds

Type	Value	Minimum	Maximum
Image Threshold	Brightness	0.1	1.0
Image Threshold	Luminance	0.0	1.0
ROI Threshold	Red Fraction	0.0	1.0
ROI Threshold	Green Fraction	0.0	1.0
ROI Threshold	Blue Fraction	0.0	1.0
Pixel Threshold	Red Channel	0.0	255.0
Pixel Threshold	Green Channel	0.0	255.0
Pixel Threshold	Blue Channel	0.0	255.0

Analyses

Analysis No	Analysis Name	Analysis Parameters	
		Parameter	Value
1	Snow Depth - SNOWDEP001	Height of the object	100
		Threshold Value	80
		Gaussian filter sigma	1
		Bias	0

D Annex: Setup reports of operational monitoring analyses

FMIPROT Setup Report | FMIPROT Webpage

Go to: Tammela FSC | Hyytiala FSC | Varrio FSC | Sodankyla Forest FSC | Sodankyla Peatland FSC | Lompolojankka FSC | Kaamanen FSC | Tammela SD | Hyytiala SD | Sodankyla SD | Sodankyla Peatland SD

Tammela FSC

Camera Selection

Camera Network	Camera Name
MONIMET	Tammela Spruce Ground

Temporal Selection

Latest one month

	Start	End
Date	N/A	N/A
Time	11:15:00	13:45:00

Masking/ROIs

Run analyses also for each polygon (ROI) separately: False

0.9879,0.4424,0.8652,0.4384,0.8394,0.6929,0.7485,0.697,0.7333,0.901,0.5227,0.903,0.5121,0.9798

Polygon	Coordinates
1	0.1227,0.9475,0.0894,0.7818,0.247,0.5495,0.2394,0.4182,0.3636,0.3576,0.4924,0.398,0.6545,0.4081,0.6318,0.6768,0.4364,0.6707,0.45,(
2	0.9894,0.9798

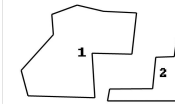

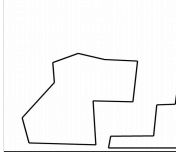

Thresholds

Type	Value	Minimum	Maximum
Image Threshold	Brightness	0.1	1.0
Image Threshold	Luminance	0.0	1.0
ROI Threshold	Red Fraction	0.0	1.0
ROI Threshold	Green Fraction	0.0	1.0
ROI Threshold	Blue Fraction	0.0	1.0
Pixel Threshold	Red Channel	0.0	254.0
Pixel Threshold	Green Channel	0.0	254.0
Pixel Threshold	Blue Channel	0.0	254.0

Analyses

Analysis No	Analysis Name	Analysis Parameters	
		Parameter	Value
1	Snow Cover Fraction - SNOWCOV001	Include Red Channel	Not Selected
		Include Green Channel	Not Selected
		Include Blue Channel	Selected
		Store mid-step and extra output data	Selected
		Use georectification	Selected
		Spatial extent	4;-4.6;13;3.6
		Spatial Extent Coordinate System	ETRS-TM35FIN(EPSG:3067) GEOID with Camera at (
		Spatial resolution	0.001
		DEM Dataset	NLS-DEM2
		Camera coordinates	60.64598306;23.80650111
		Camera coordinate system	WGS84(EPSG:4326)
		Camera Height	4
		Horizontal position	-1
		Target Direction	90
		Vertical position	23.3
		Focal length	4
		Scaling factor	0.77
		Interpolate DEM Data	Selected
		Flat terrain	Not Selected
		Radial Center	0.0;0.0
		Horizontal coefficient	0.0
		Vertical Coefficient	0.0
2	Create animation	Parameter	Value
		Duration	30
		Frames per second	12
		Resolution	720p
		Format	MP4

Hyytiala FSC

Camera Selection

Camera Network	Camera Name
MONIMET	Hyytiala Pine Ground

Temporal Selection

Latest one month

	Start	End
Date	N/A	N/A
Time	11:15:00	13:45:00

Masking/ROIs

Run analyses also for each polygon (ROI) separately: False

Polygon	Coordinates
1	0.1136,0.4525,0.1364,0.402,0.0909,0.2303,0.1682,0.196,0.2,0.2566,0.247,0.2606,0.2712,0.4768,0.3394,0.4646,0.2939,0.0828, 0.6606,0.0384,0.9333,0.3535,0.9121,0.4606,0.9818,0.5293,0.9591,0.8566,0.8894,0.9596,0.5258, 0.9859,0.503,0.2586,0.4636,0.2586,0.4606,0.5293,0.4652,0.5515,0.5136,0.5576,0.5258,0.9838,0.2455,0.9616

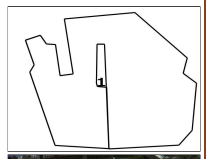

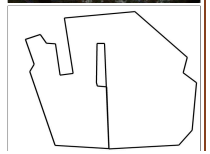

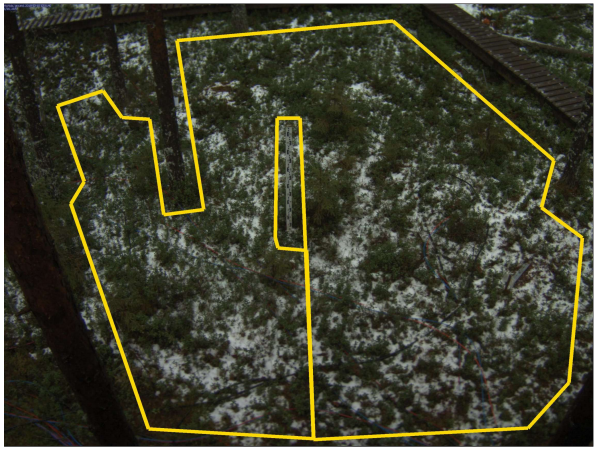

Thresholds

Type	Value	Minimum	Maximum
Image Threshold	Brightness	0.1	1.0
Image Threshold	Luminance	0.0	1.0
ROI Threshold	Red Fraction	0.0	1.0
ROI Threshold	Green Fraction	0.0	1.0
ROI Threshold	Blue Fraction	0.0	1.0
Pixel Threshold	Red Channel	0.0	254.0
Pixel Threshold	Green Channel	0.0	254.0
Pixel Threshold	Blue Channel	0.0	254.0

Analyses

Analysis No	Analysis Name	Analysis Parameters	
		Parameter	Value
1	Snow Cover Fraction - SNOWCOV001	Include Red Channel	Not Selected
		Include Green Channel	Not Selected
		Include Blue Channel	Selected
		Store mid-step and extra output data	Selected
		Use georectification	Selected
		Spatial extent	1.7;-5;10;1
		Spatial Extent Coordinate System	ETRS-TM35FIN(EPSG:3067) GEOID with Camera at Origin
		Spatial resolution	0.00075
		DEM Dataset	NLS-DEM2
		Camera coordinates	61.84740;24.29529
		Camera coordinate system	WGS84(EPSG:4326)
		Camera Height	4.3
		Horizontal position	0.0
		Target Direction	111
		Vertical position	42
		Focal length	4
		Scaling factor	0.82
		Interpolate DEM Data	Selected
		Flat terrain	Not Selected
		Radial Center	0.0;0.0
		Horizontal coefficient	0.025
		Vertical Coefficient	0.025

2	Create animation	Parameter	Value
		Duration	30
		Frames per second	12
		Resolution	720p
		Format	MP4

Varrio FSC

Camera Selection

Camera Network	Camera Name
MONIMET	Varrio Pine Ground

Temporal Selection

Latest one month

	Start	End
Date	N/A	N/A
Time	11:15:00	13:45:00

Masking/ROIs

Run analyses also for each polygon (ROI) separately: False

Polygon	Coordinates
1	0.5727,0.3899,0.4409,0.5131,0.4136,0.6869,0.4091,0.9899,0.9742,0.9717,0.9909,0.4848,0.8955,0.4606,0.8636, 0.3818,0.8197,0.3838,0.8091,0.4768,0.75,0.5677,0.6439,0.602,0.6318,0.402,0.6212,0.3697,0.5697,0.3576

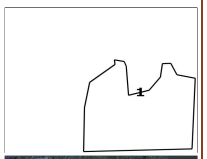

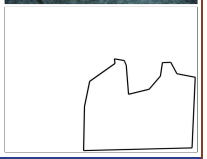

Thresholds

Type	Value	Minimum	Maximum
Image Threshold	Brightness	0.1	1.0
Image Threshold	Luminance	0.0	1.0
ROI Threshold	Red Fraction	0.0	1.0
ROI Threshold	Green Fraction	0.0	1.0
ROI Threshold	Blue Fraction	0.0	1.0
Pixel Threshold	Red Channel	0.0	254.0
Pixel Threshold	Green Channel	0.0	254.0
Pixel Threshold	Blue Channel	0.0	254.0

Analyses

Analysis No	Analysis Name	Analysis Parameters	
		Parameter	Value
1	Snow Cover Fraction - SNOWCOV001	Include Red Channel	Not Selected
		Include Green Channel	Not Selected
		Include Blue Channel	Selected
		Store mid-step and extra output	Selected

		data	
		Use georectification	Selected
		Spatial extent	-4.5;2.5;-0.5;8
		Spatial Extent Coordinate System	ETRS-TM35FIN(EPSG:3067) GEOID with Camera at Origin
		Spatial resolution	0.0006
		DEM Dataset	NLS-DEM2
		Camera coordinates	67.75492;29.60989
		Camera coordinate system	WGS84(EPSG:4326)
		Camera Height	3.5
		Horizontal position	0.0
		Target Direction	320
		Vertical position	30
		Focal length	4
		Scaling factor	1
		Interpolate DEM Data	Selected
		Flat terrain	Not Selected
		Radial Center	0.0;0.0
		Horizontal coefficient	0.08
		Vertical Coefficient	0.08

		Parameter	Value
		Duration	30
2	Create animation	Frames per second	12
		Resolution	720p
		Format	MP4

Sodankyla Forest FSC

Camera Selection

Camera Network	Camera Name
MONIMET	Sodankyla Pine Ground

Temporal Selection

Latest one month

	Start	End
Date	N/A	N/A
Time	11:15:00	13:45:00

Masking/ROIs

Run analyses also for each polygon (ROI) separately: False

Polygon	Coordinates
1	0.9725,0.9747,0.9688,0.6427,0.5956,0.6174,0.5739,0.9697
2	0.0123,0.9773,0.017,0.5631,0.0748,0.5442,0.1496,0.7551,0.2027,0.7311,0.1951, 0.5846,0.3106,0.5694,0.3191,0.8838,0.4706,0.8838,0.4801,0.9823

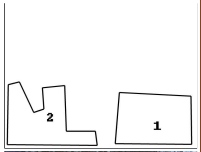

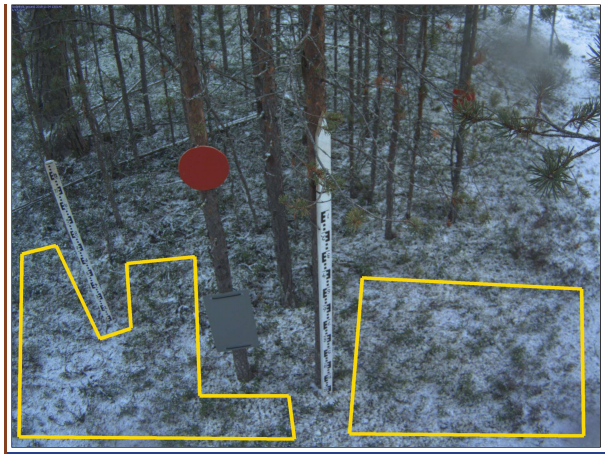

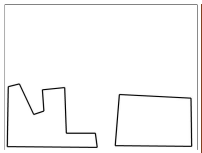

Thresholds

Type	Value	Minimum	Maximum
Image Threshold	Brightness	0.1	1.0
Image Threshold	Luminance	0.0	1.0
ROI Threshold	Red Fraction	0.0	1.0
ROI Threshold	Green Fraction	0.0	1.0
ROI Threshold	Blue Fraction	0.0	1.0
Pixel Threshold	Red Channel	0.0	254.0
Pixel Threshold	Green Channel	0.0	254.0
Pixel Threshold	Blue Channel	0.0	254.0

Analyses

Analysis No	Analysis Name	Analysis Parameters	
		Parameter	Value
		Include Red Channel	Not Selected
		Include Green Channel	Not Selected
		Include Blue Channel	Selected
		Store mid-step and extra output data	Selected
		Use georectification	Selected
		Spatial extent	1.3;-2.2;3.4;1.8
		Spatial Extent Coordinate System	ETRS-TM35FIN(EPSG:3067) GEOID with Camera at Origin
		Spatial resolution	0.0005
		DEM Dataset	NLS-DEM2
1	Snow Cover Fraction - SNOWCOV001	Camera coordinates	67.3618;26.638167
		Camera coordinate system	WGS84(EPSG:4326)
		Camera Height	2.46
		Horizontal position	0.0
		Target Direction	96
		Vertical position	35.3
		Focal length	4
		Scaling factor	0.74
		Interpolate DEM Data	Selected
		Flat terrain	Not Selected
		Radial Center	0.0;0.0
		Horizontal coefficient	0.08
		Vertical Coefficient	0.08

		Parameter	Value
2	Create animation	Duration	30
		Frames per second	12
		Resolution	720p
		Format	MP4

Sodankyla Peatland FSC

Camera Selection

Camera Network	Camera Name
MONIMET	Sodankyla Pine Peatland

Temporal Selection

Latest one month

	Start	End
Date	N/A	N/A
Time	11:15:00	13:45:00

Masking/ROIs

Run analyses also for each polygon (ROI) separately: False

Polygon	Coordinates
1	0.9864,0.3455,0.6333,0.297,0.6379,0.4566,0.9652,0.6424
2	0.5379,0.4,0.3833,0.3212,0.3818,0.2949,0.5424,0.2909
3	0.0288,0.4424,0.1985,0.3838,0.5939,0.7293,0.0242,0.7475

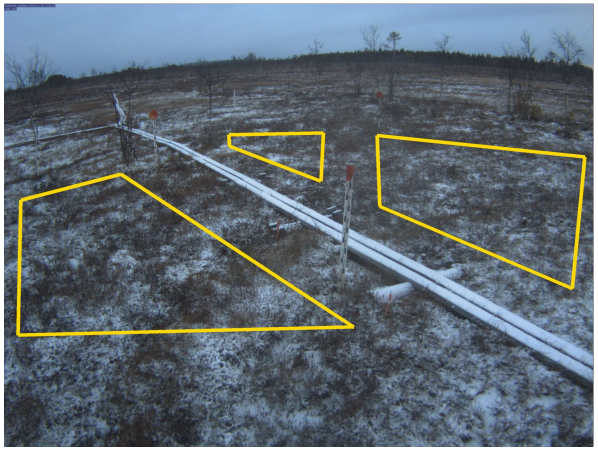

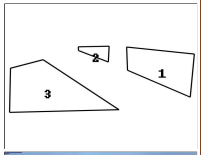

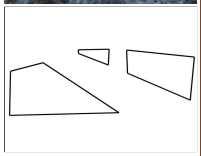

Thresholds

Type	Value	Minimum	Maximum
Image Threshold	Brightness	0.1	1.0
Image Threshold	Luminance	0.0	1.0
ROI Threshold	Red Fraction	0.0	1.0
ROI Threshold	Green Fraction	0.0	1.0
ROI Threshold	Blue Fraction	0.0	1.0
Pixel Threshold	Red Channel	0.0	254.0
Pixel Threshold	Green Channel	0.0	254.0
Pixel Threshold	Blue Channel	0.0	254.0

Analyses

Analysis No	Analysis Name	Analysis Parameters

Parameter	Value
Include Red Channel	Not Selected
Include Green Channel	Not Selected
Include Blue Channel	Selected
Store mid-step and extra output data	Selected
Use georectification	Selected
Spatial extent	-1.5;2;9.5;14
Spatial Extent Coordinate System	ETRS-TM35FIN(EPSG:3067) GEOID with Camera at Origin
Spatial resolution	0.0005
DEM Dataset	NLS-DEM2
Camera coordinates	67.368517;26.654483
Camera coordinate system	WGS84(EPSG:4326)
Camera Height	2.08
Horizontal position	-2
Target Direction	23.4
Vertical position	18
Focal length	4
Scaling factor	0.69
Interpolate DEM Data	Selected
Flat terrain	Not Selected
Radial Center	0.0;0.0
Horizontal coefficient	0.13
Vertical Coefficient	0.13

		Parameter	Value
2	Create animation	Duration	30
		Frames per second	12
		Resolution	720p
		Format	MP4

Lompolojankka FSC

Camera Selection

Camera Network	Camera Name
MONIMET	Lompolojankka Wetland Ground

Temporal Selection

Latest one month

	Start	End
Date	N/A	N/A
Time	11:15:00	13:45:00

Masking/ROIs

Run analyses also for each polygon (ROI) separately: False

Polygon	Coordinates
1	0.5833,0.4444,0.9727,0.7515,0.9742,0.9697,0.397,0.9818,0.3015,0.9051,0.0727,0.8323,0.0955,0.7232,0.2485,0.7172,0.2439,0.4384
2	0.9803,0.5838,0.6121,0.3273,0.6182,0.2525,0.8197,0.2545,0.8364,0.3131,0.8894,0.2949,0.9,0.2606,0.9848,0.2485
3	0.4485,0.3758,0.2652,0.3737,0.2591,0.2929,0.3152,0.2909,0.4182,0.3111
4	0.5576,0.297,0.5606,0.2404,0.3152,0.2162,0.203,0.2101,0.2106,0.2566,0.303,0.2545,0.3485,0.2505

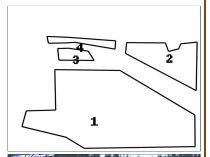

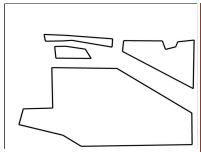

Thresholds

Type	Value	Minimum	Maximum
Image Threshold	Brightness	0.1	1.0
Image Threshold	Luminance	0.0	1.0
ROI Threshold	Red Fraction	0.0	1.0
ROI Threshold	Green Fraction	0.0	1.0
ROI Threshold	Blue Fraction	0.0	1.0
Pixel Threshold	Red Channel	0.0	254.0
Pixel Threshold	Green Channel	0.0	254.0
Pixel Threshold	Blue Channel	0.0	254.0

Analyses

Analysis No	Analysis Name	Analysis Parameters	
		Parameter	Value
1	Snow Cover Fraction - SNOWCOV001	Include Red Channel	Not Selected
		Include Green Channel	Not Selected
		Include Blue Channel	Selected
		Store mid-step and extra output data	Selected
		Use georectification	Selected
		Spatial extent	-23;2;0;31
		Spatial Extent Coordinate System	ETRS-TM35FIN(EPSG:3067) GEOID with Camera at Origin
		Spatial resolution	0.001
		DEM Dataset	NLS-DEM10
		Camera coordinates	67.997393;24.209355
		Camera coordinate system	WGS84(EPSG:4326)
		Camera Height	2.5
		Horizontal position	3
		Target Direction	341
		Vertical position	17
		Focal length	4
		Scaling factor	0.7
		Interpolate DEM Data	Selected
		Flat terrain	Not Selected
		Radial Center	0.0;0.0
		Horizontal coefficient	0.05
		Vertical Coefficient	0.05

2	Create animation	Parameter	Value
		Duration	30
		Frames per second	12
		Resolution	720p
		Format	MP4

Kaamanen FSC

Camera Selection

Camera Network	Camera Name
MONIMET	Kaamanen Wetland Ground

Temporal Selection

Latest one month

	Start	End
Date	N/A	N/A
Time	11:15:00	13:45:00

Masking/ROIs

Run analyses also for each polygon (ROI) separately: False

Polygon	Coordinates
1	0.9909,0.297,0.4121,0.3091,0.1197,0.3273,0.0076,0.3556,0.0061,0.9919,0.7667,0.9939,0.7712,0.899,0.8561,0.9091,0.85,0.5192,0.9879,0

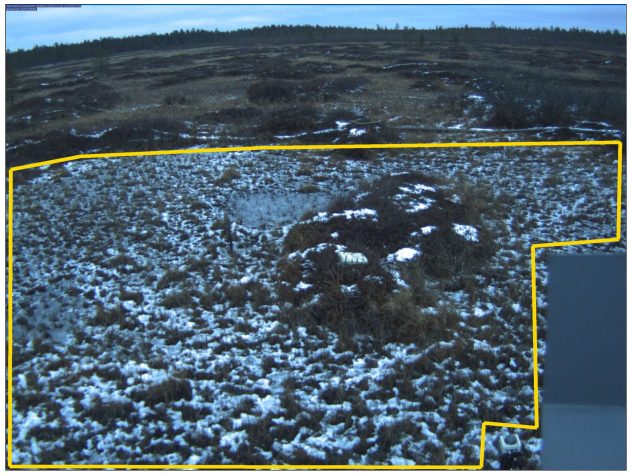

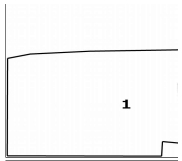

Thresholds

Type	Value	Minimum	Maximum
Image Threshold	Brightness	0.1	1.0
Image Threshold	Luminance	0.0	1.0
ROI Threshold	Red Fraction	0.0	1.0
ROI Threshold	Green Fraction	0.0	1.0
ROI Threshold	Blue Fraction	0.0	1.0
Pixel Threshold	Red Channel	0.0	254.0
Pixel Threshold	Green Channel	0.0	254.0
Pixel Threshold	Blue Channel	0.0	254.0

Analyses

Analysis No	Analysis Name	Analysis Parameters	
		Parameter	Value
1	Snow Cover Fraction - SNOWCOV001	Include Red Channel	Not Selected
		Include Green Channel	Not Selected
		Include Blue Channel	Selected
		Store mid-step and extra output data	Selected

		Use georectification	Selected
		Spatial extent	3.5;0;23;17
		Spatial Extent Coordinate System	ETRS-TM35FIN(EPSG:3067) GEOID with Camera at C
		Spatial resolution	0.001
		DEM Dataset	NLS-DEM10
		Camera coordinates	69.140583;27.269817
		Camera coordinate system	WGS84(EPSG:4326)
		Camera Height	2.6
		Horizontal position	-1
		Target Direction	55.5
		Vertical position	12
		Focal length	4
		Scaling factor	1.24
		Interpolate DEM Data	Selected
		Flat terrain	Not Selected
		Radial Center	0.0;0.0
		Horizontal coefficient	0.1
		Vertical Coefficient	0.1

		Parameter	Value
		Duration	30
2	Create animation	Frames per second	12
		Resolution	720p
		Format	MP4

Tammela SD

Camera Selection

Camera Network	Camera Name
MONIMET	Tammela Spruce Ground

Temporal Selection

Latest one month

	Start	End
Date	N/A	N/A
Time	11:15:00	13:45:00

Masking/ROIs

Run analyses also for each polygon (ROI) separately: False

0.5116,0.7051,0.4848,0.7063,0.4866,0.918

Polygon	Coordinates
1	0.4893,0.9168,0.5071,0.918

Thresholds

Type	Value	Minimum	Maximum
Image Threshold	Brightness	0.1	1.0
Image Threshold	Luminance	0.0	1.0
ROI Threshold	Red Fraction	0.0	1.0
ROI Threshold	Green Fraction	0.0	1.0
ROI Threshold	Blue Fraction	0.0	1.0
Pixel Threshold	Red Channel	0.0	255.0
Pixel Threshold	Green Channel	0.0	255.0
Pixel Threshold	Blue Channel	0.0	255.0

Analyses

Analysis No	Analysis Name	Parameter	Value
1	Snow Depth - SNOWDEP001	Height of the object	120
		Threshold Value	65
		Gaussian filter sigma	1
		Bias	0

		Parameter	Value
		Duration	30
2	Create animation	Frames per second	12
		Resolution	720p
		Format	MP4

Hyytiala SD

Camera Selection

Camera Network	Camera Name
MONIMET	Hyytiala Pine Ground

Temporal Selection

Latest one month

	Start	End
Date	N/A	N/A
Time	11:15:00	13:45:00

Masking/ROIs

Run analyses also for each polygon (ROI) separately: False

Polygon	Coordinates
1	0.4749,0.5094,0.4937,0.5087,0.4953,0.2683,0.4697,0.2697,0.4734,0.508

Thresholds

Type	Value	Minimum	Maximum
Image Threshold	Brightness	0.1	1.0
Image Threshold	Luminance	0.0	1.0
ROI Threshold	Red Fraction	0.0	1.0
ROI Threshold	Green Fraction	0.0	1.0
ROI Threshold	Blue Fraction	0.0	1.0
Pixel Threshold	Red Channel	0.0	255.0
Pixel Threshold	Green Channel	0.0	255.0
Pixel Threshold	Blue Channel	0.0	255.0

Analyses

Analysis No	Analysis Name	Analysis Parameters	
		Parameter	Value
		Height of the object	125
1	Snow Depth - SNOWDEP001	Threshold Value	40
		Gaussian filter sigma	1
		Bias	0
		Parameter	Value
		Duration	30
2	Create animation	Frames per second	12
		Resolution	720p
		Format	MP4

Sodankyla Forest SD

Camera Selection

Camera Network	Camera Name
MONIMET	Sodankyla Pine Ground

Temporal Selection

Latest one month

	Start	End
Date	N/A	N/A
Time	11:15:00	13:45:00

Masking/ROIs

Run analyses also for each polygon (ROI) separately: False

Polygon	Coordinates
1	0.5473,0.8801,0.5265,0.8851,0.5189,0.5606,0.5473,0.5492

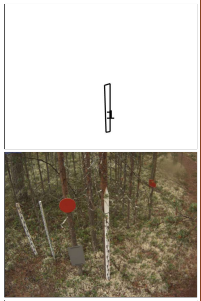

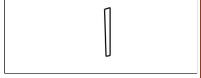

Thresholds

Type	Value	Minimum	Maximum
Image Threshold	Brightness	0.1	1.0
Image Threshold	Luminance	0.0	1.0
ROI Threshold	Red Fraction	0.0	1.0
ROI Threshold	Green Fraction	0.0	1.0
ROI Threshold	Blue Fraction	0.0	1.0
Pixel Threshold	Red Channel	0.0	255.0
Pixel Threshold	Green Channel	0.0	255.0
Pixel Threshold	Blue Channel	0.0	255.0

Analyses

Analysis No	Analysis Name	Analysis Parameters	
		Parameter	Value
		Height of the object	100
1	Snow Depth - SNOWDEP001	Threshold Value	80
		Gaussian filter sigma	1
		Bias	0
		Parameter	Value
		Duration	30
2	Create animation	Frames per second	12
		Resolution	720p
		Format	MP4

Sodankyla Peatland SD

Camera Selection

Camera Network	Camera Name
MONIMET	Sodankyla Pine Peatland

Temporal Selection

Latest one month

	Start	End
Date	N/A	N/A
Time	11:15:00	13:45:00

Masking/ROIs

Run analyses also for each polygon (ROI) separately: False

Polygon	Coordinates
1	0.5644,0.6477,0.5767,0.6503,0.5928,0.4141,0.5767,0.4154

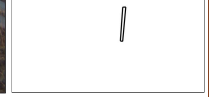

Thresholds

Type	Value	Minimum	Maximum
Image Threshold	Brightness	0.1	1.0

Image Threshold	Luminance	0.0	1.0
ROI Threshold	Red Fraction	0.0	1.0
ROI Threshold	Green Fraction	0.0	1.0
ROI Threshold	Blue Fraction	0.0	1.0
Pixel Threshold	Red Channel	0.0	255.0
Pixel Threshold	Green Channel	0.0	255.0
Pixel Threshold	Blue Channel	0.0	255.0

Analyses

Analysis No	Analysis Name	Analysis Parameters	
		Parameter	Value
1	Snow Depth - SNOWDEP001	Height of the object	100
		Threshold Value	80
		Gaussian filter sigma	1
		Bias	0
		Parameter	Value
2	Create animation	Duration	30
		Frames per second	12
		Resolution	720p
		Format	MP4